# Methods to Linearize Monochrome Inkjet Printer Response

**Understanding carbon printing**
**for the mathematically-inclined beginner**

Hendrik C. Kuhlmann

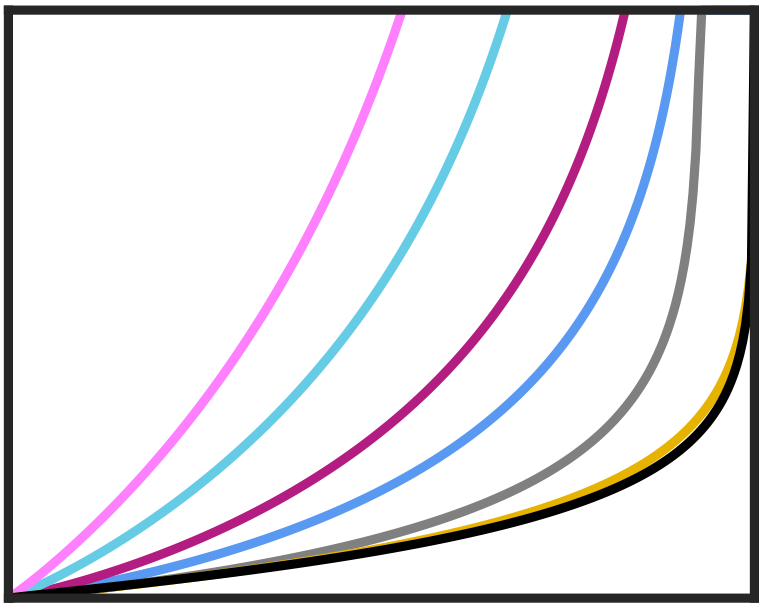

The frontispiece shows the ink amount as function of the blackness such that each ink of Paul Roark's GCVT ink set prints linearly on Hahnemühle's Photo Rag 308.

Version 2.1, September 2025


www.kuhlmann.at

# Contents

# Preface

Early in 2025 I started using refillable ink cartridges for my Epson R2880 inkjet printer, because OEM ink cartridges were no longer produced by Epson. I decided to use the Glossy Carbon Variable Tone (GCVT) ink set proposed by Paul Roark and the Windows version of Quad Tone Rip (QTR) created by Roy Harrington. Because the ink calibration for QTR was not fully clear to me, the GUI of the windows version of QTR was outdated, and because the user had only limited influence on the shape of the ink ansatz functions, I tried to find my own way through the jungle of curve creation. Initially, I wrote up my experiences only for myself. But perhaps they will also be of interest to others who are not afraid of a little math.

Essentially, a method is proposed to create a quad file for monochrome inkjet printing with multiple gray inks which prints linearly from the outset in one go. This could remove the need for iterating ink curves and even the linearization step would eventually be unnecessary. The goal is accomplished by using gray inks which are made from dilutions of the same black ink and by fitting the luminance curves of each ink from the calibration print by functions of closed form which allow to analytically predict the ink amount to make each ink channel print linearly. The blue toning required to obtain a neutrally gray print as well as the fine tuning (linearization) to achieve a print output which is linear in the blackness $K$ are addressed. The method can be generalized to create a quad file for any bijective target luminance curve, such as a gamma corrected curve. Evidence is presented that the method is very accurate and curtailed mainly by luminance measurement and printer errors. Furthermore, I suggest a method to predict the luminance of the printed output entirely based on the characteristics of the participating types of ink (PK, MK and toner). This allows for a free design of ink curves, e.g. with shapes similar as those of Piezography, such that they print linearly.

In almost all respects I am new to the field of monochrome printing with custom made inks. Therefore, the ideas presented may not all be new, my assumptions and conclusions may not always hold under all circumstances, and I may have committed mistakes. For these reasons I would be grateful for any suggestions and/or corrections by the more experienced reader.

August, 2025
H. C. K.

# 1. Introduction

Inkjet printing with pigment inks has matured over the years and today prints can be made with very high resolution, color accuracy and longevity. Black and white printing has lagged a little, because the eye is very sensitive to minute deviations from a neutral tone. But today Epson's advanced black and white mode (ABW mode) and similar ones of other printer manufacturers using multiple gray inks produce very neutral and color accurate black and white prints.

To improve black and white printing in the past a dedicated black and white printing technique was developed in which multiple gray pigment inks are used in the color channels of Epson printers. Even though black and white printing is excellent with the current state of the ABW mode, some black and white *aficionados* are still interested in using QTR with multiple gray inks. A prominent figure in this field is Jon Cone of Inkjet Mall who invented the famous Piezography system.[1] In order to control the ink flow a raster image processor is required and the shareware program Quad Tone Rip[2] (QTR) has become quite popular. Other offers, like the one of Farbenwerk,[3] focus on an easy use of multiple gray ink by relying on the Epson driver. Perhaps the most popular field is printing on transparent media to create film negatives for use in alternative contact printing processes. These negatives may require dedicated density and gradation curves. Others may just convert a printer for which OEM inks are no longer manufactured into a dedicated black and white printer which promises less expensive ink and perhaps the best possible longevity of prints on high quality papers.

The printing with QTR requires a so-called quad file which is an ASCII file providing the information for the driver to make the printer print a certain color channel or gray value. Such quad files can be created with the curve creation tool of QTR. In this process one typically tries to create a *linear curve* for black and white printing which means that the printed luminance of a gray patch is a linear function of the $K$ value which is the blackness variable (e.g. in Photoshop). To arrive at this linear curve using different gray channels in QTR usually requires a number of iterations. Experience and artful handling facilitates the process.

In the present paper I present my the idea of how to create a quad file which prints along a predefined luminance curve. Among those curves a linear curve probably is the most interesting one. The objective is to create the quad file in one go without the need for iteration. To arrive at this goal I have made several

[1] https://piezography.com/
[2] https://www.quadtonerip.com.
[3] https://www.farbenwerk.com/

measurements and calculations. I use Quad Tone Rip (QTR) for Windows to print on matte and glossy papers, using the Epson printer R2880. The QTR settings are 2880super and the dithering is set to *ordered* (standard setting). I use the Glossy Carbon Variable Tone (GCVT) ink set suggested by Paul Roark,[4] but the results are applicable to any other monochrome ink set. A QTR User Guide has been written by Moore (2005). Details and valuable information on the ink set can be found in Roark (2023).

[4] https://paulroark.com/BW-Info.

# 2. The calibration print

The calibration of an ink–paper–printer combination is usually performed by first printing the ink separation image. The image contains step wedges of 21 (or more) patches for each ink channel. The 21 steps of the wedge are designed such that within each step the ink amount $K_{\text{ink}}$[1] printed is increased by 5%, starting from 0 and up to 100% of the ink amount the printer is capable to lay down on the paper. The ink amount information is coded in the green channel G of this untagged file.

To begin the calibration process the calibration image is printed with the global ink limit set to $\alpha = 100\%$ (fig. 2.1). This parameter can be set in QTR. In this case the darkest patch is printed with the maximum ink amount the printer is capable of. Usually, this is too much ink and the dark tones of most channels, patch by patch, readily run into saturation such that the individual dark (black) gray steps are difficult to be distinguished visually anymore.

Next we have to define what we want to call 100% *black*. I shall come back to this question in section 5.3. For the moment, I define 100% black by the ink amount on the calibration print which shows the deepest black printed by the $K$ ink channel (first row in fig. 2.1) such that the next brighter step (to the left in the image) is still slightly discernable from this black and that all darker steps (to the right) cannot be visually distinguished from that step anymore. The percentage of black ink at which this condition is reached is usually set als the global ink limit $\alpha$. For

[1]The subscript 'ink' is used to distinguish the physical amount of ink $K_{\text{ink}}$ (volume of ink per area of paper, given in % of the maximum possible) from the blackness $K$ used later.

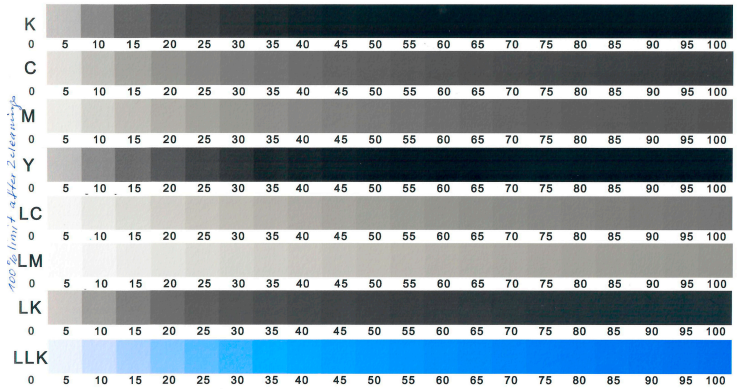


**Figure 2.1.:** Ink separation image printed on the R2880 on HFA Photo Rag 308 with the GCVT ink set. The global ink limit is $\alpha = 100\%$ (maximum possible). The numbers give the amount of ink $K_{\text{ink}}$ in percent of the maximum posssible.

Canson Arches 88 as well as for Hahnemühle Photo Rag 308 and the GCVT ink I set $\alpha = 60\%$ in the following. Therefore, 60% of the maximum possible ink will from now on correspond to 100% black. The choice of $\alpha$ sets the gray (or blackness) scale for printed images.

With the global ink limit set to $\alpha = 60\%$ in QTR the ink separation image is now printed a second time. Note the printed scale on the image is still the same, ranging from 0 to 100%. But now 100% does not mean 100% of ink the printer can deliver, but rather 100% of the ink limit $\alpha$, or 100% of the blackness on a gray scale ranging in $K \in [0, 100]\%$. Unfortunately, three different quantities are denoted with the same symbol $K$. These are

(a) $K$ can mean the *visual gray level*, the percentage of the deepest black or the blackness in the printed image. I shall keep this notation for $K$ as a measure of the blackness on the scale $K \in [0, 100]$, where $K = 0$ is the brightest and $K = 100$ the darkest tone that can be achieved. This is the $K$ scale used in, e.g., Photoshop.

(b) $K$ means the *amount of ink* per area in percent of the global ink limit $\alpha$. I shall call it *amount of ink*. The amount of ink is essentially a measure for the number of droplets per area, provided they all have the same size. In order to better distinguish between the physical ink amount and the blackness, I shall call $K_{\text{ink}}$ the ink amount in percent of the maximum amount the printer can deliver.

(c) Finally, $K$ can mean the physical ink (pigment) coverage of a pixel given in %. I shall call this physical quantity $K_{\text{cov}}$. A coverage of $K_{\text{cov}} = 100\%$ means that the pixel is completely covered with pigment. There are no open spots where the paper can pierce through.

All of the following is about the functional dependence of the blackness $K(K_{\text{ink}})$ (which is related to the visual luminance) as function of the amount of ink $K_{\text{ink}}$ required to achieve a certain appearance of the gray scale image. Up to now we have only defined the end point of the function $K(K_{\text{ink}})$ by

$$K(K_{\text{ink}} = \alpha) = 100,$$

because the darkest value achieved with $K_{\text{ink}} = \alpha$ is set to $K = 100$ for obvious practical reasons. Here and in the following, I often drop the % sign (possibly a bit unsystematic yet).

I think the Epson printer can very accurately dose the amount of ink $K_{\text{ink}}$ placed on the paper, because the piezo nozzles are precisely controlled by the printer driver and they deliver ink droplets very reliably,[2] if the nozzle check and the ink flow through the print head and the cartridges is perfect. But of course there can be

[2] For the Epson R2880 I found a *minimum* droplet volume of 3 pl. In their flyer it is stated that *Advanced MicroPiezo print head with AMC (Advanced Meniscus Control) can produce up to 3 different droplet sizes per line.*

deviations if, e.g., a nozzle is ever so slightly blocked or geometrically/mechanically imperfect.

One can find that the minimum droplet size is 3.5 pl. Moreover, the typical standard deviation of droplet volume is $\approx 5\,\%$ of the nominal value corresponding to $\approx 2\,\%$ standard deviation for the diameter of a printed droplet. Practically the same standard deviations are found for the volume and sizes when the droplets are printed with different nozzles.

# 3. A simple model for ink deposition

In the following we want to get an idea about the dependence of the luminance as a function of the ink amount $K_{\text{ink}}$ placed on the paper. To that end we make a number of idealizing assumptions which we can relax at later stage.

We consider an ink which has a completely clear base solution which contains very small black pigment particles which are completely opaque. Figure 3.1 shows a pixel (outer square) within which a droplet of ink has been placed (light gray patch) which contains some pigment particles (black patches). The area of the pixel is not relevant, it merely serves as a reference area. In any case, we select the reference area much larger than the size of a pigment particle. Furthermore, we assume that the paper is completely smooth and that the light is reflected perfectly diffuse. Moreover, it is assumed that the base solution is soaked by the paper and that the reflective properties are not changed by the base solution.

Under the above conditions I further assume that the visual luminance of the pixel is a linear function of the fraction $A$ of the pixel area which is *not* covered by pigment particles. Then[1]

$$L(A) = L_p + (L^\infty - L_p)(1 - A), \tag{3.1}$$

where $L_p$ is the luminance of the paper white (corresponding to $A = 1$) and $L^\infty$ is the luminance of the pigment particle, or the luminance of the pixel if it is completely covered with pigment ($A = 0$). This relation holds, because the human eye integrates the luminance over the area, i.e. it performs a spatial averaging. Here the pigment coverage is $K_{\text{cov}}/100 = 1 - A$.

To determine the luminance of the pixel we need to determine how the uncovered area $A$ depends on the ink amount $K_{\text{ink}}$ deposited. To that end we consider a tiny ink droplet of amount $\mathrm{d}K_{\text{ink}}$[2] which is deposited at a random location within the pixel area. I assume that a deposited droplet always has the same volume.[3] We assume that the ink is very diluted such that the droplet volume is large compared to the volume of the pigment contained which, however, is distributed in many tiny particles. Then the area within the deposit covered by pigment is considerably

[1] Usually the visual luminance is denoted $L^*$, but for convenience the asterisk is dropped here and in the following.

[2] I think the ink amount $K_{\text{ink}}$ is essentially the volume of ink deposited per area, because the maximum ink amount $K_{\text{ink}} = 100\%$ a printer can deliver is a certain volume which is placed on a certain area, determined (among other factors) by the advancement speeds of the print head and the paper. The volume per surface corresponds to a thickness of the ink layer deposited.

[3] Although the R2880 uses thee droplet sizes, it is presumably possible to print with only one droplet size ($\approx 3.5\,\text{pl}$) if the highest resolution (2880dpi) is selected in QTR. That is what I do.

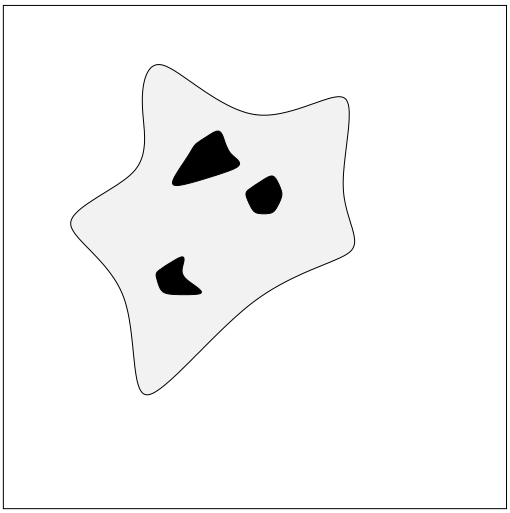

**Figure 3.1.:** A pixel (outer square) containing a droplet of ink with clear base (light gray) and three pigment particles (black). The dimensions are not necessarily to scale: A pixel printed with 720ppi has an edge length of $\approx 35\,\mu$m. A deposited 3.5 pl droplet has a diameter of $\approx 20\,\mu$m, and the diameter of a black pigment particle can range from several tens to several hundreds of a nanometer, such that $0.1\,\mu$m is perhaps a typical diameter.

smaller than the area covered by the ink droplet and the pigment particles do not fall on top of each other (they are not stacked within a single deposited droplet[4]). In that case the area covered by the pigment particles when a single drop falls on an empty area of the pixel is proportional to the ink amount $\mathrm{d}K_{\mathrm{ink}}$ of the droplet.[5] Therefore, the uncovered area $A$ is reduced by an amount proportional to $\mathrm{d}K_{\mathrm{ink}}$ and the change of the area is $\mathrm{d}A \sim \mathrm{d}K_{\mathrm{ink}}$. Now if the paper has already received many ink droplets part of the pixel is already covered by pigment. Then a pigment particle of an added droplet can fall on a spot of the pixel which is not covered by pigment, or it can fall on top of a pigment particle which has already been deposited earlier. The probability that it falls on an empty spot (and thus reduces the uncovered area) is proportional to the uncovered area $A$. Therefore, the change $\mathrm{d}A$ of the uncovered area $A$ when a single droplet of diluted ink of amount $\mathrm{d}K_{\mathrm{ink}}$ is deposited must satisfy

$$\mathrm{d}A = -sA(K_{\mathrm{ink}})\,\mathrm{d}K_{\mathrm{ink}}, \tag{3.2}$$

where the uncovered area $A = A(K_{\mathrm{ink}})$ depends on the amount of ink $K_{\mathrm{ink}}$ deposited and $s$ is a positive proportionality constant. The minus sign indicates that the uncovered area is decreasing with another droplet of ink. The constant $s$ is also proportional to the concentration $c$ of pigment particles in the ink, a point to which we shall return in section 6.1. Equation (3.2) can be integrated to yield[6]

$$\ln A(K_{\mathrm{ink}}) - \ln A(K_0^{\mathrm{ink}}) = -s(K_{\mathrm{ink}} - K_0^{\mathrm{ink}}).$$

[4] For the diluted inks this seems to be the case. But for pure black inks a certain amount of stacking of pigment particles is observed indirectly (see the data for $LK$ in fig. 6.1): When the same amount of pigment is printed, the output of the black ink appears brighter (higher luminance) than when the same amount of pigment is printed with diluted ink and more ink (more droplets). In the case of diluted ink and more droplets, the stacking is less, because already in a single droplet the stacking is less and the ink droplets cover a wider area.

[5] Due to the many pigment particles in a droplet we assume that each droplet contains the same amount of pigment in the mean.

[6] In case multiple subscripts would arise, the subscript 'ink' becomes a superscript.

For an completely uncovered pixel the amount of ink is $K_0^{\text{ink}} = 0$ and the fraction of the pixel uncovered is $A_0 = A(K_0^{\text{ink}}) = 1$. Therefore,

$$\ln A(K_{\text{ink}}) = -sK_{\text{ink}}. \tag{3.3}$$

Equation (3.1) can be solved for $A$ to obtain

$$A(L) = \frac{L^\infty - L}{L^\infty - L_p}.$$

If this relation is inserted in equation (3.3) we obtain the relation between the luminance and the amount of ink deposited

$$\ln\left[\frac{L^\infty - L}{L^\infty - L_p}\right] = -sK_{\text{ink}},$$

or, solved for $L$,

$$L(K_{\text{ink}}) = L^\infty + (L_p - L^\infty)\mathrm{e}^{-sK_{\text{ink}}}. \tag{3.4}$$

This relation should hold for diluted inks as long as the assumptions made hold true and as long as the pigment particles of a *single* droplet do not stack on top of each other when deposited.[7] Effects of high pigment particle concentrations (or similarly for large ink droplets) may be corrected by empirical laws in case no theoretical derivation is available (see section 9).

After deriving (3.4) I found that this relation is essentially the Beer–Lambert law (Beer, 1852; Lambert, 1760). Originally, it was used to describe the attenuation of the radiation intensity as a function of the depth when an absorbing substance is exposed to radiation. So there are parallels.

[7] If the concentration $c$ of the pigment particles is too large, then pigment particles of a droplet can fall on top of each other and the area covered by the pigment particles of a single droplet is no longer proportional to the ink amount $\mathrm{d}K_{\text{ink}}$ of the droplet. For such an effect, see section 6.1.

# 4. GCVT ink characteristics on Arches 88

If one measures[1] the luminance of the patches of the ink separation print on Arches 88 as a function of $K_{\text{ink}}$ one finds that the measurement points are extremely well represented by (3.4) for all ink channels. This is shown in figure 4.1. The good agreement is favored by the paper being matte and having a very smooth surface.

All ink channels have the same paper white $L_p$ (the common intersection point at $K_{\text{ink}} = 0$), but different asymptotic luminance values $L(K_{\text{ink}} \to \infty) = L^\infty$ (not shown in the plot) and different decay constants $s$. These must be determined by fitting the continuous function (3.4) to the data. The fits then yield $L_p$ and the two sets $\{L_i^\infty\}$ and $\{s_i\}$, where the index $i \in \{K, Y, LK, LLK, C, M, LC, LM\}$

[1] I use a ColorMunki Photo in spot measurement mode. The ColorMunki is supposed to have the following estimated luminance measurement errors.

- Repeatability: ±1–2% (for repeated measurements on the same sample).
- Absolute Accuracy: ±3–5% (compared to reference-grade instruments).
- Instrument Variability: Different units may have ±5% deviations.

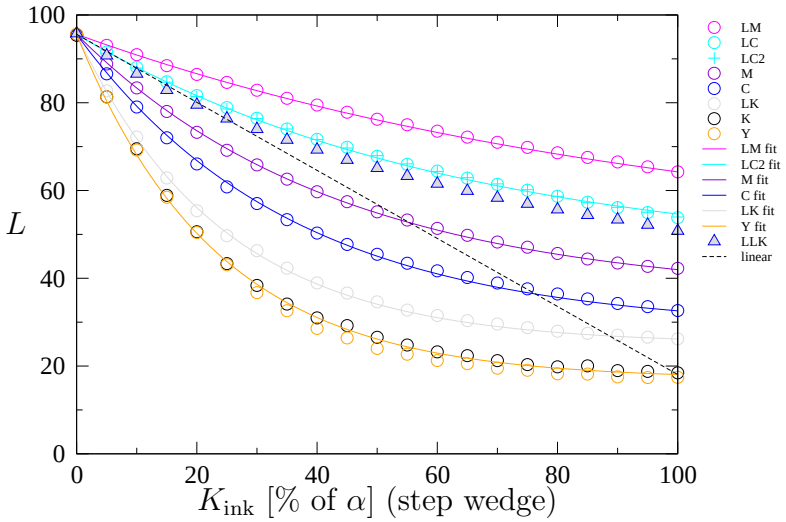


**Figure 4.1.:** Luminosities (circles) of the 21 ink patches of the ink separation print for the GCVT ink set on Arches 88 using the Epson R2880. The ink channels are colored coded. Lines represent exponential fits according to (3.4). The dashed line shows the targeted luminance curve which is a linear function of $K$. The global ink limit is $\alpha = 60\%$.

**Table 4.1.:** Fit parameters for Arches 88 using an ink limit $\alpha = 60\%$ and $L_p = 95.6$. The decay rates are based on the scale of fig. 4.1.

| ink channel | $K$ | $LK$ | $C$ | $M$ | $LC$ | $LM$ | $LLK$ |
|---|---|---|---|---|---|---|---|
| $L_i^\infty$ | 17 | 25 | 28.5 | 36 | 44 | 46 | 45 |
| $s_i$ | 0.043 | 0.041 | 0.028 | 0.023 | 0.0158 | 0.01 | 0.019 |

enumerates the different ink channels.[2] Owing to the excellent fit, equation (3.4) completely describes how an individual ink channel prints. The present fit parameters are given in table 4.1.[3]

If the luminance could be measured precisely and if the ink curves would indeed satisfy (3.4) exactly, one would only need three data points $(K_{\text{ink},1}, L_1)$, $(K_{\text{ink},2}, L_2)$ and $(K_{\text{ink},3}, L_3)$ to determine the three unknowns $L_p$, $L^\infty$ and $s$. In view of this, the 21 data points from the 21 step wedge is more than sufficient. But deviations from the ideal behavior can arise due different factors among which the properties of the paper surface is very important (see, e.g., section 9). Moreover, one needs to check for possible sources of error and the reproducibility of the measurements. One such problem is visible in fig. 4.1: In the GCVT ink set matte black is contained in both the $K$ and the $Y$ channel. Theoretically, they should print the same. But for an unknown reason,[4] I found a notable deviation (black and orange circles in fig. 4.1) which is larger than the reproducibility of the data measured with the ColorMunki Photo. The fit function for $K$ and $Y$ (the black and orange curves) is a kind of compromise.

The ultimate goal of the calibration and linearization process is to obtain an even distribution of the luminance $L$ over the whole scale of blackness $K$. This means the luminance must be a linear function of $K$, satisfying

$$L(K) = L_{\text{lin}}(K) = L_p - (L_p - L_m)\frac{K}{100} \tag{4.1}$$

where $K$ is the visual blackness. For this function, $L_{\text{lin}}(K = 0) = L_p$ is the brightest white and $L_{\text{lin}}(K = 100) = L_m$ is the deepest black. It is similar to the function $L(A)$ mentioned above when the coverage $K_{\text{cov}}/100 = (1 - A)$ is replaced by $K/100$ and $L^\infty$ by $L_m$. In this sense/approximation, the ink coverage $K_{\text{cov}}$ (better pigment coverage) is equivalent to the blackness $K$.

The targeted linear behavior (4.1) is shown as a dashed line in fig. 4.1. But it is obvious also from (3.4) that the luminance is not a linear function of the ink amount $K_{\text{ink}}$. Therefore, we must distinguish between $K$ and $K_{\text{ink}}$ even though

[2] In the GCVT ink set the $LLK$ channel contains the blue toner ink. This ink is only used later to obtain a neutral gray. Moreover, both the $K$ and $Y$ channel contain MK ink.

[3] At this stage I determined the parameters by trial and error. A better job is done later by a least squares method.

[4] The measurements were based on the first ink load of the new set of refillable ink cartridges. Later I found that the priming of the cartridges has a decisive influence on the ink flow. Thus a possible reason could be that the $K$ cartridge was just not completely primed.

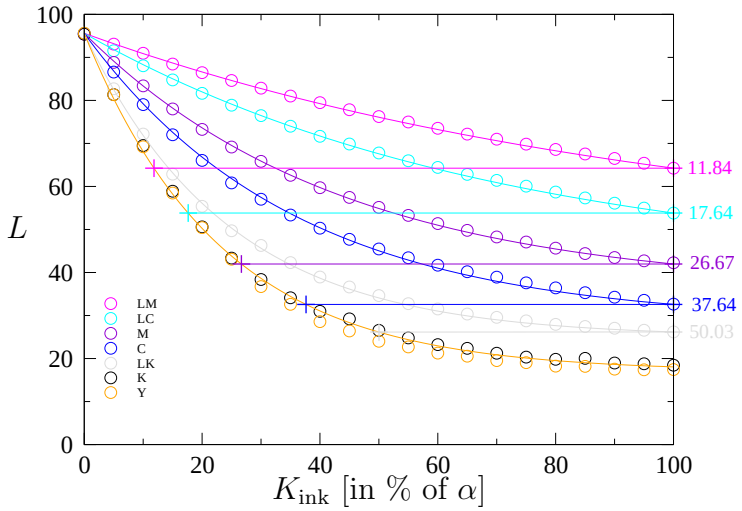


**Figure 4.2.:** QTR recommendation: Correlating the luminance of all gray inks with the one of the $K$ ink at the anchor points $\bar{K}_i$ (plusses) defined by $L_i(K = \alpha) = L_K(\bar{K}_i)$. The $K$ values at these anchor points are given by numbers in the right margin. Same curves and conditions as in fig. 4.1.

they both range in $[0, 100]$, and ask: How much ink $K_{\text{ink}}$ is required to obtain the linear dependence (4.1) of the luminance on the visual blackness $K$, in particular, if more than one gray ink is used?

# 5. Total linearization

## 5.1. The idea

From the calibration plot the luminance of each ink as a function of $K_{\text{ink}}$ is known (fig. 4.1). Thanks to the very good exponential approximation (3.4) the ink response curves are mathematically accessible in closed form. This offers the possibility to accurately linearize the luminance. Moreover, it enables to realize the following idea.

> One can linearize each ink curve separately to accurately map the luminance to a unique desired linear curve.[1] Within a certain range of $K$ each ink would then print linearly and the luminance of all inks (when printed alone) would lie on the same linear curve. Then one could smoothly blend the ink amounts among each other with only very little restrictions.

This idea has the advantage that all inks print the same luminance for all gray values $K$ (within their accessible range), and not only at the anchor points $\bar{K}_i$ of QTR (pluses in fig. 4.2). The blending of different inks would work out, if a blend of inks (which print the same luminance) would also print the same luminance if their weights sum up to 1. Luckily, this is the case to good accuracy.[2] For a test of this hypothesis, see fig. 9.4 below. It is also important to notice that the available range of $K$ is restricted for the gray inks (derived from PK), because their luminance saturates on matte paper before reaching blackness $K = 100$.

For the following it is important to be able to accurately measure the calibration print. Furthermore, one should be aware of possible sources of error, some of which are listed here.

1. The ColorMunki Photo may exhibit systematic deviations and random errors. But I found a very good reproducibility. Therefore, the random error seems quite small.

2. Nozzles of the print head may be very slightly uneven or partially blocked. Quite generally, the ink flow may also be imparted by the state of the ink

[1] One could also map the exponential ink functions to other curves, see section 10.

[2] In principle there could be interactions among different inks. But since in the GCVT ink set all gray inks derive from the same PK ink, this is not the case. See also section 6.1.

in the ink cartridges. In my case, a slightly varying ink flow is probably the most important source of error.[3]

3. The fit functions do not exactly reproduce the measured data.

4. The paper structure and its absorbance properties in combination with the ink may vary locally. But this is not very likely. However, the paper structure may have some influence on the luminance and the fit functions may need to be adapted (see section 9).

## 5.2. Linearizing the $K$ channel

The exponential curves $L_i(K_{\text{ink}})$ are very different from the intended a linear variation (dashed line in fig. 4.1). In particular, the $K$ channel (orange curve) always prints much darker than linear. Therefore, the ink amount $K_{\text{ink}}(K)$ needs to be reduced.

To find the correct ink amount reduction we first need the targeted linear luminance variation (4.1), for convenience repeated here,

$$L_{\text{lin}}(K) = L_p - (L_p - L_m)\frac{K}{100},$$

where $L_m = L_K(K_{\text{ink}} = \alpha)$ is the minimum luminance (deepest black) that can be obtained (within the global ink limit $\alpha$ selected, see section 5.3). Note that the asymptotic value of the luminance $L_K^\infty$ of the $K$ channel must be slightly smaller than $L_m$, $L_K^\infty < L_m$.

To find the mapping for the $K$ channel (for instance for K-only (KO) printing) we consider a certain fixed value of $L$ and relate the value $K_{\text{ink}}$ which produces this luminance in the calibration plot to the blackness variable $K$ which produces the same luminance if the luminance would be a linear function of $K$. This is explained graphically in fig. 5.1 for a general gray channel. The relation between $K_{\text{ink}}$ and $K$ is obtained by expressing the same $L$ value by the exponential function (3.4) of $K_{\text{ink}}$ (blue curve in fig. 5.1) and by the linear function (4.1) of $K$ (full black line in fig. 5.1). This yields (the subscript $K$ denotes the black ink channel)

$$L_K(K_{\text{ink}}) = L_{\text{lin}}(K),$$

or

$$L_K^\infty + (L_p - L_K^\infty)\exp(-s_K K_{\text{ink}}) \stackrel{!}{=} L_p - (L_p - L_m)\frac{K}{100}.$$

[3] Most likely, this is the reason why the $K$ and $Y$ curves in fig. 4.1 deviate from each other. Also the ink amount of individual droplets typically vary by approximately 5%, corresponding to a deposited area variation of 2% (see footnote 2 above).

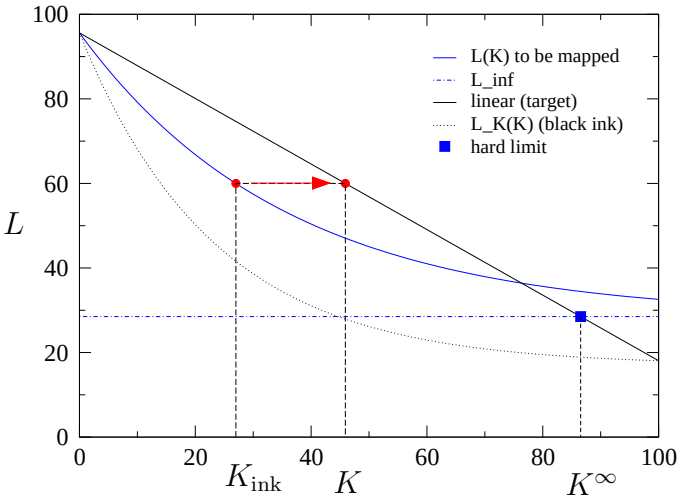


**Figure 5.1.:** Mapping of $K_{\text{ink}}$ to $K$ for $L = 60$ (red dots and arrow) for a gray ink (blue line). The mapping can only be carried out within $K \in [0, K_c]$ (blue square), because values $L < L^{\infty}$ (dash-dotted blue line) are not accessible by the ink. Note: The scale for $K_{\text{ink}}$ is in % of the ink limit $\alpha$.

From this equation we can express $K_{\text{ink}}$ as

$$K_{\text{ink}} = -\frac{1}{s_K} \ln \left[ \frac{L_{\text{lin}}(K) - L_K^{\infty}}{L_p - L_K^{\infty}} \right] = -\frac{1}{s_K} \ln \left[ 1 - \frac{L_p - L_m}{L_p - L_K^{\infty}} \frac{K}{100} \right]. \tag{5.1}$$

Now we can interpret $K_{\text{ink}}$ in (5.1) as the *ink amount* which should be printed in order to obtain the luminance $L$ on the linear curve at the *blackness* $K$ (gray level). The amount of black ink $K_{\text{ink}}$ required for a linear output is shown as the black line in fig. 5.2.

For the black ink (dotted line in fig. 5.1) the ink amount $K_{\text{ink}}$ required to achieve the gray level $K$ for a given luminance is always less than $K$. This can also be seen from fig. 5.2. This is the reason why one has to always use positive values in the fields *Highlight* and *Shadow* under the *Gray Curve* tab of QTR in the Curve Creator modus. The maximum possible brightening (by the functions implemented in QTR) by means of the highlight parameter, the shadow parameter and their combination is shown in fig. 5.2 as a blue, a red and a green line, respectively. One can see that the maximum possible brightening (for Gamma = 1) in the shadows does not reduce the ink amount to the one required for linearizing the $K$ channel (full black line). Therefore, one has to further reduce the ink amount in QTR by reducing the individual ink limit for the darker inks in this region of $K$, approximately $K \in [60, 100]$. This may, on the other hand, counteract the deepest black which would then have to be compensated by a black boost. But these characteristics are typically remedied by the linearization in QTR.

## 5.3. Selecting the black point

In the foregoing we have made a selection of the black point defined by the couple $(\alpha, L_m)$, where $\alpha$ is the global ink limit and $L_m$ the luminance of the deepest black which should be achieved at $K = 100$ or $K_{\text{ink}} = \alpha$. The situation is explained in

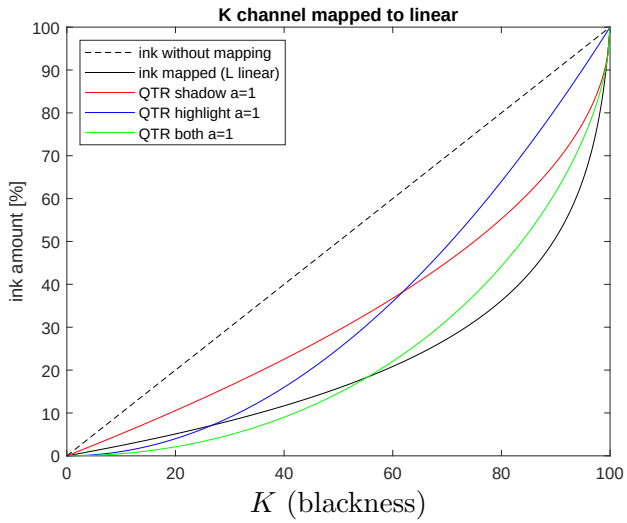


**Figure 5.2.:** The mapping function (ink amount) $K_{\text{ink}}(K)$ as function of the blackness $K$ according to (5.1) (full black line) for GCVT black ink ($K$) on Arches 88. This function represents the ink amount (here in units of the global ink limit $\alpha = 60\%$) required for a linear relation $L(K)$ in the print. The uncorrected linear ink amount with $K = K_{\text{ink}}$ resulting from the uncorrected exponential decay of $L_K(K_{\text{ink}})$ (orange curve in fig. 4.1) is shown as a dashed black line. For comparison, also the QTR ink amount function for $K$ only (highlight and shadow parameters set to zero, Gamma = 1, dashed line) are shown for the maximum possible highlight brightening ($a = 1$, blue line), maximum possible shadow brightening ($a = 1$, red line) and the combination of both (green line).

fig. 5.3 which shows the exponential $L_K$ curve (black line) on the full scale $K_{\text{ink}}$ of ink not limited by $\alpha$, where $K_{\text{ink}} = 100\%$ is the maximum ink the printer can deliver.

For the purpose of illustration we assume here an ink limit of $\alpha = 40\%$ (vertical dotted line). The choice of $\alpha$ is not really critical. What is important, however, is the choice of the minimum luminance $L_m$ which we want to achieve at the ink limit, at $K_{\text{ink}} = \alpha = 40\%$ in the present example. Thus far we have defined $L_m$ as the measured (or fitted) luminance $L_m = L_K(K_{\text{ink}} = \alpha)$ (blue circle and dashed blue line). If $\alpha$ is a good choice, then the luminance $L_K(K_{\text{ink}} = \alpha)$ is probably low enough (dark enough). This choice would lead to the linear ink curve 1 (full blue line) for the black channel by mapping all points on $L_K(K_{\text{ink}} < 40\%)$ to the linear blue line. By the mapping to curve 1 (blue) the ink amount is reduced for all $K_{\text{ink}} < 40\%$ as described above (full black line in fig. 5.2).

But from fig. 5.3 we notice that the theoretically deepest black is represented by $L_K^\infty$ (red square and dashed red line). This choice would lead to the linear ink curve 2 (full red line). The mapping to the linear curve 2 can be accomplished by (5.1), and it would brighten all $K_{\text{ink}}$ values to the left of the intersection point of line 2 with $L_K(K_{\text{ink}})$ (black diamond) and darken all $K_{\text{ink}}$ values to the right of the intersection point (black diamond). As can be seen, this darkening would require a very high ink load and would even exceed the capacity of the printer ($K_{\text{ink}} > 100\%$)

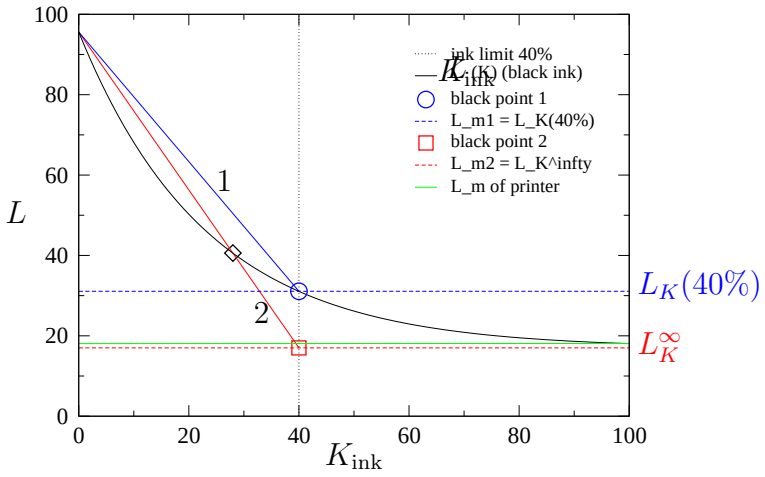


**Figure 5.3.:** Sketch illustrating possible choices for the black point (see text). Shown on the full $K_{\rm ink}$ scale are the luminance of the $K$ cannel (full black line), the global ink limit $\alpha = 40\%$ (vertical dotted line) is selected for demonstrative purposes, and two choices for the black point (blue circle, red square). The full blue line 1 and the red line 2 represents the luminance of the $K$ channel after linearization according to (5.1).

for the lowest luminance values. This is so, because the luminance $L_K^\infty$ of black point 2 (red square) can only be reached theoretically at an infinite ink load. Therefore, $L_m$ should stay away from $L_K^\infty$ and one should select $L_m > L_K^\infty$, slightly larger. If the maximum ink load for black should be 100% of what the printer can deliver, then one should increase $L_m$ from $L_K^\infty$ to $L_m = L_K(K_{\rm ink} = 100)$ which indicated by the green horizontal line. This would correspond to a black boost up to 100% of the printer's capacity. For practical reasons, one could perhaps also accept a black point which is $\Delta L = 0.5$ above the asymptotic value and set $L_m = L_K^\infty + 0.5$.

Now I am discussing the ink amount curve as shown in by the full black line in fig. 5.2. For the choice $L_m = L_K(K_{\rm ink} = \alpha)$ the ink amount curve for the $K$ channel would exactly end in the point $(K, K_{\rm ink}) = (100, \alpha)$. This is the case in fig. 5.2, where $K_{\rm ink} = 100\%$ corresponds to the global ink limit $\alpha$ (see figure caption). If $L_m < L_K(K_{\rm ink} = \alpha)$ is selected smaller than $L_K(K_{\rm ink} = \alpha)$ to obtain darker blacks, the global ink limit would be reached before the blackness $K$ reaches $K = 100$ and the ink amount at $K = 100$ would exceed the global ink limit. In the extreme case for $L_m = L_K^\infty$, the ink amount curve would diverge with an asymptote to $K = 100$. For even smaller values $L_m < L_K^\infty$, the mapping (5.1) will not have a real solution anymore and the solution becomes complex. Such small values for $L_m$ are absolutely prohibited.

## 5.4. Linearizing all ink channels

We can apply the same mapping (5.1) from section 5.2 to each of the ink curves of fig. 4.1. The equation for the mapping of a channel $i$ is the same as (5.1), but with channel specific values $L_i^\infty$ and $s_i$. The general mapping reads

$$K_i^{\rm ink} = -\frac{1}{s_i} \ln\left[\frac{L_{\rm lin}(K) - L_i^\infty}{L_p - L_i^\infty}\right] = -\frac{1}{s_i} \ln\left[1 - \frac{L_p - L_m}{L_p - L_i^\infty}\frac{K}{100}\right], \tag{5.2}$$

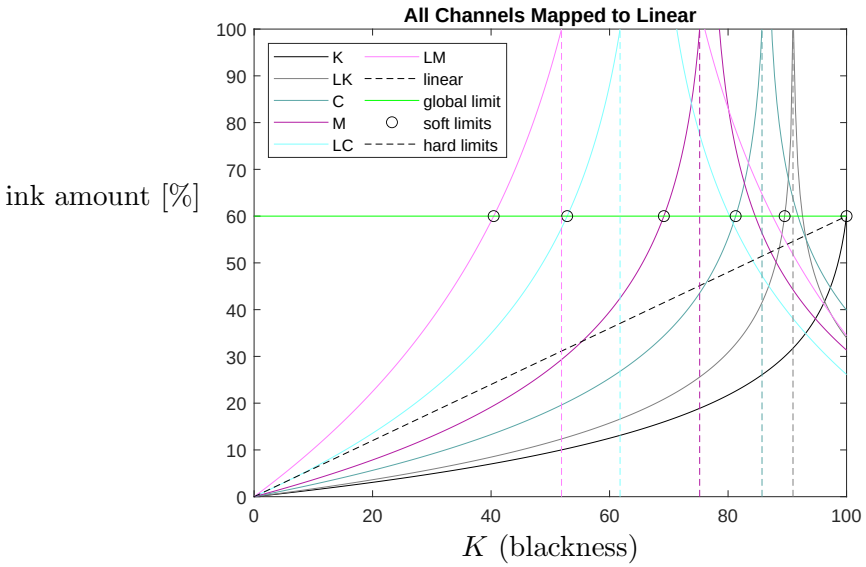


**Figure 5.4.:** Amount of ink $K_{\text{ink}}$ in % of the maximum possible (100%, $y$ axis) for all ink channels $i$ (color) as functions of the blackness $K$ ($x$ axis). The real part $\Re(K_{\text{ink}})$ is plotted. The horizontal green line indicates the current global ink limit of $\alpha = 60\%$. It sets the scale for the darkest black. The vertical dashed lines indicate the 100%-limits $K_i^{100}$ according to (5.4) for each ink channel. $\alpha$-limits are indicated by circles. All curves are for GCVT ink on Arches 88.

where $K_i^{\text{ink}}(K)$ is the amount of ink $i$ (in percent of the global ink limit) which will print the gray level $K$. The mappings for the GCVT inks on Arches 88 and printer R2880 are shown in fig. 5.4.

Different from the $K$ channel which sets the gray scale, we cannot map the lighter ink channels to large $K$, simply because the saturation luminance $L_i^\infty > L_m$ is higher than the deepest black at $K = 100$ which is printed at $L_m$. So there will not be a real solution to (5.2) for a mapping of $L_i(K_{\text{ink}})$ to $L_{\text{lin}}(K) < L_i^\infty$. The associated hard limiting value $K_i^\infty$ (infinity limit) has been indicated by a blue square in fig. 5.1. At this value the argument of the logarithm in (5.2) becomes zero, i.e.,

$$\text{Infinity-limit:} \qquad \frac{K_i^\infty}{100} = \frac{L_p - L_i^\infty}{L_p - L_m}. \tag{5.3}$$

For $K > K_i^\infty$ (5.2) has no real solution anymore and the solution becomes complex. In the graphs of the real part of the ink amount $K_{\text{ink}}(K)$ as a function of the gray level $K$ (fig. 5.4) these infinity limits show up as sharp spikes of the real part of the solution. For the $LK$ ink (100% PK in the GCVT ink set, gray curve in fig. 5.4) one can see the sharp spike at $K_{LK}^\infty$ indicating the break down of the real solution of (5.2). For the other inks one can also see the real part of the solution beyond the break down point. These solution branches for $K > K_i^\infty$ are irrelevant here.

But there is another type of limit which is encountered even before the infinity-limit (5.3) if only the channel $i$ is printing. This other limit is characterized by

the total ink amount printed being 100% of what the printer can deliver. These 100%-limits ($K_i^{100}$) are indicated by vertical dashed lines in fig. 5.4. From the condition[4]

$$L_{\text{lin}}(K_i^{100}) = L_i^{\infty} + (L_p - L_i^{\infty}) \exp(-s_i \times (100/\alpha))$$

together with (4.1) we find

$$\text{100\%-limit:} \qquad K_i^{100} = 100 \times \frac{L_p - L_i^{\infty}}{L_p - L_m} \{1 - \exp[-s_i \times (100/\alpha)]\}\,. \tag{5.4}$$

Obviously, one should also stay away from $K_i^{100}$ and should not use the ink $i$ for $K > K_i^{100}$. However, in practice this limit will not typically be exceeded, since an ink channel is usually never printing alone (expect possibly for the black channel).

The ink channels should perhaps only be used up to the $K$ value on the $x$ axis at which they print with $\alpha = 60\%$ ink amount (global ink limit, green horizontal line in fig. 5.4), because the exponential fits of type (3.4) shown in fig. 4.1 are made only for data up to the global ink limit. These soft $\alpha$-limits are obtained by the intersection points of the ink amount curves in fig. 5.4 with global ink limit $K_i^{\text{ink}} = \alpha$ or, equivalently by the condition

$$L_{\text{lin}}(K_i^{\alpha}) = L_i^{\infty} + (L_p - L_i^{\infty}) \exp(-s_i \alpha),$$

resulting in

$$\alpha\text{-limit:} \qquad K_i^{\alpha} = 100 \times \frac{L_p - L_i^{\infty}}{L_p - L_m} [1 - \exp(-s\alpha)]\,. \tag{5.5}$$

These $\alpha$-limits are indicated by circles in fig. 5.4. The abscissas $K_i^{\alpha}$ may thus be considered save upper limits on the blackness $K$ up to which the respective ink channel $i$ should be used. But also in this case, the limit will typically not be a problem.

If one wants to use the inks up the 100%-limits $K_i^{100}$, it is recommended to fit the ink curves over the full range of ink delivery (first calibration print) using $\alpha = 100\%$ such that the full range is well represented by the fit. This approach is considered later in section 9, where also deviations from the pure exponential law (3.4) are treated. The only severe limit for the present method is the infinity-limit, because in the present approach, we rely on the capability of each ink to be able to print a the demanded gray level even if printed alone. This is a significant restriction. But it pays by achieving a linear output in one go, as we shall see.

## 5.5. Linearity check

After the mapping (5.2) has been implemented for each channel and corresponding quad files have been created, one can print a step wedge for each ink channel to see

[4] Remember the $s_i$ were determined for global ink limit $\alpha$.

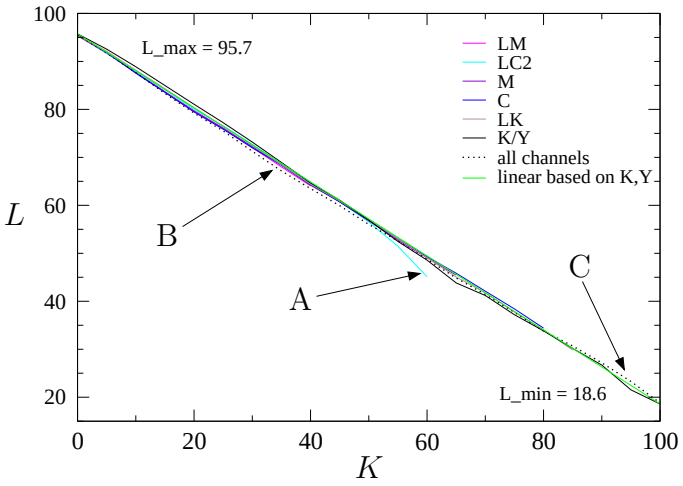


**Figure 5.5.:** Measured $L(K)$ after linearizing each channel individually. The characteristics of each channel, when printed alone, is indicated by a colored line. The dotted line shows the result when printing with all channels, based on the ink curves presented in section 6. The $LC$ channel is printed beyond its soft limit $K^{\alpha}_{LC}$ (A). Locally, all channels print slightly too dark (B) or slightly too bright (C). GCVT ink on Arches 88.

if the channel is linearized. The result is shown in fig. 5.5. The response of each channel individually is quite linear. An exception is the $LC$ channel, which was also printed for $K > K^{\alpha}_{LC}$, exceeding the soft $\alpha$-limit (region (A) in fig. 5.5). The $K$ and $Y$ channels (both containing 100% MK ink) show two slight irregularities, at $K = 65$ and $K = 95$. The reason is unknown. It is perhaps due to some uncertainty in the measurement or the printing. We have seen previously (see fig. 4.1) that the printing of the $K$ and $Y$ channels was not very consistent.

The combination of all the inks according to the ink curves discussed in section 6 is shown as a black dotted line in fig. 5.5. One can notice that in region (B) the combined inks print slightly darker than any of the participating individual ink. This could be due to some error. But it could also be due to the combined printing of inks.[5] In the latter case the effect seems to be weak. In region (C) of fig. 5.5 one may think that the combination of channels prints slightly too bright, but in this region only the $K$ channel is used. The amount of $LK$ at $K = 85$ is only $\approx 10\%$ of $K$. Yet it might have had some influence.

[5]This point is considered later again in section 9.4.

# 6. Blending the inks

## 6.1. Why does it work?

In order to achieve a smooth transition between the $K$ ranges within which each ink is printed one could select Gauß functions to partition the inks on the $K$ scale (see the next section 6.2). These functions are perfectly smooth. Later other functions will be used.

When different inks are blended these Gauß function have an overlap. In these regions only fractions of the inks must be used. The working hypothesis is as follows.

> **Hypothesis**: *If each ink, when printed alone, produces the same luminance $L$ for any given $K \in [0, K_i^\infty]$ (within its infinity-limit), then also a linear combination of fractions of different inks will produce the same luminance if the sum of the ink fractions is 1.*

If this assumption is true the linearity of all inks described in section 5.4 would add to the smoothness of the ink transitions.

However, at this stage it is not strictly proven that the superposition of different inks, which produce the same luminance if printed alone, will also produce the same luminance. In particular, the luminance of an ink is a nonlinear function of the ink amount $K_{\text{ink}}$ and it is unclear which luminance will result from a superposition of inks with different concentrations of black pigment yielding different tones and different $L_i^\infty$ and different solvents (for MK and PK). The hypothesis could be tested by printing a corresponding wedge of the same nominal gray level but different relative ink amounts. In section 9.4 this is done with a mixture of 50% each of the $M$ and $C$ inks. So far I have not found any significant interaction effect. In the following, and in section 12 and 13, arguments based on the amount of pigment and pigment coverage are provided that the above ink blending hypothesis is true.

To get a better clue, we consider the concentration of pigment in the diluted PK inks. Let the mass concentration $c_{LK}$ of the 100% PK ink be normalized to

**Table 6.1.:** Dilutions of the PK ink in different ink channels for the GCVT ink set. The mass fraction of PK ink is denoted $c_i$.

| ink | $LK$ | $C$ | $M$ | $LC$ | $LM$ |
|---|---|---|---|---|---|
| $c_i$ | 1 | 0.5 | 0.3 | 0.15 | 0.9 |

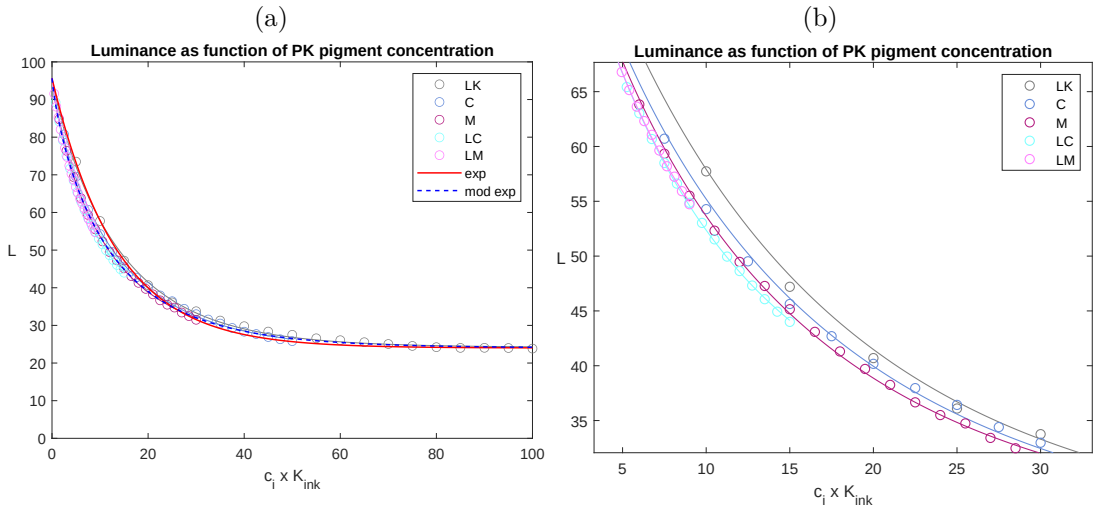


**Figure 6.1.:** (a) Luminance as function of the normalized amount of pigment $c_i K_{\text{ink}}$ for different dilutions ($c_i$) of PK ink printed on HFA Photo Rag 308. Symbols are measurements and lines are fits according to (9.1). The bold red line indicates the function $24 + (L_p - 24)\exp(-0.075K)$ and the blue dashed line represents $24 + (L_p - 24)\exp(-0.13K^{0.83})$, both with $L_p = 95.65$. The ink characteristics are based on the fit in fig. 9.1. (b) is a zoom into (a).

1. Then the pigment concentration $c_i$ of the diluted ink $i$ is the mass fraction[1] of the 100% PK ink in the gloss optimizer solvent (GLOP). For the GCVT inks these mass fractions are given in table 6.1. In section 3 we have considered the luminance as a function of the amount of ink $K_{\text{ink}}$ and derived the luminance based on the paper coverage by the pigment particles. Since the amount of pigment particles is proportional to the mass concentration of pigment in the ink, also the decay rate $s_i = \sigma c_i$ should be proportional to the mass concentration of pigment, where $\sigma \approx s_{LK}$ is a universal constant valid for each ink derived from the same PK ink. Therefore, the luminance should be $\sim \exp(\sigma c_i K_i^{\text{ink}})$, where $c_i K_i^{\text{ink}}$ is the normalized (via $c_{LK} = 1$) mass of the pigment being printed. The luminance of an ink patch as function of the normalized mass of pigment printed is shown in fig. 6.1(a). The curves do not exactly follow the pure exponential decay law (3.4) (red line), but are rather well represented by a slight modification (blue dashes, see section 9). The important observation is the curves for all inks collapse on a single curve within narrow error bounds. Therefore, the luminance printed is only a function of the amount of pigment. It does not matter which dilution (ink channel) is used.[2]

This means that the ink amount of any single ink to achieve a certain luminance (in particular on a linear curve) contains the same amount of pigment. Therefore, it does not matter whether this amount of pigment comes form one ink only, or is contributed by fractions of the specific ink amounts (to achieve the same gray level

[1] I diluted the $LK$ ink based on weight.

[2] The best global fit of all data computed with weights given by $c_i$ is $L^{\text{fit}} = 23.94 + (L_p - 23.94)\exp(-0.1248K^{0.8304})$ with $L_p = 95.65$.

alone) of different inks when these fractions sum up to 1. This proves the above hypothesis true and we follow the idea of a superposition of inks within their $\alpha$-($K \in [0, K_i^{\alpha}]$) or 100%-limits ($K \in [0, K_i^{100}]$), depending on within which range the fit of the ink characteristics was made.

From fig. 6.1(a) it is noticed that the $LK$ channel prints lighter than the other diluted inks. I have made repeated experiments and the systematic deviation from the universal curve characterized by $\sigma$ was confirmed. A possible explanation for this deviation is the concentration of pigment in the pure PK ink is so large such that pigment particles from a single droplet stack on top of each other. This effect reduces the area covered by the pigment in a single deposited PK ink droplet. Conversely, the uncovered area is increased which leads to a larger luminance. This effect is predominant at low $K_{\text{ink}}$ where a considerable area of the paper is yet uncovered by pigment, and vanishes for large $K_{\text{ink}}$, because most of the area is already covered by pigment. Luckily, the region $K_{\text{ink}} \lesssim 30$, where the deviation is significant, is typically outside of the region where the $LK$ channel is used. It may thus have little effect on the present ink blending. A careful inspection facilitated by the zoom in of fig. 6.1(b) shows that the $LK$ ink prints slightly lighter than the $C$ ink which is lighter than the $M$ ink which is lighter than the $LC$ ink. It might be possible that these very small deviations are also due to the stacking of pigment particles contained in a single droplet. The stacking can always occur, merely its probability decreases with the dilution of the ink.

The good collapse of the curves in fig. 6.1(a) may seem a bit surprising given the different values for $L^{\infty}$ of the inks. The different values for $L^{\infty}$, therefore, seem to be related to the limited range of $K_{\text{ink}} < 100$ over which the fit can be made.

Concerning printing on matte paper, the pigment in the MK ink, its coating, its concentration and its solvent are different from that of the PK ink. Therefore, the $K$ and $Y$ channels containing MK ink do not collapse on the almost universal curve in fig. 6.1(a) for the PK inks. However, by mapping the luminance of the $K$ channel to the linear curve, its characteristics is taken into account and hopefully the luminance of the $LK$ channel merges smoothly with that of the $K$ channel in the transition range of $K$. This is not trivial, however, and the prediction of the luminance of the GCVT ink on matte paper is described later in section 13.

## 6.2. Blending functions and their superposition

## 6.3. Gauß functions

For blending the inks one can use the Gauß functions

$$I_i^{(0)}(K) = X_i \exp\left[-\sigma_i (K - \hat{K}_i)^2\right], \tag{6.1}$$

where $i$ enumerates the different ink channels. The positions $\hat{K}_i$ specify the gray level at which the ink functions $I_i^{(0)}(K)$ peak. $\hat{K}_i$ and the constants $\sigma_i = 4\ln(2)/d_i^2$,

where $d_i$ is the full width at half maximum, are selected freely. But there is a restriction: Care must be taken that the ink function $I_i^{(0)}(K)$ has become sufficiently small when the infinity-limit $K_i^\infty$ for ink $i$ is approached (the 100%-limit $K_i^{100}$ is usually not a problem). The coefficients $X_i$ in (6.1) could be used to give different inks a different weight. But for the present method this is not necessary and I use the same weight $X_i = 1$ for all inks. An example for the basic ink functions (6.1) is shown in fig. 6.2(a).

We now superpose the basic ink functions (6.1) and scale them such that their sum is normalized to unity for all $K$

$$\frac{1}{N(K)} \sum_i I_i^{(0)}(K) = 1.$$

To satisfy this relation, the normalizing denominator $N(K)$ must depend on $K$ such that

$$N(K) = \sum_i I_i^{(0)}(K).$$

This way we obtain the scaled ink functions ($X_i = 1$)

$$I_i^{(1)}(K) = \frac{I_i^{(0)}(K)}{N(K)} = \frac{\exp\left[-\sigma_i (K - \hat{K}_i)^2\right]}{N(K)}, \tag{6.2}$$

which are no longer Gaussian. My current selection $\{d_i, \hat{K}_i\}$ for Arches 88 with $\alpha = 60\%$ can be found in table B.1 below. The resulting scaled ink functions are shown in fig. 6.2(b) with the sum of all ink functions indicated by the red line.

The ink arrangement in fig. 6.2(b) gives only the relative use of the individual inks. For instance for $K \to 0\%$ and $K \to 100\%$ only one ink is used, the most diluted ink $LM$ and the matte $K$ ink, respectively. When it comes to selecting the locations $\hat{K}_i$ of the peaks of the individual inks the following aspects may play a role.

1. A bright ink cannot be used for dark tones (large $K$) on matte paper, because the targeted luminance cannot be achieved by that ink due to its infinity-limit $K_i^\infty$.

2. On the other hand, dark inks should not be used in the bright regions of a print (small $K$), because only very little ink may be required such that the graininess of the dark ink may become visible in the bright regions of the print. This is the case for KO ($K$ only) printing, where this effect might even be desired.

3. The light inks should not be used for darker tones, because more ink is required to realized a dark tone by a light ink as compared to a dark ink. This

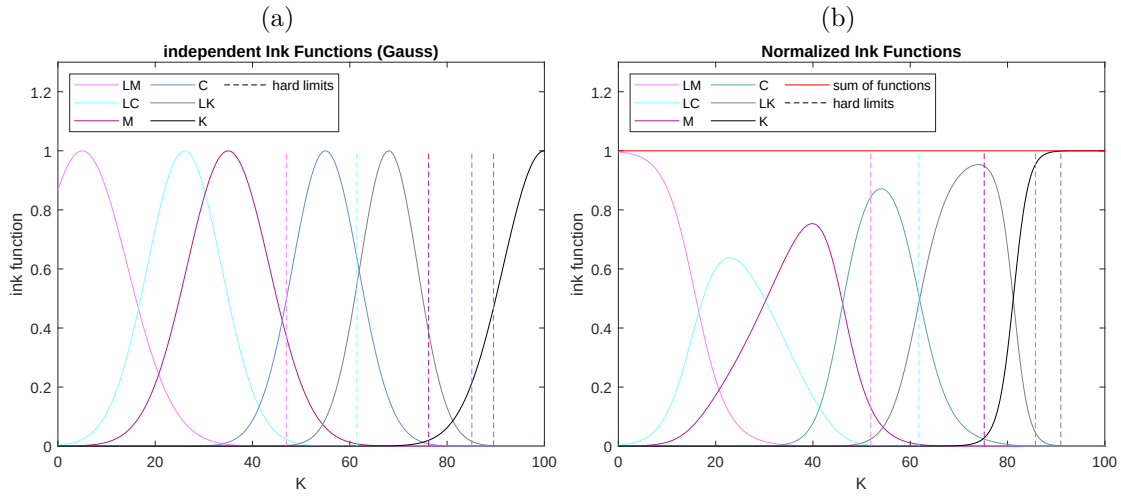


**Figure 6.2.:** (a) Example for Gauß functions $I^{(0)_i(K)}$ according to (6.1). (b) Normalized ink functions $I^{(1)_i(K)}$ (6.2) (color) and their sum (red). The vertical dashed lines indicate the 100%-limits $K_i^{100}$ (5.4), which are not so critical, though.

may result in a very wet paper and can lead to significant bending, because the ink-loaded paper in the middle of the print will expand, while the dry border of the paper does not. This may lead to head strikes.

4. The overlap of the ink functions should be sufficient, because otherwise the tonal range will not be represented smoothly enough (visible, e.g. in a bull's eye plot) despite an apparent linearity of printed 21-step wedge data.

For the above reasons the inks should be ordered according to their luminance and the peak locations $\hat{K}_i$ should not be moved too close to $K = 100$.

We have not yet applied the ink amount necessary for each ink to obtain the same gray level at the same $K$. The final ink amount $I_i(K)$ for each ink as a function of the gray level $K$ is obtained by multiplication of each relative ink function (6.2) with the respective ink amount function $K_i^{\text{ink}}(K)$ from (5.2). This leads to the final result for ink $i$

$$I_i(K) = K_i^{\text{ink}}(K)\frac{I_i^{(0)}(K)}{\sum_j I_j^{(0)}(K)} = K_i^{\text{ink}}(K)\frac{\exp[-\sigma_i(K-\hat{K}_i)^2]}{N(K)}. \tag{6.3}$$

The sum over all contributions is then $I(K) = \sum_i I_i(K)$. The individual contributions (6.3) to the final ink amount are shown in fig. 6.3 as colored lines. Using this ink distribution the printed output should theoretically be linear. The dashed lines represent the fine tuning described in the section 7. Note: for the present method, the darker tones on matte paper are printed only by the $K$ channel, because of the limitation $K < K_{LK}^{\infty}$ for the darkest gray ink ($LK$).

Of course, using a free construction of the ink distribution one can use the $LK$ channel down to $K = 100$ for matte paper, but the relatively brighter $LK$ ink would

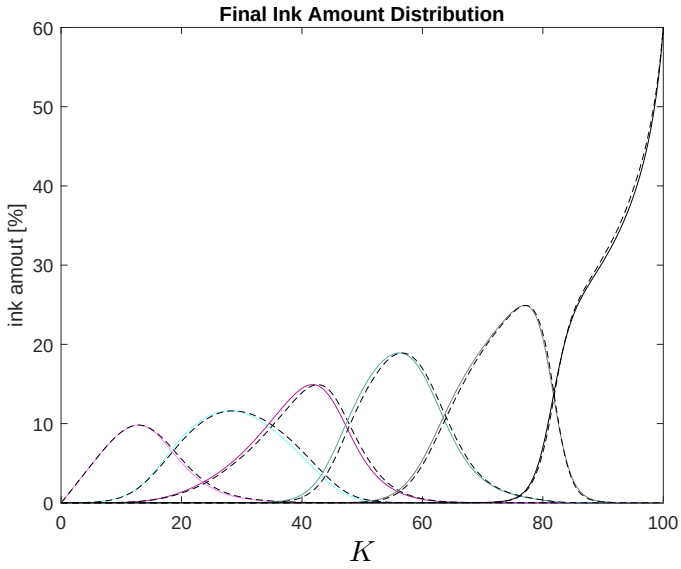


**Figure 6.3.:** Final ink amounts $I_i(K)$ according to (6.3) (colored lines) given in percent of the maximum possible (the global ink limit is 60%) shown as functions of $K$ for GCVT ink on the matte Arches 88. The dashed lines show the fine tuning of the ink distribution described in section 7.

have to be compensated by even more black ($K$) ink. This particular characteristics results from using the GCVT ink set which must use PK as well as MK inks on matte paper. For glossy paper for which only the PK inks are used, this peculiarity does not arise.

## 6.4. Cubic Hermite splines

Somewhat more flexible ink functions can be constructed by using cubic Hermite splines. These are piecewise cubic polynomials which are constructed on finite-length intervals. This is different from the Gauß functions which are defined on the full real axis. Here I use ansatz functions $I_i^{(0)}(K) = H_i(K)$ which are composed of two Hermite splines per each ink. They are defined by a set of left- ($K = l_i$) and right boundary points ($K = r_i$), a set of center points $K = C_i$ and a set of amplitudes ($A_i$). For the cubic Hermite splines the value and the slope can be prescribed at the end points of the definition interval. For the present purpose I select

$$H_i(l_i) = H_i(r_i) = 0, \quad H_i(C_i) = A_i, \tag{6.4a}$$
$$H_i'(l_i) = H_i'(r_i) = H_i'(C_i) = 0. \tag{6.4b}$$

Modifications merely may apply to the brightest and the darkest inks in the set of inks used. For instance, if one uses a freely designed ink distribution and the brightest tones are only printed by the $LM$ channel, then it is useful and desired that the spline increases linearly from $K = l_{LM} = 0$ (green curve in fig. 6.4). Other

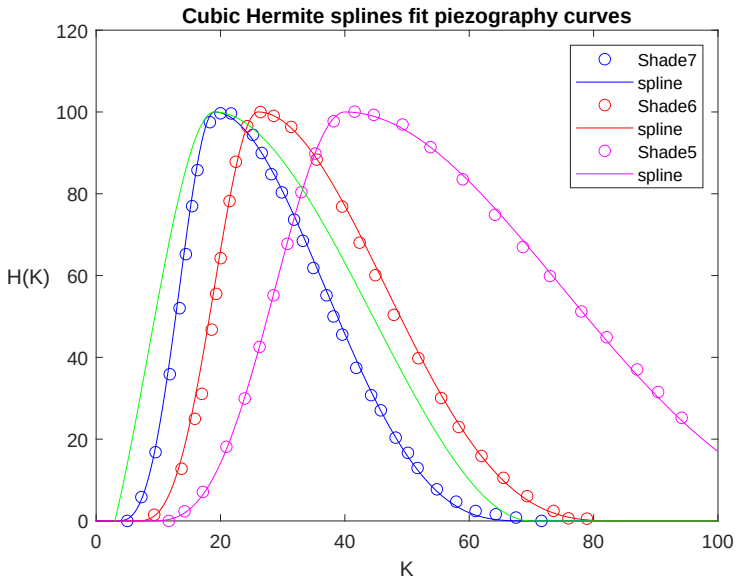


**Figure 6.4.:** Discretization of three Piezography curves (symbols) for shades 5, 6 and 7. Corresponding cubic Hermite splines raised to the power of 1.7 are shown as lines. The origin in $K$ is arbitrary. For the green curve the Hermite spine is not raised to the power of 1.7 and it has been modified to be linear when $H(K)$ intersects the axis $H = 0$. This latter property is beneficial for the brightest ($LM$) ink which is often the only ink in the highlights and should therefore print linearly for the lowest $K$ values.

than the Gauß functions the cubic Hermite splines also allow for asymmetric shapes, a feature which is praised by Piezography for their ink distribution functions. This property allows for smoother tonal transitions by long tails towards $K = 100$ of light ink ansatz functions.

Since I was wondering if the cubic Hermite splines can mimic the curves of the Piezography system, I sampled some of the Piezography curves (Vermont PhotoInkjet, 2014) and tried to match them with Hermite splines. Pure Hermite splines cannot achieve this, because the peaks of the Piezography ink curves are narrower. But raising the cubic Hermite splines to the power of 1.7 seemed to do the job. This is shown in fig. 6.4. The effect of raising the spline to the power of 1.7 can be seen by comparing the blue curve with the right part (negative slope) of the green curve.

The cubic Hermite splines can be used similarly as the Gauß functions in order to automatically arrive at a linear output. In this case the linear slope at $K = 0$ of the first Hermite spline is not necessary. But the Hermite ansatz functions can also be used for freely designed ink distributions in which the governing parameters $l_i < C_i < r_i$ and $A_i$ are freely selected. For such free design of the ink distribution it would be extremely useful to be able to monitor the expected luminance during the design stage. We shall come back to this issue in section 13.

Similar as for the Gauß functions the ink amount printed when using the Hermite

ansatz function is

$$I_i(K) = K_i^{\text{ink}}(K)\frac{H_i(K)}{N(K)}, \tag{6.5}$$

with normalizing denominator

$$N(K) = \sum_i H_i(K).$$

When using the Hermite splines $H_i(K)$ which are non-zero only in the interval $K \in [l_i, r_i]$, it makes sense to define an ink overlap parameter of neighboring Hermite splines. Typically, I use a constant overlap parameter in $K$ of $\Delta K_o := r_i - l_{i+1} = 15$ with some modification near $K = 0$ and $K = 100$. If it turns out, e.g. by printing a bull's eye, that the ink distribution is not sufficiently smooth the overlap parameter $\Delta K_o$ can be increased, which usually solves the issue.

# 7. Fine tuning

The luminance output achieved using (6.3) would be exactly linear if the following conditions hold.

1. The measurement of the calibration print is exact.
2. The ink characteristics exactly follow the exponential law (3.4).
3. The superposition hypothesis for the ink amount (section 6.1) is correct.
4. No error is involved in the amount of ink the printer lays down on the paper.

It turns out that a good linearity is usually achieved (see, e.g., the dotted line in fig. 5.5). However, due to errors and deviations violating the above conditions the final result may not be exactly linear. From the dotted line in fig. 5.5 the current maximum deviation of $L(K)$ from linearity is only about 1.5 units of Lab-$L$. Perhaps this is not something to really worry about.

Nevertheless, one can try to correct this in a final linearization step, similar as in QTR. This correction is necessary anyway in case a toner is used to neutralize the output, and it is also necessary if the ink distribution is designed freely. For the fine tuning a step wedge is printed using the ink amount functions (e.g. (6.3))

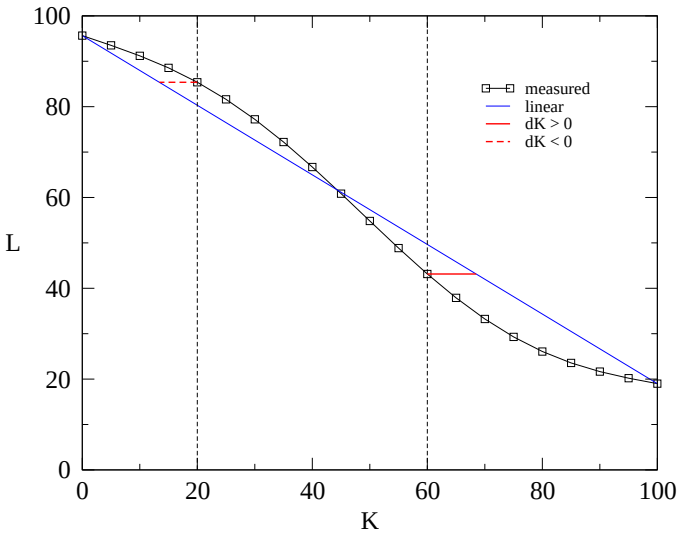


**Figure 7.1.:** Sketch of the linearization by shifting $K$ to $K' = K + \Delta K$ (red) for the measured luminance $L(K)$.

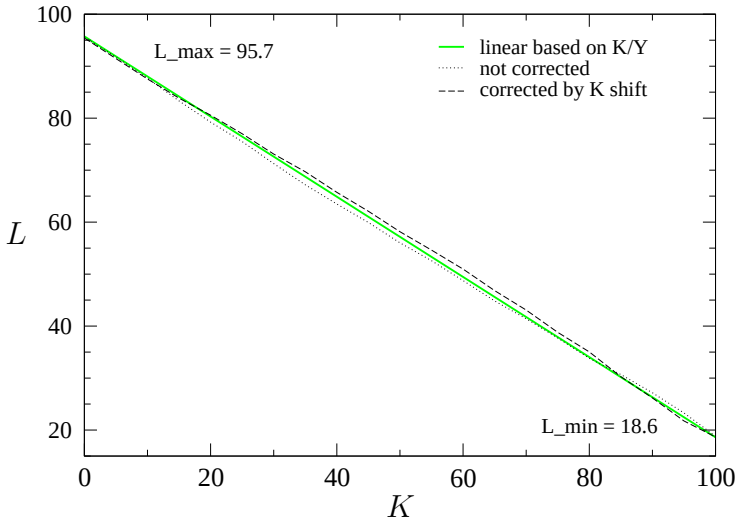


**Figure 7.2.:** Measured $L(K)$ as indicated in the legend. The uncorrected basic curve is dotted. The corrected curve is dashed. GCVT ink on Arches 88.

and the discrete 21 data points $[K, L(K)]$ are measured and stored in a file which can serve as an input file for the fine tuning.

As an example, consider the sketch in fig. 7.1 and the off-linear luminance at $K = 60$. The luminance $L(K = 60)$ should appear under a value of $K' = K + \Delta K$ which is obtained by finding the intersection point of the line $L(K = 60)$ with the targeted linear curve (4.1). The local shifts $\Delta K_i^{21}$ for the 21 values $K_i^{21} = 5i$ with $i \in [0, 20]$ are linearly interpolated to the fine grid of $2^8$ points required for the quad file. This results in 256 shift values $\Delta K_i^{256}$, $i \in [0, 255]$. The targeted ink amounts $I^{256'}$ for linear printing are then evaluated at the shifted $K$ values $K_i^{256'} = K_i^{256} + \Delta K_i^{256}$. Rather than computing $I^{256'}$ from the continuous functions (6.3) I use a linear interpolation of the available data $I_i^{256} = I_i(K_i^{256})$ on the equidistant $2^8$ grid $K_i^{256}$. The couples $[K_i^{256}, I^{256'}]$ are then written to the quad file. The resulting refined ink distribution curves are shown as dashed lines in fig. 6.3. As can be seen the correction is very small. Too make the shift function $\Delta K_i^{256}$ smoother, running averages may be useful (see e.g. section 14.1).

The measured luminance values of a step wedge using the refined ink distribution is shown in fig. 7.2. The refinement (linearization) procedure corrected the original luminance curve (dotted) to the corrected curve (dashed line). But both are very close to the ideal linear behavior (green line) such that any deviation is likely to have been caused by the measurement error, printer variability or print drying time. Probably, the original luminance curve was already as linear as is possible with the current equipment. A more substantial correction is required when using a toner (cf. fig. 8.3). It should be noted that errors made by fitting the ink characteristics to exponential functions do not influence the result of the fine tuning. Theoretically, the fine tuning should be exact, if the printer prints exactly and if the ColorMunki would be exact.

# 8. Neutralization

The pure carbon prints obtained with the quad generated in the above way has a brownish tint. In the GCVT ink set the brown tint is compensated with a blue toner which resides in the $LLK$ channel. How should the tint be neutralized within the present framework?

One idea would be to linearize the toner as well and then determine the fraction of the toner which would yield the desired result. Then the output would be linear from the outset. But this approach does not work, because the blue toner runs into saturation and cannot print at low luminance. Another idea could be that the toner is selected in proportion to the amount of black ink required for linearity from figure 5.2 (full line). I tried this for the PK inks only, since the MK ink is not as brown on matte paper as the PK ink is. But when the highlights are neutralized the darker tones turn out too blue. It seems the interaction of the blue ink with the darker tones of the carbon ink is not easy to predict mathematically.

Therefore, as shown fig. 8.1, I made a very coarse grid of control points, $K = 0, 20, 40, 60, 80, 100$,[1] and set corresponding toner ink amounts which should compensate the brown tint. The control points are shown by circles. The toner ink at the control points is then interpolated by cubic splines (blue line in fig. 8.1) to obtain the toner ink amount on the fine grid of 256 points required for the quad.[2] The quad file obtained is then used to print the step wedge. Based on the measured Lab-$b$ values of the step wedge the control points are adapted to finally arrive at a neutrally printing step wedge. This may require a few iterations. This iteration is probably similar to what is required when using QTR, where the toner ink function must be entered by decimal numbers. The amount of blue ink at the control points suitable for Arches 88 are given in table 8.1.

Since the toning adds some extra ink, the neutral step wedge prints slightly too dark. Therefore, a linearization is required after toning. For the present method the shift of the ink curves, using the fine tuning described in section 7 is shown in fig. 8.2. The shift of the ink curves mainly to larger $K$ brightens the print. As can be seen the shift is significant.

Finally, the result of measuring the step wedge is shown in fig. 8.3. In the figure the luminance of the pure carbon ink (black dashed line in fig. 8.3, see the dotted line in fig. 5.5) is almost linear. But the brownish tint shows in the positive Lab-$b$ value (dashed blue line on the $a, b$ scale) with a maximum of about $b \approx 7$. When

[1] I later refined it to steps with $\Delta K = 10$.

[2] As a general rule, care must be taken not to produce negative values for the ink amount when writing the quad file.

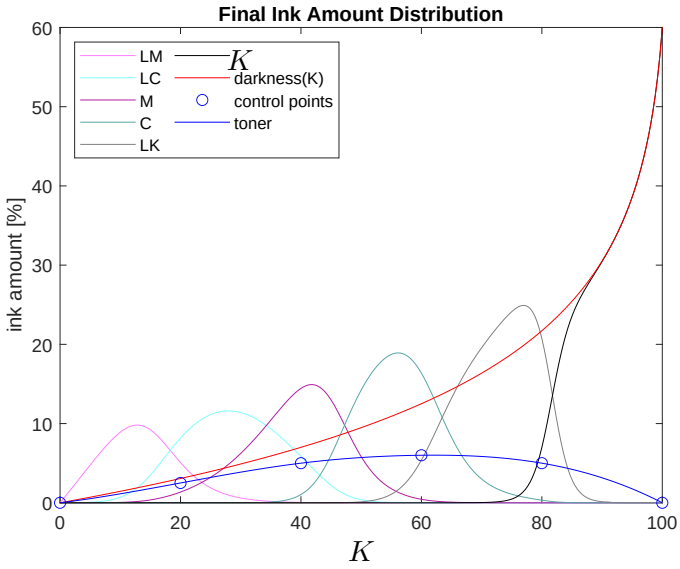


**Figure 8.1.:** Ink amount (in percent of the maximum possible, $\alpha = 60\%$) including the toner ink $LLK$ (blue line). The equivalent ($K$) ink amount curve (red, same as in fig. 5.2) does not include the toner ink. GCVT ink on Arches 88.

**Table 8.1.:** Amount of blue toner ($LLK$ channel) at the control points to make Arches 88 appear neutral as in fig. 8.1. The ink limit is $\alpha = 60\%$. The resulting distribution of Lab-$b$ is shown in fig. 8.3 (full blue line).

| control point $K$ | 0 | 20 | 40 | 60 | 80 | 100 |
|---|---|---|---|---|---|---|
| ink amount [%] | 0 | 2.5 | 5.0 | 6.0 | 5.0 | 0 |

this is compensated by the blue toner, the luminance is reduced (orange line on the $L$ scale). This must be compensated by the fine tuning, shifting the ink curves including the toner curve. The final luminance curve (full black line) is almost linear. The brownish tint has been eliminated such that now $b \lesssim 2$ (full blue line).

I think the result is well acceptable. The minimum luminance at $K = 100$ is about $L(K = 100) \approx 18$. Possibly the luminance can be further reduced to $L \approx 17.5$ (see section 5.3). But this may hardly be visible.

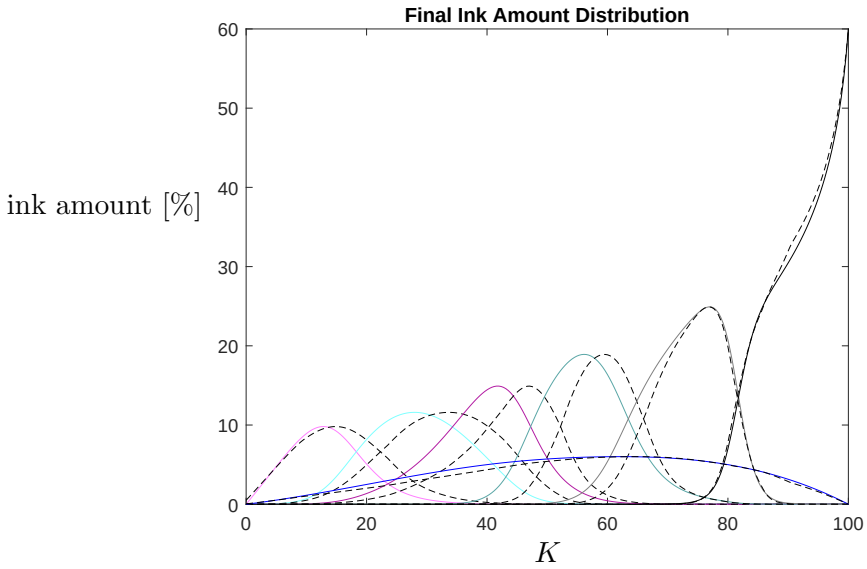


**Figure 8.2.:** Necessary shift of the ink curves to linearize the luminance $L(K)$ which prints too dark due to the toner ink. Before the shift: color, after the shift: dashed lines. GCVT ink on Arches 88.

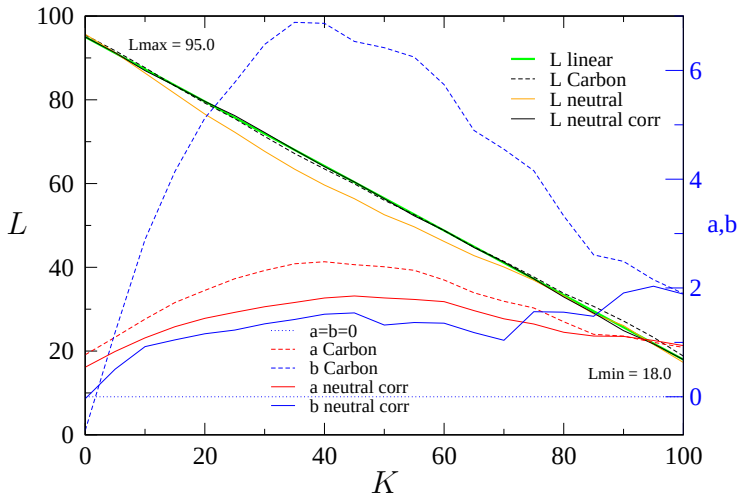


**Figure 8.3.:** Linearizing the $L(K)$ response: $L$ of the neutral ink before (full orange) and after linearization (full black). The Lab-$b$ before neutralization (dashed blue) is significantly reduced after neutralization and linearization (full blue). GCVT ink on Arches 88.

# 9. Beyond exponential fitting

## 9.1. Modified exponential fit

Depending on the ink and paper combination, the exponential fit according to (3.4) may not always represent the measured luminance with sufficient accuracy. A better approximation may be obtained by some generalization of the exponential fit function. Not only the fit of the ink characteristics can be improved, also the whole linearization process can be carried out with such modifications. Merely, the fit functions become somewhat more complicated.

Perhaps the easiest way to improve the fit is to introduce a phenomenological exponent $n$ and to fit the data to the modified exponential law

$$L(K_{\text{ink}}) = L^{\infty} + (L_p - L^{\infty})\mathrm{e}^{-sK_{\text{ink}}^{n}}. \tag{9.1}$$

This law may be related to the Yule–Nielsen equation for the reflectance (Arney and Yamaguchi, 1999) in which another empirical $n$ factor is introduced which depends on the paper and ink combination through the sharpness of the halftone dot edges and through the scattering of light within the ink itself. Apparently, the exponent $n$ deviates more from $n = 1$ when printing on Photo Rag 308 than when printing on Arches 88 which was considered in section 4 above. For Arches 88 the pure exponential fit (3.4) worked quite nicely ($n = 1$). I speculate that the main reason for the deviations from (3.4) when using Photo Rag 308 is caused by its more structured paper surface, whereas the surface of Arches 88 is much smoother.

To avoid fitting the data by trial and error, I made a little code to perform the modified fitting for all channels automatically. The paper white is obtained beforehand as the mean value of the measured luminance values at $K = 0$ of all ink channels $i$. For PR308 I got $L_p = (1/8)\sum_{i=1}^{8} L_i(K = 0) = 95.51$. The remaining unknowns $L_i^{\infty}$, $s_i$ and $n_i$ were then obtained by the least-squares method. The result of the least-squares fit for all channels is shown in fig. 9.1 for ink limit $\alpha = 100\%$. As can be seen, the fit works nicely. For the $M$ and $C$ channels the modified fit (9.1) is significantly better than the exponential fit (3.4). For the lightest inks the exponential fit is sufficient. The fit parameters are collected in table 9.1. The decay rates $s_i(\alpha = 100\%)$ are the values obtained directly from the fit over the full range of the ink amount $K_{\text{ink}} \in [0, 100]$. The decay rates $s_i(\alpha = 60\%)$ are the decay rates which need to be used when an ink limit is applied (the typical case), here 60%. The transformation between the two decay rates is described in section 9.2.

As can be seen from table 9.1 and from fig. 9.2,[1] the luminance functions $L_K$

[1] The data correspond to $L_p = 95.65$. When the data in the table and in the figure were computed,

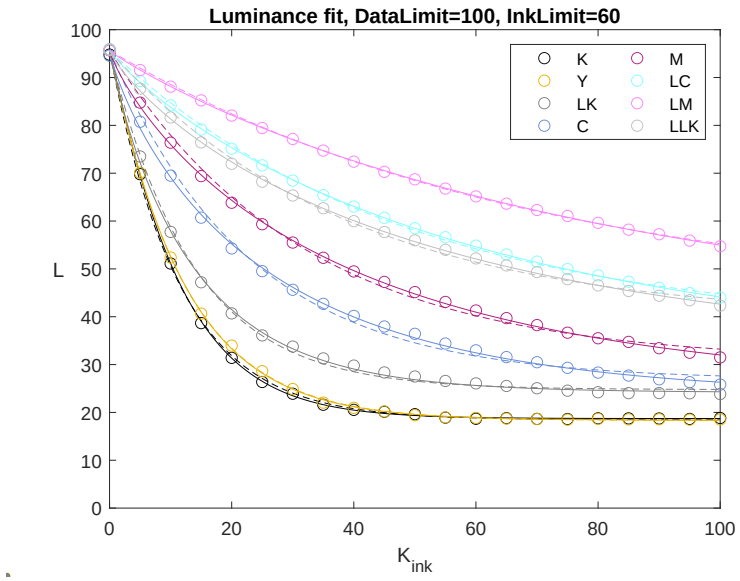


**Figure 9.1.:** Calibration of the GCVT ink on Hahnemühle Photo Rag 308 for a global ink limit $\alpha = 100\%$. Measured data for the ink channels (color coded) are shown by circles. Full lines are modified exponential fits according to (9.1) by least-squares. For comparison the pure exponential fits according to (3.4) are shown by dashed lines.

**Table 9.1.:** Fit parameters for the GCVT ink on Hahnemühle Photo Rag 308 obtained by least-squares curve fitting for $\alpha = 100\%$ and $L_p = 95.65$. The last column gives the decay rates according to (9.3) which must be used when utilizing the result in the presence of an ink limit of $\alpha = 60\%$.

| Channel | $L_i^\infty$ | $n_i$ | $s_i(\alpha = 100\%)$ | $s_i(\alpha = 60\%)$ |
|---|---|---|---|---|
| $K$ | 18.7142 | 1.0634 | 0.074695 | 0.043388 |
| $Y$ | 18.3813 | 1.0138 | 0.078907 | 0.047012 |
| $LK$ | 24.1714 | 0.91782 | 0.090697 | 0.056751 |
| $C$ | 23.3160 | 0.84346 | 0.065457 | 0.042543 |
| $M$ | 24.6009 | 0.84380 | 0.046408 | 0.030157 |
| $LC$ | 30.7429 | 0.89238 | 0.025910 | 0.016424 |
| $LM$ | 36.1862 | 0.93044 | 0.015881 | 0.009875 |
| $LLK$ | 31.1981 | 0.83798 | 0.036471 | 0.023771 |

($L_Y$) with $n = 1.0634 \approx 1$ (1.0138) are very well represented by the exponential fit (3.4) which corresponds to $n = 1$. With $n = 0.84$ the luminance functions $L_C(K_{\text{ink}})$ and $L_M(K_{\text{ink}})$ exhibit the largest deviations from a pure exponential decay.

Before carrying out the fit, care must be taken that the ink flow from the cartridges is not hindered. Figure 9.2 shows such an example. The first measurement (circles and squares) were made despite of 4 nozzles being blocked in the magenta

the value of the paper white was determined independently in advance. But this value does not deviate much from the mean value 95.51 obtained from the measurements.

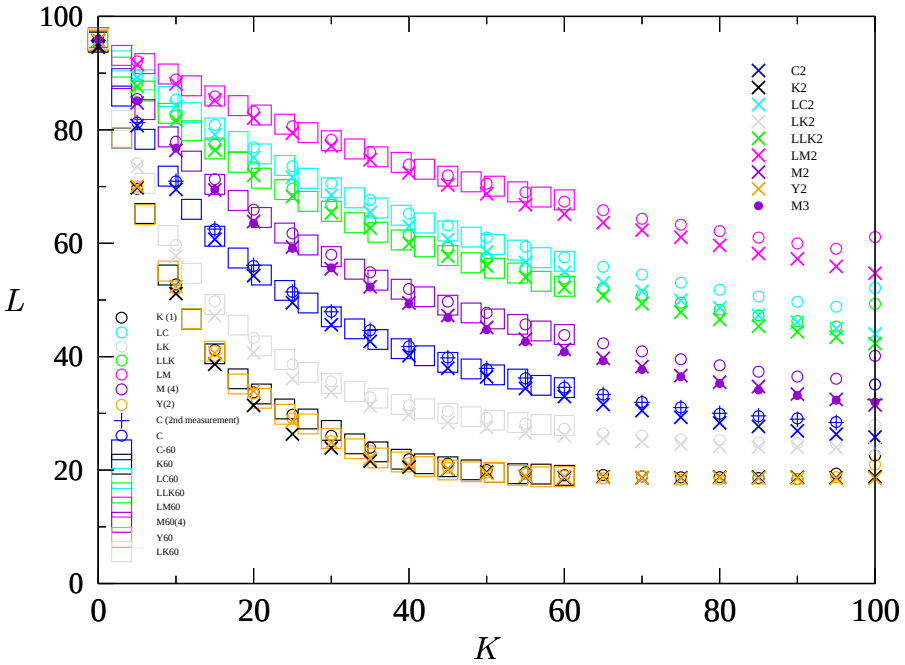


**Figure 9.2.:** Calibration of the GCVT ink on Hahnemühle Photo Rag 308 for global ink limit $\alpha = 100\%$ (circles and crosses). Also shown are data for an ink limit $\alpha = 60\%$ (squares). The data were obtained before (circles and squares) and after 2 head cleanings (crosses). The numbers in parentheses in the legend denote the number of clogged nozzles. $M3$ denotes a 3rd measurement (reproducibility). The luminance for ink limit $\alpha = 100\%$ (circles, clogged nozzles) at $K_{\text{ink}} = 100\%$ was too high, because the data suffered from the well-known banding phenomenon (a problem for small format Epson printers) close to the edge of the paper.

channel. The crosses are measurements after two head cleanings. One can see the improved ink flow by the luminance being shifted to lower values. In any case, the reproducibility of the ColorMunki measurements was confirmed by a repeated measurement on the other day: compare the blue pluses and circles, and the violet crosses and dots.

Clearly, a fit based on $\alpha = 100\%$ gives a much better value for $L^\infty$ and for the global dependence of the ink curves on $K_{\text{ink}}$ than when a ink limit $\alpha < 100\%$ is applied. For that reason, at the moment, I tend to base the generation of the quad file on the fit of the data for $\alpha = 100\%$. If necessary the decay rates can be transformed according to (9.3) to any other ink limit.

## 9.2. Full-scale fit and ink limit $\alpha < 100\%$

The data for the $K$ channel at $\alpha = 100\%$ suggest to use the black point of $\alpha = 60\%$ with $L_K(\alpha) = 19.1$. At this point $L_K(\alpha) = L_K^\infty + 0.5$. Note that $L_K^\infty = 18.62$ (or $L_Y^\infty = 18.38$, table 9.1) is the deepest black possible with this ink set on Photo Rag 308 (plus/minus the error range of the ColorMunki and the uncertainty in the

ink delivery). How are the fit parameters obtained for $\alpha = 100\%$ on an ink scale $K_{\text{ink}} \in [0, 100]$ related to those for $\alpha < 100\%$, e.g. for $\alpha = 60\%$? Using an ink limit $\alpha$ corresponds to the linear coordinate transform

$$K_{\text{ink}}^{\alpha} = \frac{100}{\alpha} K_{\text{ink}}^{100}, \tag{9.2}$$

for the ink amounts in the calibration print, where $K_{\text{ink}}^{\alpha}$ is the ink amount variable we use in units of $\alpha$ and $K_{\text{ink}}^{100}$ is the ink amount in units of the maximum possible. Thus, when $K_{\text{ink}}^{100} = \alpha$ (ink limit) we obtain $K_{\text{ink}}^{\alpha} = 100$. Now we insert this transformation into (9.1), where $s_{100} = s(\alpha = 100\%)$ (also shown in table 9.1) is the decay constant for a 100% ink limit for which the fit was made. We obtain

$$\begin{aligned} L(K_{\text{ink}}) &= L^{\infty} + (L_p - L^{\infty})\mathrm{e}^{-s_{100}(K_{\text{ink}}^{100})^n} \stackrel{!}{=} L^{\infty} + (L_p - L^{\infty})\mathrm{e}^{-s_{100}(\alpha K_{\text{ink}}^{\alpha}/100)^n} \\ &= L^{\infty} + (L_p - L^{\infty})\mathrm{e}^{-s_{100}(\alpha/100)^n (K_{\text{ink}}^{\alpha})^n} = L^{\infty} + (L_p - L^{\infty})\mathrm{e}^{-s_{\alpha}(K_{\text{ink}}^{\alpha})^n} \end{aligned}$$

from which we identify the decay rate in the presence of an ink limit $\alpha < 100\%$

$$s_{\alpha} = \left(\frac{\alpha}{100}\right)^n s_{100}. \tag{9.3}$$

For $\alpha = 100\%$, simply $s_{\alpha} = s_{100}$. For a pure exponential fit with $n = 1$ we both decay rates are linearly related by the simple scale factor $\alpha/100$. Equation (9.3) is the decay rate which must be used in (9.1) when an ink limit is applied (typical case), but the fitting is done on the full scale with ink limit 100%. Of course the transformation (9.3) must not be applied if the ink luminance is directly fitted to the ink data on the scale restricted to $\alpha$ (second calibration print), which is the procedure suggested in Moore (2005).

## 9.3. Modification of the transformation formulae

With the modified exponential fit (9.1), the transformation formulae must be slightly modified as well. In particular, when solving for the ink amount required for linearity (5.2), the replacement of $K_{\text{ink}}$ by $K_{\text{ink}}^n$ in (9.1) now demands to take the $1/n$-th power of the right-hand side of (9.1). Therefore, the ink mapping (5.2) changes to

$$K_i^{\text{ink}} = \left[-\frac{1}{s_i} \ln\left(1 - \frac{L_p - L_m}{L_p - L_i^{\infty}} \frac{K}{100}\right)\right]^{1/n}. \tag{9.4}$$

Furthermore, the $\alpha$-limit (5.5) on $K$ (when $K_i^{\text{ink}} = \alpha$) up to which a gray ink should be used will change to

$$K_i^{\alpha} = 100 \times \frac{L_p - L_i^{\infty}}{L_p - L_m} \left[1 - \exp(-s\alpha^n)\right]. \tag{9.5}$$

The ink distribution functions, the fine-tuning process and the toning are not affected.

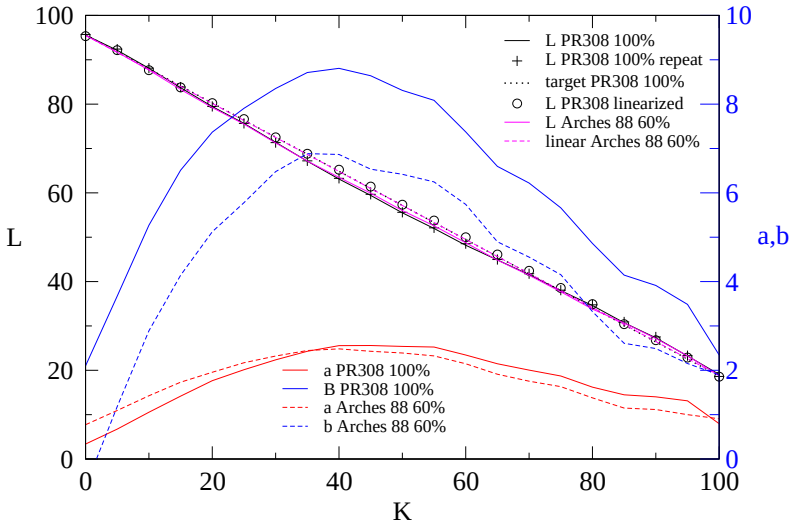


**Figure 9.3.:** Lab values measured from a printed step wedge using the quad file created for PR308 based on the modified fit (9.1) over the full range up to 100% ink (black line). The measurement was repeated the other day (pluses). The targeted linearity ($L_p = 95.65$, $L_m = 18.7$) is indicated by a black dotted line. The correction of the quad file by linearization is shown as circles. For comparison the uncorrected result for Arches 88 using the pure exponential fit (3.4) based on the 60% ink limit print (2nd calibration print) is shown as a magenta line.

## 9.4. Quality of the quad files: Linearity check

The Lab values measured from a print of a step wedge using the quad file for HFA PR 308 based on the modified exponential fit (9.1), where the decay rates $s_i$ have been obtained over the full ink range up to 100%, and on the automatic linearization (6.3) using Gauß functions is shown as a black line in fig. 9.3. The quad prints slightly too dark in the mid range and slightly too bright for $K > 85$. I found no obvious reason for this deviation, because in the mid range $K \approx 40...60$, where the deposited ink comes mainly from the $M$ and $C$ channels, one cannot identify a significant deviation of the calibration ink data from the fit (full lines in fig. 9.1). It is interesting to note that the quad for Arches 88 (exponential fitting (3.4) over the range up to the ink limit $\alpha = 60\%$) shows almost the same small deviation from linearity (magenta line, see also fig. 7.2). Anyway, the linearization according to section 7 makes the output (black circles) linear with good accuracy (black dotted line). The ink distribution functions used can be found in Appendix B.1. The targeted black point was $L_m = 18.7$.

To check if the deviation from linearity in fig. 9.3 is due to a combination of two inks, which both print linear, I made the test shown in fig. 9.4. Both individual inks, $M$ and $C$, print linearly as per construction over the full range of ink delivery, up to their 100%-limits $K_M^{100} = 82.7$ and $K_C^{100} = 90.1$, respectively. The combination of both inks with an amount of 50% each yields the same linear luminance. This shows that there is no effect of combining inks with different shades of gray if both

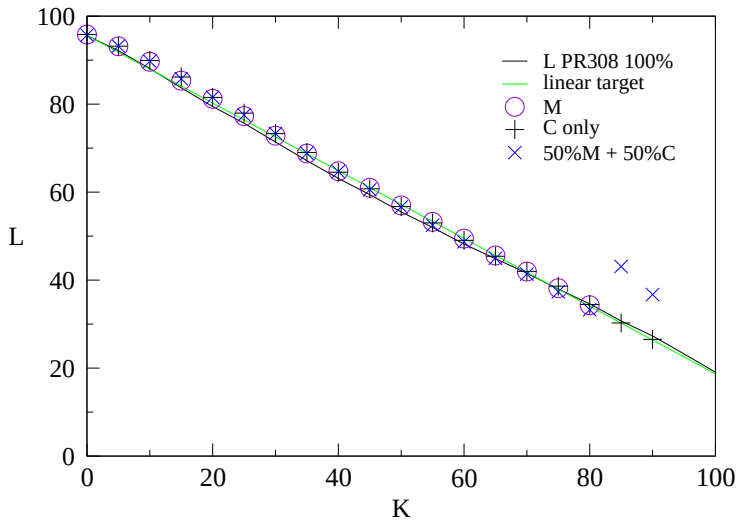


**Figure 9.4.:** Deviations from linearity. Shown are the Lab-$L$ responses of the pure carbon quad from fig. 9.3 using all inks (black line), the output of the $C$ channel alone (pluses), the output of the $M$ channel alone (circles) and the 50% combination of the $M$ and the $C$ channels ($\times$). The targeted linear response is indicated by the green line. GCVT ink on PR308.

individual ink responses are linear. The data for the $C+M$ combination at $K = 85$ and 90 are due to the $M$ channel being absent (100%-limit $K_M^{100}$ exceeded), thus only for 50% $C$. In fact, we see that the luminance of the individual inks as well as their combination (symbols) print slightly too bright for $K \in [5, 20]$. I conclude that the small deviations from linearity in fig. 9.3 and in fig. 9.4 are mainly due to the variation of the printer output and, to a minor extent, to the error in the ColorMunki measurements.

Finally, we see that the carbon ink appears slightly warmer on PR308 than on Arches 88. The Lab-$b$ values are shifted to higher values by about $\Delta b \approx 2$ compared to Arches 88. The reason is the warmer paper base of PR308 compared to Arches 88.

## 9.5. Comparison of the ink characteristics of Arches 88 and Photo Rag 308

Figure 9.5 shows a comparison between the ink characteristics of Arches 88 (circles, measured on the 60% scale) and Photo Rag 308 (crosses, measured on the 100% scale but shown only on the 60% scale). Regarding the luminance both papers are very similar.[2] But it seems the matte black $(K, Y)$ prints slightly darker on PR308 for small $K$. But in this range $K$ is typically not used, except for KO printing.

[2] Arches 88 subjectively appears brighter, only because the paper is slightly more blue (Lab-$b$ of the paper color is less, see fig. 9.3).

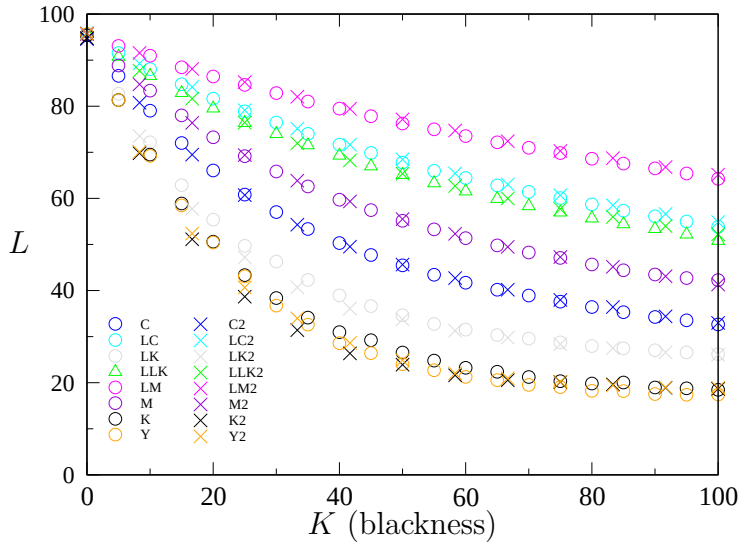


**Figure 9.5.:** Comparison of the measured ink data for Arches 88 (circles) and Photo Rag 308 (×, 100%) both obtained for $\alpha = 60\%$.

For Arches 88 (symbols), one can notice a little bump in the $L_K$ data near $K \approx 45$. The $L_Y$ data seem smoother. The reason is unknown.[3] Also the deviation between the $K$ and the $Y$ channel indicates the sensitivity of the data with respect to the ink flow in different channels. Some further calibration plots for Hahnemühle's Photo Rag 308 are provided in Appendix B.1.

[3] In the forum under https://groups.io/g/QuadToneRIP/topic/qtr_51_step_linearisation/38411565 Tyler Boley mentioned that ... *smaller printers are all variable dot and I think that may be a large factor in their more bumpy linearity per ink.* On the other hand, I also found on https://groups.io/g/QuadToneRIP that only the smallest drop size is used by the printer if the highest resolution 2880dpi is selected.

# 10. Gamma correction

The quad files produced by QTR after linearization, as well as the quads produced using the present technique, print with a linear luminance as a function of $K$. The prints appear relatively bright with *opened-up* shadows. This look of the prints is different from the impression of the image on the screen, on which the darker tones are closer together. The Epson printer driver is probably designed as to (hopefully) better match the printed image to the visual impression of the image on screen. Obviously, this requires a luminance output which deviates from linear. Paul Roark has accomplished this by further darkening the darker grays in Photoshop by use of a corresponding Photoshop curve. Here, I want to try to burn the correction into the quad file itself by directly targeting a nonlinear $L(K)$ curve.

## 10.1. Defining the gamma correction

I do not know of any generally reference luminance curve $L_{\text{ref}}(K)$ which should be targeted in order to produce a print which most closely resembles the image as seen on screen. It appears that all printer manufactures have their own firmware tweak of the linear luminance which is probably the best reference function and which is targeted by QTR.. Therefore, I have measured the luminance of a 21 step wedge printed on PR308 with the R2880 using the ABW mode (neutral, darker, highest quality) and OEM vivid magenta K3 inks.[1] The measured luminance, shown as circles in fig. 10.1, deviates from linearity (black dashed line).

The mappings (5.2) or (9.1) intend to map the luminance of all the inks to the same linear curve. But one can map all the inks also to any other luminance curve, as along as the target luminance is a bijective function of $K$. Since the luminance of the print produced by Epson's ABW driver is (and must be) bijective, it is possible to map the luminance curves of all the inks to the luminance curve which the Epson driver produces. Let us call this the *G-curve* (gamma), even though it is not strictly a $\gamma = 2.2$ correction of the QTR curve (see fig. 10.1).[2] The correction of the linear response that the Epson driver provides is more like a general *tone mapping* which is intended to make the print look like the image on screen.

[1] This seems to be the standard setting among the different luminance settings the ABW mode of the Epson driver offers.

[2] It seems that all nonlinear tone curves are called *gamma-corrected* curves, even though no specific exponent $\gamma$ can be given. The $\gamma = 2.2$ correction is only used for converting the electrical signal sent to a display to make the display look right. It is also used in ICC transforms. But the value $\gamma = 2.2$ has nothing to do with the luminance curve of a printed image.

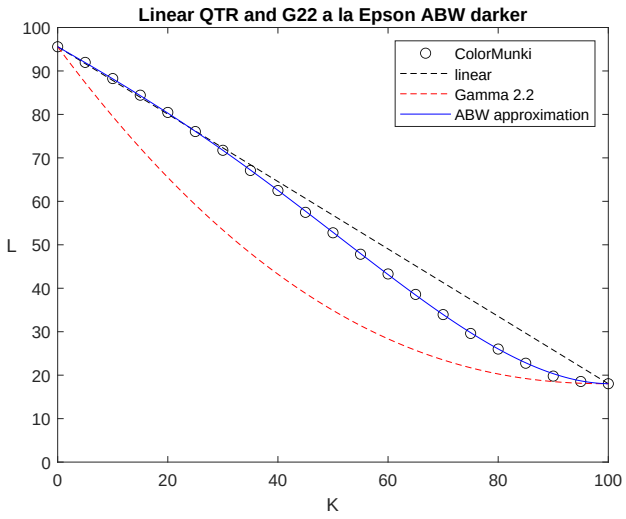


**Figure 10.1.:** Measured luminance (circles) of a 21 step wedge printed on PR308 using the ABW mode (neutral, darker). The full blue curve is a smooth approximation of the data ($L_\mathrm{G}$ curve). The black dashed line indicates a linear luminance and the red dashed line is an unrealistic strict $\gamma = 2.2$ mapping of the linear QTR curve. GCVT ink on PR308.

To determine the ink amount $K_\mathrm{ink}$ of the ink $i$ which is necessary to achieve the luminance $L_\mathrm{G}(K)$ (target G-curve) we must require

$$L_i(K_i^\mathrm{ink}) \stackrel{!}{=} L_\mathrm{G}(K).$$

Solving for $K_i^\mathrm{ink}$ and using the modified exponential law (9.1) we get

$$K_i^\mathrm{ink} = \left[ -\frac{1}{s_i} \ln \left( \frac{L_\mathrm{G}(K) - L_i^\infty}{L_p - L_i^\infty} \right) \right]^{1/n}. \tag{10.1}$$

In order to handle $L_\mathrm{G}(K)$ in this equation, we need a smooth continuous function of $K$. To that end the deviation $\Delta L_\mathrm{G}(K) = L_\mathrm{G}(K) - L_\mathrm{lin}(K)$ of the measured G-curve from the linear curve is evaluated for the 21 points of the step wedge. For Photo Rag 308 the result is shown as circles in fig. 10.2. In the next step the $\Delta L_\mathrm{G}(K)$ data are fitted by a fourth-order polynomial (red dashed line) yielding

$$f(K) = a_4 K^4 + a_3 K^3 + a_2 K^2 + a_1 K + a_0,$$

with coefficients given in table 10.1. Since the fit does not exactly vanish at $K = 0$

Usually, a gamma correction $L \to L'$ would read

$$L'(K) = L_p \left( \frac{L(K)}{L_p} \right)^\gamma.$$

Applied to the linear luminance we have this would correspond to

$$L'(K) = L_m + (L_p - L_m) \left( 1 - \frac{K}{100} \right)^\gamma.$$

The luminance function $L'$ for $\gamma = 2.2$ is shown in fig. 10.1 as a red dashed line. But this is not how the Epson driver prints.

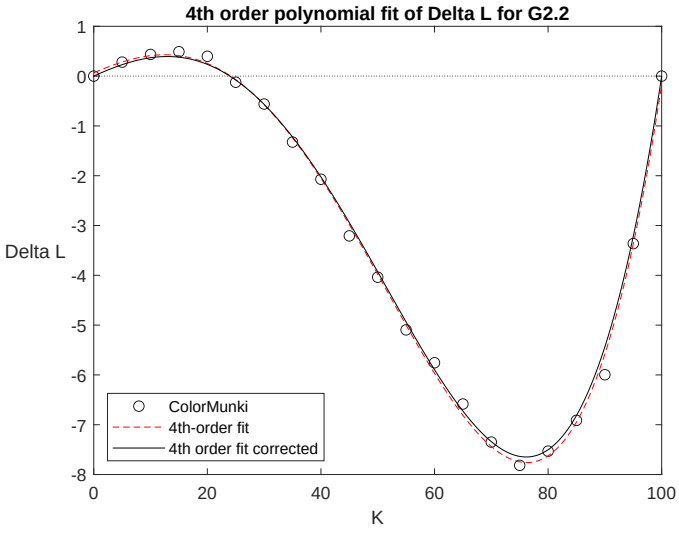


**Figure 10.2.:** Luminance deviation $\Delta L_{\mathrm{G}}(K)$ of the Epson driver output in ABW mode (neutral, darker) from a linear behavior on PR308. Shown are measured data (circles), a 4th-order polynomial fit $f(K)$ (red dashes) and a modified polynomial fit of $\Delta L_{\mathrm{G}}(K)$ to such as to satisfy the boundary conditions $\Delta L_{\mathrm{G}}(K = 0) = \Delta L_{\mathrm{G}}(K = 100) = 0$ (full black curve).

**Table 10.1.:** Polynomial fit coefficients in $L_{\mathrm{G}}(K)$ (10.2) to approximate the luminance data obtained with the ABW mode of the Epson driver.

| $a_0$ | $a_1$ | $a_2$ | $a_3$ | $a_4$ |
|---|---|---|---|---|
| $6.4917 \times 10^{-2}$ | $4.939 \times 10^{-2}$ | $-8.1265 \times 10^{-4}$ | $-7.47 \times 10^{-5}$ | $7.7656 \times 10^{-7}$ |

and $K = 100$ (a property certainly good to have), I have subtracted a very weak linear ramp to obtain

$$\Delta L_{\mathrm{G}}(K) := f(K) - \left[ f(0) + \frac{f(100) - f(0)}{100} K \right]. \tag{10.2}$$

As can be seen from fig. 10.2 $\Delta L_{\mathrm{G}}(K)$ is quite nicely represented. The same is true for the full luminance curve

$$L_{\mathrm{G}}(K) = L_{\mathrm{lin}}(K) + \Delta L_{\mathrm{G}}(K) \tag{10.3}$$

in fig. 10.1 (blue curve).

Since the paper white $L_p$ and the black point $L_m$ are very similar for Arches 88 and PR308, the same tone mapping (10.2) can be used. It still has to be tested if the same data can even be used for glossy papers. Therefore, at the time being, equation (10.2) together with the coefficients from table 10.1 is implemented and used to generate the $2^8$ data points for each channel required for the quad.

One problem when targeting the gamma-corrected quad is, that the target luminance $L_{\mathrm{G}}(K)$ (10.3) is not directly invertible to access $K(L_{\mathrm{G}})$, whereas this is the case for $L_{\mathrm{lin}}(K)$. The inversion is required for determining the $\alpha$- and 100%-limits on $K_i$. Using the notation $L_{\mathrm{target}} \in [L_{\mathrm{lin}},\ L_{\mathrm{G}}]$ the soft ($K_i^{\alpha}$) and hard limits ($K_i^{100}$) can generally be phrased as

$$L_{\mathrm{target}}(K_i^{\alpha}) = L_i^{\infty} + (L_p - L_i^{\infty}) \exp(-s_i \alpha^n), \tag{10.4a}$$
$$L_{\mathrm{target}}(K_i^{100}) = L_i^{\infty} + (L_p - L_i^{\infty}) \exp\left[-s_i \times (100/\alpha)^n\right], \tag{10.4b}$$

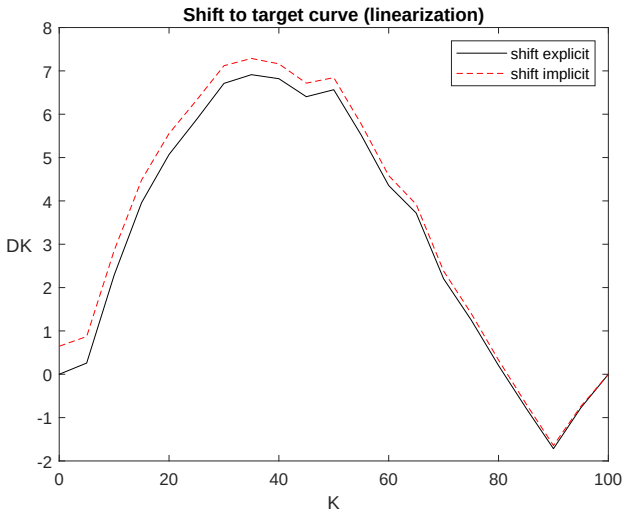


**Figure 10.3.:** Shift $\Delta K(K)$ to linearize the luminance curve for PR308 in the presence of a toner (see also table B.4 and fig. B.5). Shown are the results for two methods of determining the shift (see text). The deviation is due to the difference in the targeted linear curve (different values for $L_p$).

where one has to solve for $K_i^\alpha$ and $K_i^{100}$. To treat both cases with the same code, both limits are obtained by finding the abscissa $K$ of the intersection point of the luminance function $L_{\text{target}}(K)$ with the constant right hand sides of (10.4). This functionality can easily be implemented in the code.

## 10.2. Refinement of the gamma correction equivalent to linearization

The same functionality must also be used for the refinement process, e.g. for the linearization process or, more generally, for the fine-tuning of a luminance curve which deviates from the target curve. To that end the measured deviating luminance curve must be mapped to the target curve by shifting the $K$ values. In case of a linear target (classical linearization) ($L_{\text{target}} = L_{\text{lin}}$) the shift $\Delta K(K)$ from the equidistant values of $K$ (from the measurement) to the target values of $K$ can be explicitly determined, because $L_{\text{lin}}$ is invertible. The full black line in fig. 10.3 represents the shift $\Delta K(K)$ (based on the measured (nonlinear) luminance data, see also table B.4 and fig. B.5) which is necessary to linearize the luminance on PR308 after the output has been made neutral by use of the blue toner channel ($LLK$). Alternatively, one can (and must in case $L_{\text{G}}$ is targeted) use the implicit method based on the above mentioned method of finding the intersection point. The corresponding result for $\Delta K(K)$ is shown as a dashed red line in fig. 10.3. The small deviation between both shift data results from using the theoretical target with $L_p = 95.65$ for the implicit method, whereas the explicit inversion used the measured data $L_p = 95.325$ for $K = 0$ (first data point). These differences lead to slightly different linear target curves.

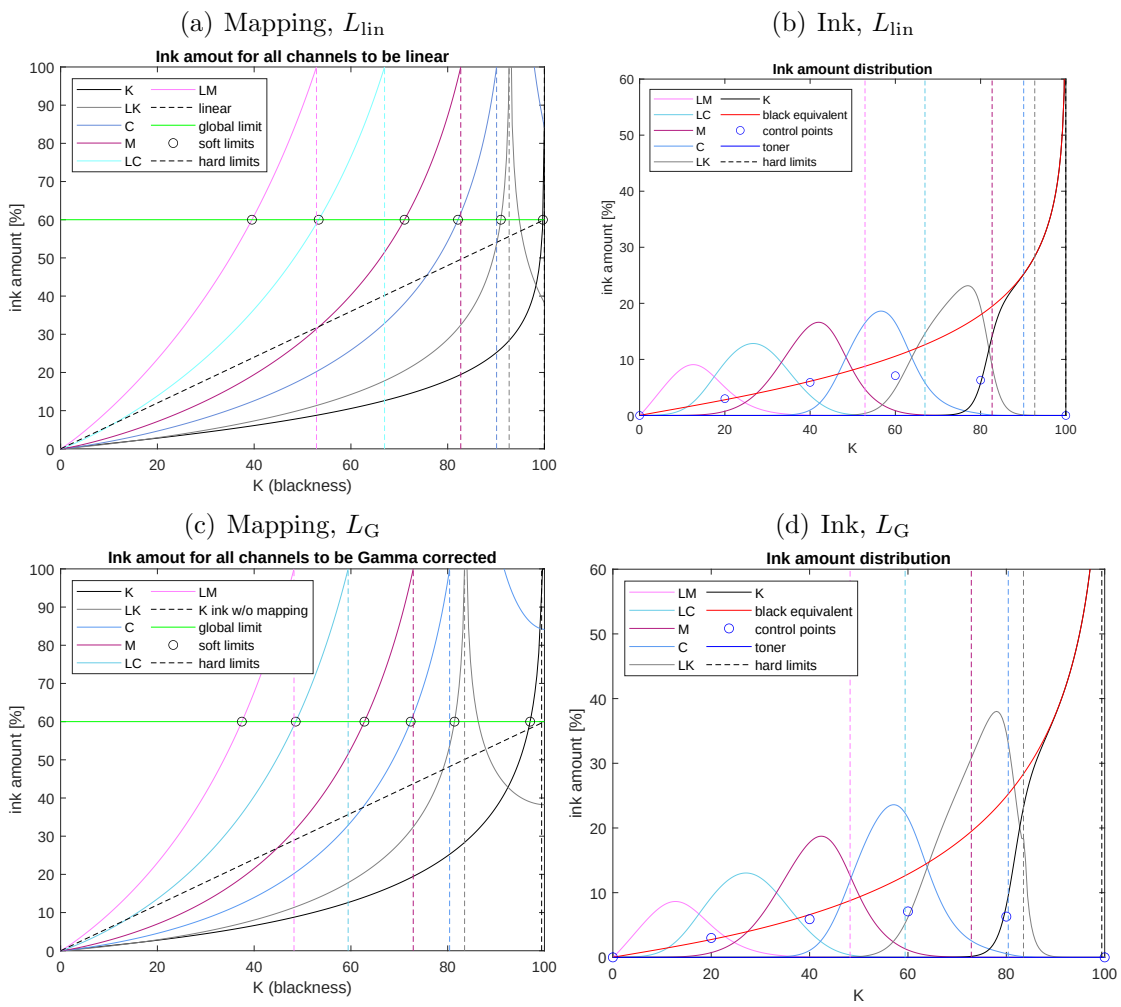


**Figure 10.4.:** Comparison of the mapping of individual ink channels to the target curve being linear (a) or of gamma type (c). Also shown are the final ink distributions (b,d) for the same ink ansatz functions. Note that the $LK$ channel in (d) is partly used beyond its infinity-limit $K_{LK}^{\infty}$ (vertical gray dashed line). GCVT ink on PR308.

## 10.3. Test of the gamma correction

Figure 10.4 shows ink mapping and ink distribution when the linear curve $L_{\mathrm{lin}}(K)$ (fig. 10.4(a,b)) or the gamma-corrected curve curve $L_{\mathrm{G}}(K)$ (fig. 10.4(c,d)) is targeted. Figure 10.4(c) indicate that the ink amount is increased (the mapping curves are shifted to the left) if all ink channels are forced to print on the $L_{\mathrm{G}}$ curve instead of printing on the $L_{\mathrm{lin}}$ curve (fig. 10.4(a)). Using the same basic ink functions, this is also reflected in the final ink amounts shown in figs. 10.4(b,d). From fig. 10.4(d) one can see that the $LK$ channel has already significantly exceeded its 100%-limit $K_{LC}^{100}$ (vertical dashed line) when using the present ink distribution functions. $K_{LC}^{100}$ is very close to the singularity (infinity-limit $K_{LK}^{\infty}$) such that for $K > K_{LC}^{\infty}$ the ink amount according to the mapping in fig. 10.4(b) is determined by the real part of

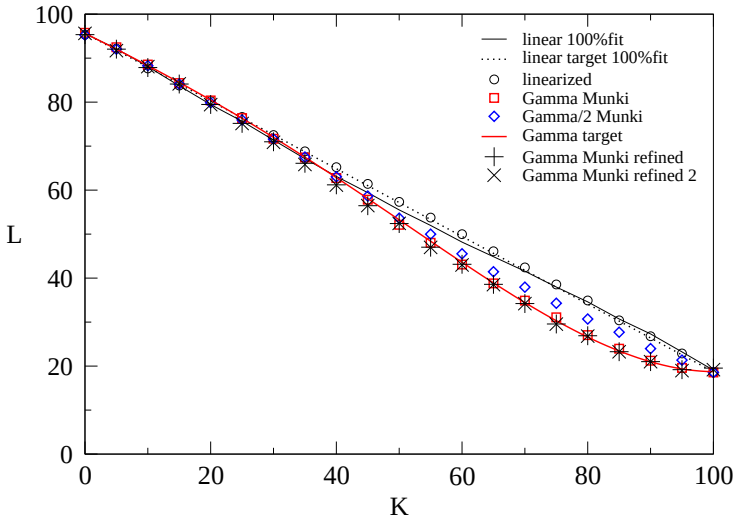


**Figure 10.5.:** Targeting different luminance curves, $L_{\text{lin}}$ and $L_{\text{G}}$, for PR308 (carbon only) when the fit coefficients for the ink characteristics have been determined over the full range (100%) of ink, $\alpha = 60\%$ and resolution 2880s dpi. Shown is the target cuve $L_{\text{G}}$ for the gamma-corrected output (full red line) as in fig. 10.1 together with the measured data of the output using a corresponding quad file (red squares). Targeting half the gamma correction yields the blue diamonds. For comparison, also shown is the luminance when targeting $L_{\text{lin}}$ (full line) and the result of the linearization by fine tuning (circles). The + and × symbols show the result of a repeated measurement of the step wedge from a quad created in a refinement step (a la linearization).

the complex solution.[3] The location $\hat{K}_{LC}$ of the maximum of the ink distribution function $I^{(0)}_{LK}(K)$ (6.1) should thus be moved to lower $K$ values. We also see from fig. 10.4(c) that the $K$ channel reaches its 100%-limit $K^{100}_K$ already before blackness $K = 100$. This is related to the selection of $L_m = 18.7$ and, in particular, to the gamma-correction curve: From fig. 10.1 (blue line) one can notice that the slope of the gamma curve at $K = 100$ is almost zero (horizontal tangent). Perhaps the gamma correction is already a tad too strong.

Figure 10.5 shows the result of the step wedge printed with two different quads generated by the present method. When using $L_{\text{G}}(K)$ as the target curve (red line) the measured luminance (red squares) fits quite nicely. This proves that the present approach works. From the red squares a fine tuning ($K$ shift to the target curve) does not even seem necessary. Also shown are measurements for a quad in which the only half of the gamma correction (10.2) was applied (blue diamonds). Also this results is convincing.[4]

[3] This is due to the current implementation in which each channel is forced to print on the target curve.

[4] Remark: The data point for $K = 100$ for the measurements (red squares and blue diamonds) have been taken from the measurement of the linear curve (black line), because the data was missing on the print. The reason was I have set the maximum ink for the $K$ channel to $2^{16}$, whereas it must be $2^{16} - 1$, because also the 0 counts. ;-)

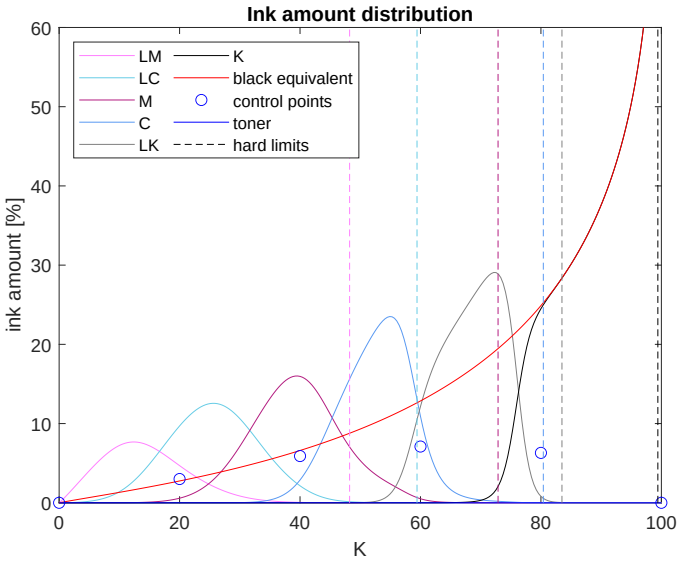


**Figure 10.6.:** Adapted ink distribution when targeting $L_{\mathrm{G}}$ (gamma correction) on which the data (red squares) in fig. 10.5 are based. PR308, 2880s dpi, $\alpha = 60\%$, ink fit over 100%.

The quad files used for fig. 10.5 have been created with an adapted distribution of the basic ink functions in order not to exceed the infinity-limits (as seen in fig. 10.4(d)). The ink distribution for targeting $L_{\mathrm{G}}$ which belongs to fig. 10.5 (red squares) is shown in fig. 10.6. The ink amount for the $K$ channel exceeding the ink limit of $\alpha = 60\%$ can be viewed as a *black boost* (here up to 100%).

Even though a further refinement by $K$-shifting to the gamma target curve is not necessary, I performed the fine tuning. The necessary shift is shown in fig. 10.7. The zero shift at the end points $K = 0$ and $K = 100$ is enforced. The magnitude of the $K$-shift is less than $\Delta K \leq 1$, throughout, meaning it is only less than 1% on the $K$ scale, thus practically insignificant. One can notice that the largest shift occurs isolated at $K = 50$. Probably the measured data $L(K)$ at $K = 50$ (red square) in fig. 10.5 is an outlier such that this shift is comparatively large (but in fact still very small). Yet, the isolated positive shift is reflected in the refined ink curves in fig. 10.8 at $K = 50$ by small indentations in the $C$ and $M$ curves. Perhaps one can do better than linear interpolation between the shift data in order to smooth the outliers. One possibility is a polynomial fit (red dashed line in fig. 10.7). The $K$ curve in fig. 10.8 rises up to the ink amount $K_{\mathrm{ink}} = 100$. The luminance of the 21 steps obtained from the refined quad are shown in figure 10.5 as + and × (two repeated measurements). In the mid range of the gray scale the original quad seems to be even better than the refined one. I suspect the deviations only indicate the errors made in the printing and measurement processes involved with the current equipment (R2880 printer/cartridges and the ColorMunki Photo).[5] The results

[5]For example the shift at $K = 40$ should be $\Delta K = +0.099$ (see also fig. 10.7). But the refined printed data point in fig. 10.5 (plus, cross) measures a negative shift of about $\Delta K \approx -1.75$(!)


**Figure 10.7.:** Computed $K$-shifts $\Delta K(K)$ to move the measured $L$ values (red squares in fig. 10.5) to the target gamma curve $L_{\mathrm{G}}(K)$ (red line in fig. 10.5). The red dashed line is a 6th-order polynomial fit of the shift data. The shifts are enforced to vanish at $K = 0$ and $K = 100$. GCVT ink on PR308.

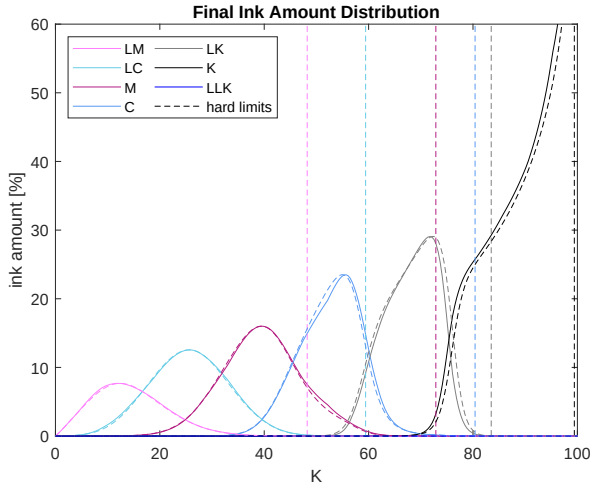


**Figure 10.8.:** Ink distribution after a refinement step (full lines) in comparison with the ink distribution before (dashed lines, fig. 10.6). GCVT ink on PR308. Target $L_{\mathrm{G}}(K)$.

suggest that indeed the quad generated in the present one-go procedure are almost perfect and only hampered by the deficits of the equipment.

from the reference gamma curve.

# 11. Proof or disproof of concept

Theoretically, the above concept is fine. But the proof of the pudding is in the eating. To that end I created a bull's eye file in which the blackness increases radially from 0 to 100. The human eye can easily discover any deficits in the smoothness of the gray transition. Unfortunately, the transition between gray values in the bull's eye plot were not as smooth as expected, despite of the linearity of the luminance values at the 21 discrete points of the step wedge (see fig. 14.5). The lack of smoothness was most prominently with glossy paper. I trace this back to the relatively steep transitions between inks provoked by the Gauß functions and the narrow overlap between the ansatz functions selected. This may have led to a sensitivity which could amplify any imperfections of the printer and the measurement device.

To remedy this deficit for matte paper, I changed the ansatz functions and increased the overlap. In fact, testing has shown that the ansatz functions in QTR are based on functions which are triangular. For these functions the ink amount is linearly reduced to zero on a variation of $K$. While I found no negative effect on the visual smoothness using ansatz functions which have a discontinuous slope, I preferred to have smoother ansatz functions and thus selected cubic Hermite splines. Form these cubic functions one can require to have a maximum at a nodal point and that they vanish with zero slope at the end points of their support (section 6.4).

One problem with matte paper and the linearization of all inks is the fact that the darkest gray ($LK$, 100% PK ink) by far cannot reach the blackness of the MK ink. Therefore, due to the present concept of linearizing all ink channels, the $LK$ ink has to vanish before the infinity-limit ist reached. This makes it more difficult to create a smooth transition as compared to glossy paper, where the $LK$ channel can provide a very deep black. Nevertheless, I think I succeeded for matte paper by using cubic Hermite splines and a wide overlap among the inks.

# 12. Ink blending based on pigment

## 12.1. Using a single global mapping

For glossy paper, another linearization strategy may be used. It is based on the observation that all inks of the glossy subset of the GCVT set are made of dilutions of the same PK ink. As a result, all ink curves can be mapped to a more or less unique luminance curve as a function of the relative amount of pigment contained. We have seen this before in fig. 6.1. For the GCVT ink set the relative (mass) amount of pigment is given by the mass concentrations of PK ink which are 0.09 (for $LM$), 0.15 (for $LC$), 0.30 (for $M$), 0.50 (for $C$) and 1.0 (for $LK$). From this observation one can conclude that the luminance is only determined by the amount of pigment, no matter from which dilution (ink channel) it originates.

Therefore, suitable functions can be constructed with suitable pigment weights and all pigment curves are then mapped to a linear curve using the overall modified exponential law whose coefficients were obtained by all data points of all inks. This overall curve is similar to the luminance curve of the $LK$ channel (PK ink). However, since there are small deviations of the individual inks from the mean luminance curve, this method does not exactly produce a linear luminance curve, but a very good initial raw curve which can be linearized. Here we consider Hahnemühle Fine Art Baryta (FAB) with paper white $L_p = 96.41$ and an ink limit of $\alpha = 80\%$. The minimum luminance targeted at $\alpha$ is $L_m = 2.5$.

The superposition is as follows. Let us define the relative pigment amount as $p_i = c_i K_{\text{ink}}$. Assume we have found the global fit $L_g(K_{\text{ink}}) \approx L_{LK}(K_{\text{ink}})$ to which all ink curves (e.g. figure 12.1) collapse (see fig. 12.2 and 12.3). Then all luminance curves only depend on a single variable, the pigment amount $p = p_i$. The global fit (blue dashed lines in fig. 12.2 and fig. 12.3) of the usual form

$$L_g(p) = L_g^\infty + (L_p - L_g^\infty)\mathrm{e}^{-s_g p^{n_g}} \tag{12.1}$$

can be mapped to the desired target curve $L_{\text{tar}}(K)$ (linear or any other shape) by

$$p_g(K) = \left[-\frac{1}{s_g}\ln\left(\frac{L_{\text{tar}}(K) - L_g^\infty}{L_p - L_g^\infty}\right)\right]^{1/n_g}. \tag{12.2}$$

For the paper FAB the fit from fig. 12.3 yields the parameters $L_g^\infty = 0.5$, decay rate $s_g = 0.058$ and exponent $n_g = 0.94$.[1] The amount of ink $i$ needed to print the target luminance at $K$ when used alone, is then given by $K_i^{\text{ink}}(K) = p_g(K)/c_i$.

[1] These data relate to the fitting by hand, not to the automatic fit described further above.

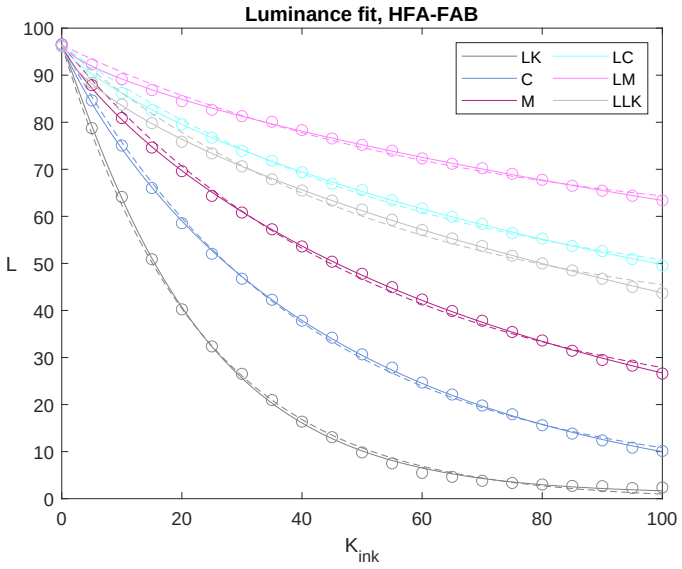


**Figure 12.1.:** Individual ink curves of GCVT ink on FAB.

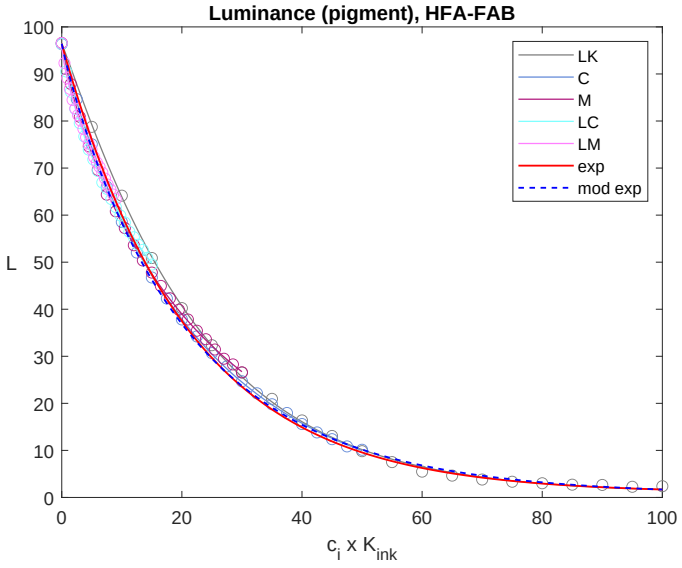


**Figure 12.2.:** Luminance of all GCVT glossy inks as function of the relative pigment amount $p = c_i K_i^{\text{ink}}$ on FAB.

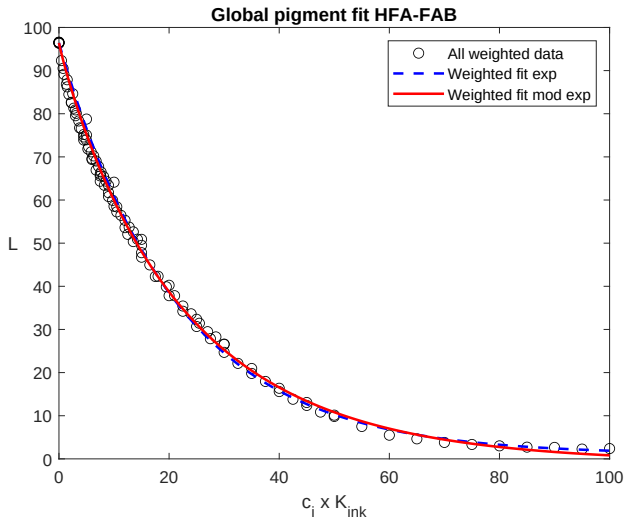


**Figure 12.3.:** Fitting all data by a pure exponential decay (blue dashes) or a modified exponential decay function. The data points are the same as in fig. 12.2. For the fit, the data points have been weighted inversely proportional to their density. GCVT on FAB.

The pigment amounts from different inks must add up to

$$p_g(K) = \sum_i p_i(K). \tag{12.3}$$

Consider now the ink ansatz function $I_i^{(0)}(K)$ and superpose them such that their sum is unity. Similar as in section 6.3 we then have the normalized ansatz functions

$$I_i^{(1)}(K) = \frac{I_i^{(0)}(K)}{N(K)}, \quad \text{with} \quad N(K) = \sum_i I_i^{(0)}(K). \tag{12.4}$$

Note that with this selection the relative weight given to an ink channel in the mixture of all channels is proportional to the amount of ink. To achieve the target luminance curve $L_g(K)$, the functions $I_i^{(1)}(K)$ need to be weighted by $p_g(K)$. This yields the final pigment amount functions for each ink

$$p_i(K) = p_g(K) I_i^{(1)}(K), \tag{12.5}$$

equivalent to the ink amount for ink $i$

$$K_i^{\text{ink}}(K) = \frac{p_g(K)}{c_i} I_i^{(1)}(K) = p_g(K) \frac{I_i^{(0)}(K)}{c_i \sum_i I_i^{(0)}(K)}. \tag{12.6}$$

This ink distribution (dashed lines in fig. 12.4) is very similar to the one which would result from linearizing all ink channels individually, as in section 6.3, where each ink amount is also given equal importance.

If not the sum of the ink functions, but rather the sum of the concentration-weighted ink functions are used for the normalization, one arrives at the alternative formulation

$$K_i^{\text{ink}}(K) = p_g(K)\frac{I_i^{(0)}(K)}{\sum_i c_i I_i^{(0)}(K)}, \tag{12.7}$$

where the concentrations appear in the normalizing factor. Both variants (12.6) and (12.7) yield the same total pigment amount, which can be checked by taking the sum over all pigment contributions

$$p_g(K) = \sum_i p_i(K) = \sum_i c_i K_i^{\text{ink}}(K). \tag{12.8}$$

But the pigment amounts per ink are different: one gets (dependence on $K$ suppressed)

$$\text{from (12.6)}: \qquad p_i = p_g\frac{I_i^{(0)}}{\sum_i I_i^{(0)}}, \tag{12.9a}$$

$$\text{from (12.7)}: \qquad p_i = p_g\frac{c_i I_i^{(0)}}{\sum_i c_i I_i^{(0)}}. \tag{12.9b}$$

This means that when using a combination of inks according to (12.7) those inks with small concentrations of pigment (the lighter inks like $LM$) are given less importance than those with high pigment concentration (the darker inks). The resulting ink distributions are shown in fig. 12.4. The normalization (12.6) corresponds to the dashed lines, while (12.7) results in the ink distribution shown by full lines. The higher importance of the lighter inks for (12.6) is visible by the larger ink amounts and the shift of the dashed ink curves to larger $K$.

## 12.2. Effect of the global mapping on the individual inks

The luminance of ink $i$, if printed alone and if mapped to the target luminance via the pigment amount $p_g(K)$ according to (12.2) is obtained from the equivalent ink amount $K_i^{\text{ink}} = p_g(K)/c_i$. This ink amount is now inserted into the luminance function for ink $i$ to yield

$$L_i^{\text{map}}(K) = L_i^{\infty} + (L_p - L_i^{\infty})\exp\left[-s_i(p_g(K)/c_i)^{n_i}\right], \tag{12.10}$$

where $s_i$ is the decay rate on the 100% scale. So far we have not used any ink limit.

$L_i^{\text{map}}(K)$ is the luminance which would result, if the ink $i$ is printed with the pigment amount equivalent to the one of the global mapping to the target curve. This luminance must not necessarily be the luminance $L_g(K)$, because the luminance

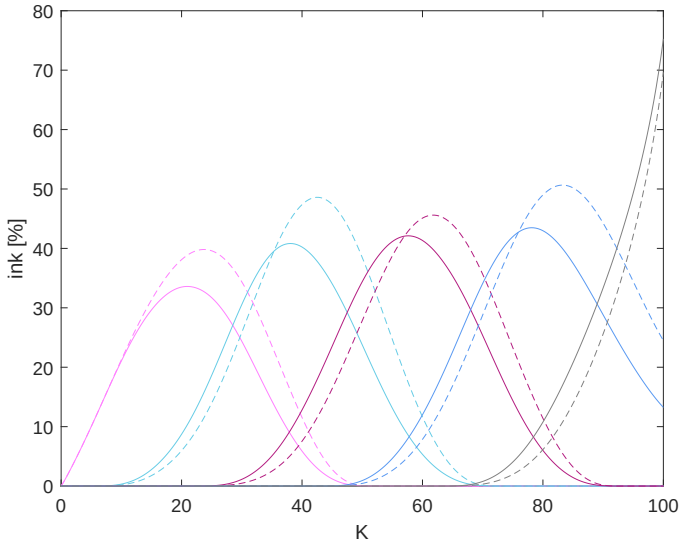


**Figure 12.4.:** Different normalizations when printing with GCVT ink on HFA FAB lead to different ink distributions: dashed lines represent (12.6), while full lines correspond to (12.7). Both distributions lead to the same total pigment-amount distribution $p(K)$. Linar target function.

curves of all inks deviate slightly. The effect of the global mapping on the mapping of the individual ink channels is shown in fig. 12.5 for FAB. One can see that the ink channels (full lines in color) are only approximately linear (red dotted linear target curve). This is due to the deviation of the individual ink luminance curves $L_i(p)$ from the global approximation $L_g(p)$.

To obtain the effect on the luminance of combining all channels, we consider the luminance reduction $R_i(K)$ from the paper white $L_p$ which is caused by ink $i$

$$R_i(K) = \frac{c_i I_i^{(0)}(K)}{\sum_i c_i I_i^{(0)}(K)} \left[L_p - L_i^{\text{map}}(K)\right] > 0. \tag{12.11}$$

If ink $i$ would the only ink used (1 ink only), the reduction would be $L_p - L_i^{\text{map}}(K)$ (second factor). But this is not typically the case. The first factor thus gives the relative weight the ink $i$ is given in the superposition of the inks (see (12.7)). If we assume that the luminance reduction is additive, the total luminance due to all the inks can be obtained by subtracting all luminance reductions from the paper white $L_p$. This way we obtain a predicted luminance curve

$$L_{\text{pred}}(K) = L_p - \sum_i R_i(K). \tag{12.12}$$

This yields the dash-dotted black line for $L_{\text{pred}}(K)$ in fig. 12.5 (FAB). The deviations from the target curve are quite small and qualitatively the same as in the measurement (open black circles in fig. 14.4). This seems to confirm the viability of the approach, although it is not strictly proven that the luminance reductions can be superposed.

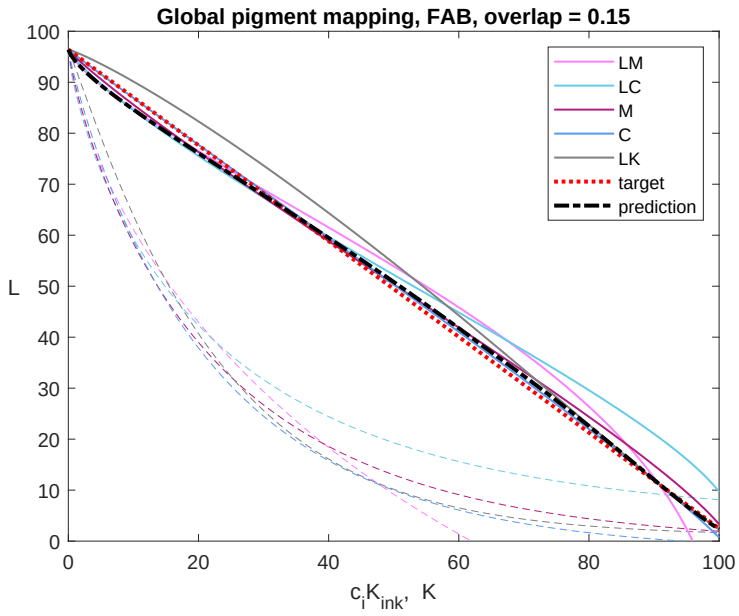


**Figure 12.5.:** FAB, glossy carbon, $L_g^\infty = 0.5$, decay rate $s_g = 0.058$ and exponent $n_g = 0.94$. Dashed lines indicate the original ink characteristis on the pigment scale $c_i K_{\text{ink}}$. Full lines are the luminance curves of the individual links on the $K$ scale, if mapped according to the global pigment mapping. Only the $LK$ cuves are directly comparable (full and dashed gray lines). For the other inks the scales are different, because $c_i \neq 1$. The thick dash-dotted curve is the luminance prediction based on the global pigment mapping for given ansatz functions. It does not deviate very much from the linear target (red dotted line).

## 12.3. Some thoughts on the GCVT ink set

One aspect that comes to my mind relates to the ink ansatz functions. If black ink is used in the highlights, only a few black dots would be visible perhaps leading to some graininess. To obtain the same degree of light gray, many more ink dots must be laid down when printing with a light gray. As a result (gray of the dots , amount of the dots) the gray appears much smoother. Therefore, light ink is preferred for the highlights. But a similar argument applies to the dark end of the $K$ scale. If only black ink would be used for dark tones, then a few white spots would remain (showing the paper white) in order to have a very dark but not completely black tone. This is a graininess which is the negative of the graininess at light gray tones. Therefore, the dark tones should not only be printed by pure black ink, but also by a dark gray ink.

From this perspective, it would be beneficial if a large number of inks with finely graded lightness/darkness covering the full scale would be employed. But using a large number of inks may lead to other problems. It is probably for this reason why the Piezography ink distribution functions have such long tails towards 100% black. The very dark tones are made by several of the darker inks. This leads of course also to a higher ink load, but the graininess is largely suppressed. This

approach is viable, if each ink of the set is diluted from the same black ink such that, theoretically, each ink can produce the same deep black, if only enough ink is used. This is the case for the glossy subsect of the GCVT ink set of Paul Roark. Within this subset all luminance values ($L > L_m$) can be obtained by each ink. It is only a matter of ink amount. This property is also in favor of a linearization of each ink channel separately. Since ideally all glossy inks have the same saturation luminance, there should not occur any singularity in the mapping of a channel to a linear curve.

For matte papers there arises a problem with the GCVT ink set. On matte paper the saturation luminance of the darkest gray (PK ink in the $LK$ channel) is considerably lighter than the matte black (MK). Therefore, the gray inks cannot be linearized for $K$ values larger than $K_{\text{linear}}(L_{\text{sat}})$, where $L_{\text{sat}}$ is the common saturation luminance of the gray inks. In the mapping of a glossy ink channel to a linear luminance, a corresponding singularity will occur, and it is not possible to print tones darker than the saturation luminance with this glossy ink. Therefore, one would either have to refrain from using the glossy inks beyond this point, or give up the idea of mapping all gray levels to a linear curve. If one gives up the linearization of each ink channel, then the gray inks can also used down to $K = 0$. But because they print too light, this brightening effect has to be compensated by increasing the black (MK) ink amount. In any case the ink amount of the gray inks must vanish at $K = 0$, because a gray ink at $K = 0$ could only be compensated by an infinite amount of black (MK) ink. In case of the glossy subset (and also for the Piezography inks) this restriction is removed and gray inks can be used with finite amounts also at $K = 0$, where they contribute to the black coverage.

# 13. Luminance prediction

The combination of MK and PK inks in the GCVT ink set when printing on matte paper prohibits the use of PK inks for the darkest tones if one uses the linearization of all ink channels. This is due to the divergence of the mapping at the infinity-limits of the PK inks. Therefore, if one wants to use the PK inks down to $K = 100$, the linearization of all ink channels must be given up and the ink distribution must be designed freely. But how to design the ink distribution? A great help in this process would be a monitoring tool which could reliably predict, or at least provide a good approximation of, the luminance $L(K)$ for a given free ink distribution. The ink distribution functions could then be adjusted, while observing the changes of the predicted luminance. This way it would be possible to come up with a pretty good initial ink distribution which could then be fine-tuned to make the ink distribution to perfectly print according to the target function.

In the following I suggest a prediction of the luminance $L(K)$ based on the area covered by pigment and the associated reduction of the luminance. Let us first consider the PK inks $i \in [LM, LC, M, C, LK]$ only.

## 13.1. Carbon on glossy paper (PK inks only)

We first note that the relative pigment amount of PK ink as a function of $K$ is given by

$$P_{\mathrm{PK}}(K) = \sum_{i=LM}^{LK} c_i I_i(K), \tag{13.1}$$

where $c_i$ is the pigment concentrations of ink $i$ and $I_i(K)$ the actual ink amount used in the given free ink distribution during the ink curve design process. This pigment amount is different from the pigment amount $p_g(K)$ which is a result of the *global* fit in (12.2). Here, $P_{\mathrm{PK}}(K)$ is the actual pigment amount of any arbitrary ink distribution which is used to print a pixel (or any other reference area) with blackness $K$.

The luminance which would result, if the pigment amount $P_{\mathrm{PK}}$ would be printed by a single channel $i$ is given by

$$L_i^P(K) = L_i^\infty + (L_p - L_i^\infty) \exp\left[-s_i \left(P_{\mathrm{PK}}(K)/c_i\right)^{n_i}\right]. \tag{13.2}$$

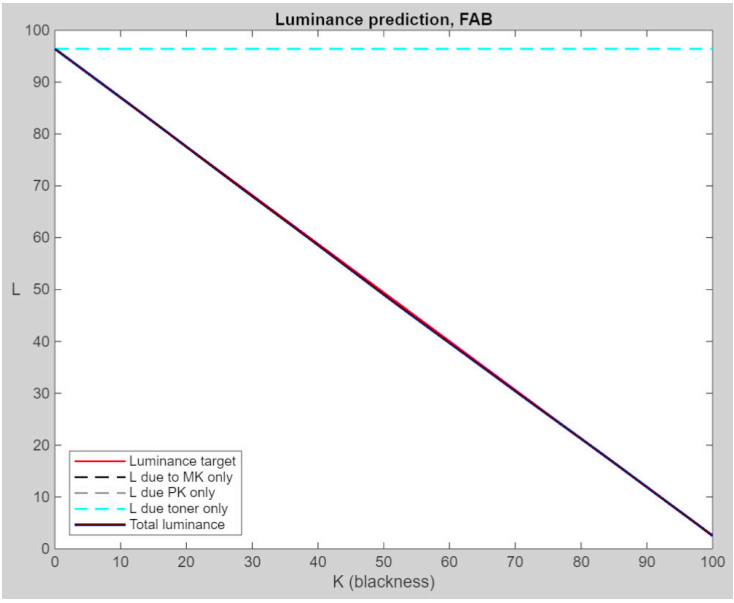


**Figure 13.1.:** Luminance prediction according to (13.12) (blue) for an ink distribution for FAB ($L_p = 96.4$, $L_m = 2.5$) in which all ink channels have been linearized. The red line is the linear target curve.

From this we expect the luminance reduction of channel $i$ to be (as in (12.11))

$$\begin{aligned} R_i(K) &= \frac{c_i I_i^{(0)}(K)}{\sum_i c_i I_i^{(0)}(K)} \left[L_p - L_i^P(K)\right] \\ &= \frac{c_i I_i^{(0)}(K)}{\sum_i c_i I_i^{(0)}(K)} (L_p - L_i^\infty) \left[1 - \exp\left\{-s_i \left(\frac{P_{\mathrm{PK}}(K)}{c_i}\right)^{n_i}\right\}\right]. \end{aligned} \tag{13.3}$$

Here, the first factor gives a weight to the ink $i$ as in (12.11). The total luminance reduction from all PK inks then is

$$R_{\mathrm{PK}}(K) = \sum_i R_i(K), \tag{13.4}$$

and the luminance is predicted to be

$$L_{\mathrm{pred}}^{\mathrm{glossy}}(K) = L_p - R_{\mathrm{PK}}(K). \tag{13.5}$$

The result has been tested for an ink distribution obtained by a total linearization of all ink channels. The corresponding ink amounts $I_i(K)$ enter $P_{\mathrm{PK}}$. The predicted luminance for glossy carbon is excellent (fig. 13.1).

It should be noted that this luminance prediction relies on the knowledge of the ansatz functions $I_i^{(0)}(K)$. Thus the prediction is only applicable to ink distributions which are generated in the present way. The luminance prediction is not needed (or almost trivial) if the ink distribution is created in one go such as to be linear or gamma-like by the present method. However, one might be interested in a particular nonlinear ink distribution. Such a distribution can be created freely based on ansatz functions by `MakeQuad`. In such case the luminance prediction (13.5) is very useful and reliable.

On the other hand, one might be interested to quickly check the luminance (without printing and measuring) which would result from a distribution of GCVT inks which are generated by another method, e.g. by QTR. For such ink distributions the prediction (13.5) cannot be used, because the ink ansatz functions $I_i^{(0)}(K)$ are not known. In this case one might read the quad file and convert the data into ink amount functions on the 100%-scale. Thereafter, the more complicated method described in section 13.6 could be used which is based on pigment luminance $L_i^\infty$ and the probabilities for the various pigment stacking configurations which are possible.

## 13.2. Carbon on matte paper (PK and MK inks)

Now we consider the superposition of matte and glossy black inks on matte paper. The PK (glossy) ink cannot reach the same level of black on matte paper as the MK (matte) ink. This is clearly seen by comparing the luminance for $K = 100$ of the $LK$ and the $K$ channels in fig. 9.1.

An important relation is the linear dependence of the luminance $L(A)$ on the pigment coverage $A \in [0, 1]$, where $A$ is the fraction of the total area of the pixel covered with pigment. They are related by (see also (3.1))[1]

$$L(A) = L_p - (L_p - L^\infty)A, \tag{13.6}$$

where $L^\infty$ implies full coverage, because it is reached for $K_{\text{ink}} \to \infty$. The linear relation is due to the human eye interpolating the luminance of an irregular pattern linearly. As a consequence of (13.6) the pigment coverage $A$ can be deduced from the luminance $L = L(A) = L(K)$ as

$$A_{\text{MK}}(K) = \frac{L_K(K) - L_p}{L^\infty - L_p} = 1 - \exp\left\{-s_K[I_K(K)]^{n_K}\right\}, \tag{13.7}$$

where we have inserted the fitted luminance of the MK black ink ($K$ channel) and the actual ink amount used is expressed as a function of the blackness variable $K$ with help of (6.3) or (6.5). If, on the other hand, only PK ink is used, the pigment coverage can be deduced from the above luminance reduction (13.5) as

$$A_{\text{PK}}(K) = \frac{R_{\text{PK}}(K)}{L_p - L_{LK}^\infty}. \tag{13.8}$$

The denominator represents the maximum possible luminance reduction which can be achieved by the PK ink, expressed through $L_{LK}^\infty$.

If both PK and MK inks are printed at the same time, it can happen that a randomly placed pigment particle covers a previously uncovered spot on the paper, or it can fall on top of a spot which has been already been covered by a pigment

[1] Note that here $A$ is the pigment-covered area, whereas in section 3 $A$ was the area left blank.

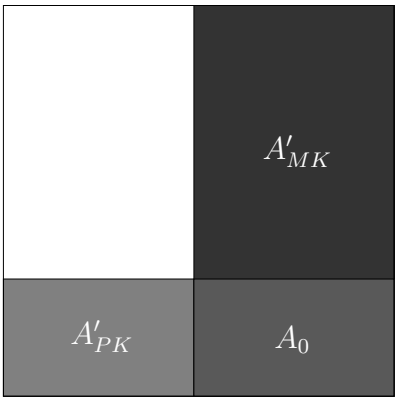


**Figure 13.2.:** A pixel (reference area, outer square) in which area fractions $A$ are indicated by rectangles which are completely covered with MK pigment, PK pigment, or a combination of both pigments. The total area of the pixel (reference area) is 1.

particle of the other ink. If the droplets all have the same size and if the deposition time and place are randomly distributed, then the areas (a) covered by a single pigment of MK, (b) covered by a single pigment particle of PK and (c) the area covered by both pigment particles can be obtained from the above individual pigment coverages of the two kinds of ink. This is graphically illustrated in fig. 13.2.

If each ink alone would cover the fractions $A_{\mathrm{PK}}$ and $A_{\mathrm{MK}}$, then from the figure the fraction of the area which is covered by both pigments is

$$A_0 = A_{\mathrm{MK}} A_{\mathrm{PK}}, \tag{13.9}$$

and the area fractions which remain covered by only one kind of pigment are reduced to

$$A'_{\mathrm{MK}} = A_{\mathrm{MK}} - A_0, \tag{13.10a}$$
$$A'_{\mathrm{PK}} = A_{\mathrm{PK}} - A_0. \tag{13.10b}$$

Now we have to take into account the luminance reductions due to each of these areas which are covered by pigment. These luminance reductions are[2]

$$R'_{\mathrm{MK}} = A'_{\mathrm{MK}}(L_p - L^{\infty}_K), \tag{13.11a}$$
$$R'_{\mathrm{PK}} = A'_{\mathrm{PK}}(L_p - L^{\infty}_{LK}), \tag{13.11b}$$
$$R_0 = A_0 \left[ L_p - \frac{L^{\infty}_K}{2} - \frac{L^{\infty}_{LK}}{2} \right], \tag{13.11c}$$

where it is assumed that in the region $A_0$ both types of pigment particles, MK and PK, have the same probability of being placed on top of the respective other one. The luminance prediction $L^{\mathrm{matte}}_{\mathrm{pred}}(K)$ is then obtained by subtracting these luminance reductions from the luminance $L_p$ of the paper white

$$L^{\mathrm{matte}}_{\mathrm{pred}}(K) = L_p - R'_{\mathrm{MK}}(K) - R'_{\mathrm{PK}}(K) - R_0(K). \tag{13.12}$$

[2]The prime should indicate that these luminance reductions differ from the reductions when only one ink is printed. For instance for $R'_{\mathrm{PK}}$ this is due to the reduction of the area from $A_{\mathrm{PK}}$ to $A'_{\mathrm{PK}}$ due to the stacking of pigments which is considered separately ($A_0$).

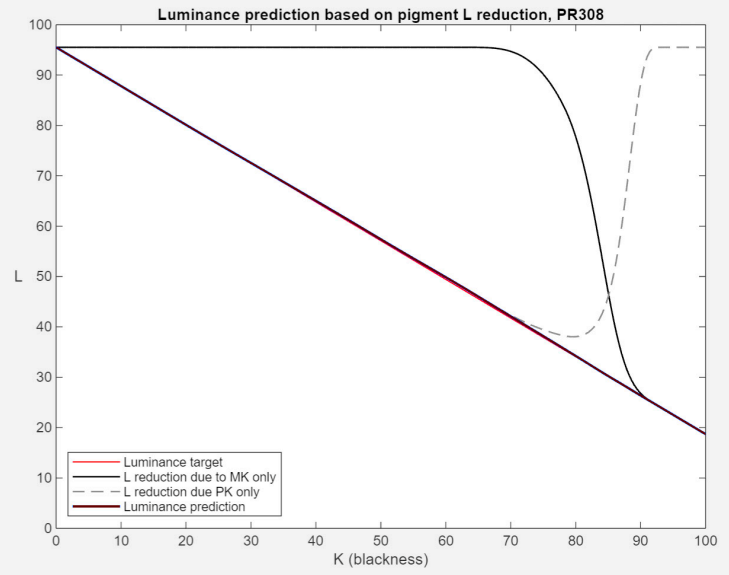


**Figure 13.3.:** Luminance prediction according to (13.12) (blue) for an ink distribution for PR308 in which all ink channels have been linearized. The black and the gray dashed line represent the luminance of the MK ink ($K$ channel) and the PK ink (all PK channels), respectively, when printed alone. The red line is the linear target curve.

Equation (13.12) has been tested by using an ink distribution for HFA PR 308 which was obtained by a linearization of all ink channels and which is known to print almost linearly. For this distribution the PK ink is not used for $K > 92$. Figure 13.3 shows that the above prediction method indeed reproduces the linear luminance of the ink distribution for HFA PR 308 which was proven to be linear. This test is a strong indication that (13.12) can accurately predict the luminance and can therefore be used in freely designing superpositions of matte and glossy inks on matte papers in order to match a given target luminance curve.

The geometrical consideration with help of fig. 13.2 can perhaps better be replaced by a statistical consideration. If an arbitrary point within a pixel whose area is normalized to 1 is probed, the pigment coverage $A_{\mathrm{MK}}$ is the same as the probability to find this point covered by an MK pigment particle. The same holds for the PK coverage and probability. Since the placement of the pigments is considered to be random and independent, the probability to finding both pigment particles at the same point then is the product of the probabilities, i.e. $A_{\mathrm{MK}}A_{\mathrm{PK}}$ which corresponds to the area fraction $A_0$ in fig. 13.2.

## 13.3. Freely designed ink distribution

The practical proof needs printing with a quad file generated from a freely designed ink distribution. For the test on the matte paper PR308 the PK ink is used up to $K = 100$. However, the ink amount of $LK$ must vanish at $K = 100$, because any PK pigment with $L_i^\infty > L_K^\infty$ cannot be compensated with a finite amount of MK ink.[3] In the test the ink definition parameters $l_i$, $C_i$, $r_i$, $A_i$ for the cubic

[3]The $LK$ (PK) ink amount (and thus the luminance reduction) vanishes quadratically, owing to the current state of the design of the Hermite splines (violet curve at $K = 100$)). But it might be better to make the $LK$ spline vanish linearly at $K = 100$.

**Table 13.1.:** Parameters defining the ink functions shown in fig. 13.5. The parameters $b_i$ are the exponents to shape the MK ink curves which are made from power laws with zero slope at $l_i$ (for $b_i \geq 2$).

| $i$ | 1 | 2 | 3 | 4 | 5 | 6 | 7 |
|---|---|---|---|---|---|---|---|
| channel | $LM$ | $LC$ | $M$ | $C$ | $LK$ | $K$ | $Y$ |
| type | PK | PK | PK | PK | PK | MK | MK |
| $l_i$ | 0 | 7.072 | 20.37 | 33.67 | 45.88 | 63.34 | 90.48 |
| $C_i$ | 17.74 | 32.40 | 48.96 | 65.15 | 79.54 | – | – |
| $r_i$ | 47.00 | 66.35 | 92.19 | 99.79 | 100.2 | – | – |
| $A_i$ | 14.99 | 17.76 | 17.34 | 15.91 | 11.96 | 44.95 | 19.72 |
| $b_i$ | – | – | – | – | – | 2.114 | 13.52 |

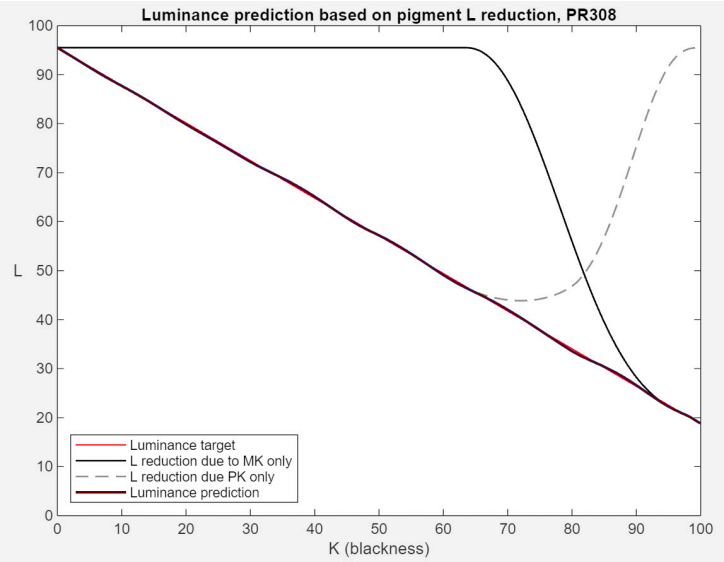


**Figure 13.4.:** Luminance prediction for the ink distribution shown in fig. 13.5.

Hermite splines are interactively adapted while observing the luminance prediction. For the parameters given in 13.1 the prediction according to (13.12) with a linear target output is shown in fig. 13.4 (blue curve). The associated ink distribution is displayed in fig. 13.5.

The print of a 21 step wedge on PR308 using a quad file created with this free ink distribution is shown in fig. 13.6 (red circles). Indeed the linearity of the printed step wedge is not too bad. But the print is slightly too dark for $K < 65$ and slightly too bright for $K > 65$. The same trend has been observed before in fig. 9.3 for PR308. This slight variation may have to do with the fit of the calibration data. Perhaps one cannot do better with the present equipment. Also shown is the result for a quad file which was obtained by a linearization of all ink channels (black crosses). It follows the same trend. Merely, the patch at the end of the scale $L(K = 100) = 21.0$ is somewhat too bright. Perhaps this is due to a variation of the paper property. It might have been mechanically touched before printing, thus slightly changing the reflective properties.

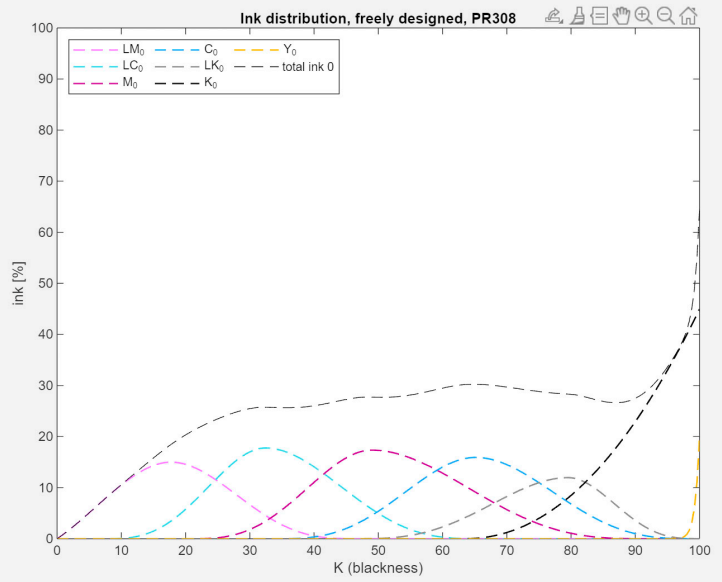


**Figure 13.5.:** Ink functions which produce the luminance predictions shown in fig. 13.4.

The very good news, however, is that the luminance of the freely designed ink curves and the resulting quad are very close to linear. This verifies the above approach and makes possible the luminance prediction via (13.12) also for GCVT inkset, despite of the glossy and matte inks being combined.

## 13.4. Glossy paper with toner ink

The method can be extended to include the effect of the toner in the $LLK$ channel on the luminance. In case of glossy paper the combination of the PK pigments with the toner pigments would have to be considered, which themselves are a mixture of blue and cyan, see the recipe of Roark (2023). For a prediction merely the luminance properties of the MK ink in (13.12) have to be replaced by the luminance properties of the toner ink ($LLK$). This yields

$$L_{\text{pred}}^{\text{glossy,toner}}(K) = L_p - R'_{\text{toner}}(K) - R'_{\text{PK}}(K) - R_0(K), \tag{13.13}$$

where now[4]

$$R'_{\text{toner}} = A'_{\text{toner}}(L_p - L^{\infty}_{LLK}), \tag{13.14a}$$
$$R'_{\text{PK}} = A'_{\text{PK}}(L_p - L^{\infty}_{LK}), \tag{13.14b}$$
$$R_0 = A_0 \left[ L_p - \frac{L^{\infty}_{LLK}}{2} - \frac{L^{\infty}_{LK}}{2} \right] h, \tag{13.14c}$$

[4]Since the value $L^{\infty}_{LLK} \approx -25$ is unrealistic (see table 15.1), I have used $L^{\infty}_{LLK} = 0$. This selection yields realistic predictions in the tests below.

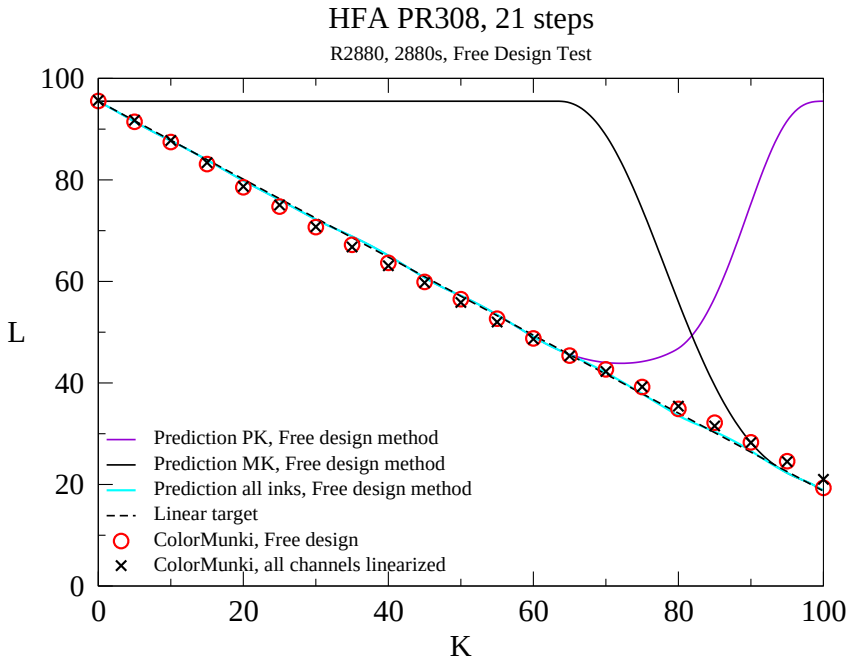


**Figure 13.6.:** Luminance measurements for a freely designed ink distribution (red circles). The shape and amlitude of the individual ink curves (not shown) were adjusted such that the luminance prediction (13.12) results in a linear curve (cyan curve with small residual waviness). The PK inks (violet curve) are used up to $K = 100$ where their amount vanishes. For comparison, measurements were made of a 21 step wedge printed with a quad based on the linearization of all channels (black crosses).

and the area fractions are

$$A'_{\text{toner}} = A_{\text{toner}} - A_0, \tag{13.15a}$$
$$A'_{\text{PK}} = A_{\text{PK}} - A_0, \tag{13.15b}$$

with

$$A_0 = A_{\text{toner}} A_{\text{PK}}, \tag{13.16}$$

and

$$A_{\text{toner}}(K) = 1 - \exp\{-s_{LLK}[I_{LLK}(K)]^{n_{LLK}}\}, \tag{13.17a}$$
$$A_{\text{PK}}(K) = \frac{R_{\text{PK}}(K)}{L_p - L^{\infty}_{LK}}, \tag{13.17b}$$

where $I_{LLK}(K)$ is the actual toner ink amount used at blackness variable $K$.[5]

To demonstrate the quality of the luminance prediction in the presence of a toner, the luminance of two ink distributions are considered. Since I have extended `Make-`

[5]The ink amount for the toner is not constructed via ansatz functions, hence the toner ink amount is denoted $K^{\text{ink}}_{LLK}(K)$ and not $I_{LLK}(K)$.

(a) before linearization (b) after linearization

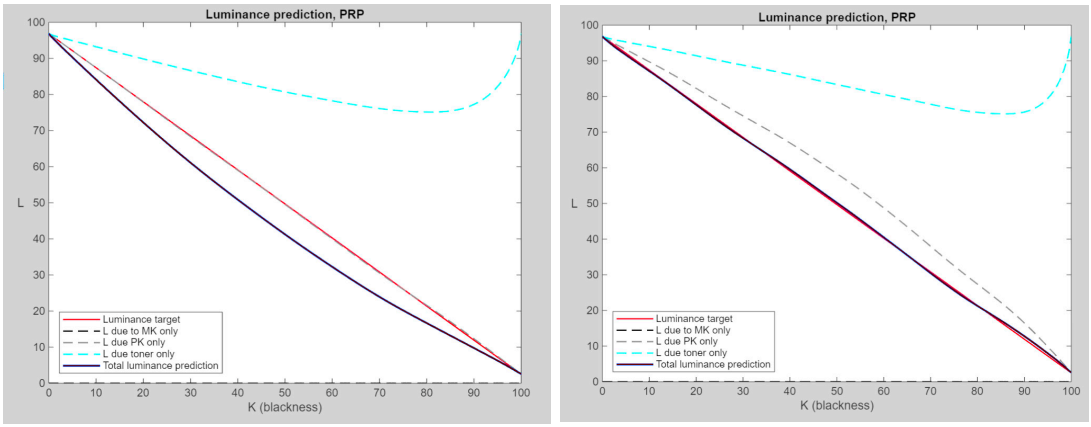


**Figure 13.7.:** Luminance prediction (not a measurement!) based on the ink distribution for printing on the glossy paper HFA Photo Rag Pearl (PRP) in the presence of a toner ink. The luminance due to the PK inks alone (gray dashed line) and that of the toner ink alone (cyan dashed line) are also shown. The neutralized ink distribution before linearization (a) is predicted to print too dark (blue line). After linearization (b) the ink distribution is predicted to print almost linearly. This is confirmed by measurement in fig. 15.6.

`Quad` to be able to read quad files,[6] I loaded the quad belonging to a neutralized (but not linearized) ink distribution on PRP. This ink distribution was made starting from a pure carbon version created by linearizing all ink channels. Then toner ink is added such that the print looks neutral (for the measurements, see fig. 15.6). The luminance predicted for the neutral (but not linearized) ink distribution is shown in fig. 13.7(a). The quad would print too dark (blue line in (a)). The luminance prediction for the quad file obtained by linearization is shown in fig. 13.7(b). By comparison with the measurement(s) in fig. 15.6 below the present luminance prediction is considered rather good.

The luminance prediction for pure carbon printing can be used as a predictive tool to achieve the targeted luminance during freely designing the ink distribution. When a toner is present, however, the prediction of the luminance alone is of little value, because one typically wants to also predict Lab-$b$ as a function of $K$ in order to achieve a neutrally looking print. Therefore, one would need to be able to predict Lab-$b$ as well. Even for pure carbon this is, however, a non-trivial task, because one would have to consider the subtractive color mixing of the paper white with the carbon pigment, and eventually the toner pigment(s). Therefore, it is not so easy to even predict the Lab color of the carbon print as a function of $K$. To my current understanding this would require to establish the absorption spectrum of the paper and that of the pigment. These would have to be superposed according

[6] This feature is useful for quickly monitoring the ink distribution of a quad. `MakeQuad` can also linearize a given quad, provided the luminance of a step wedge has been measured which was printed using this (nonlinear) quad.

to the pigment coverage in order to obtain the spectrum of the reflected light. From the spectral power distribution $I(\lambda)$ of the illuminant (e.g. the reference illuminant D55) and the spectral reflectance $S(\lambda)$ of the surface one could then obtain the tristimulus values $X$, $Y$ and $Z$ by integration over the wavelength $\lambda$

$$\begin{pmatrix} X \\ Y \\ Z \end{pmatrix} = \frac{1}{N} \int_\lambda S(\lambda) I(\lambda) \begin{pmatrix} \bar{x} \\ \bar{y} \\ \bar{z} \end{pmatrix} \mathrm{d}\lambda, \tag{13.18}$$

where $\bar{x}$, $\bar{y}$ and $\bar{z}$ are the CIE standard observer functions (human eye sensitivities). The normalizing denominator is[7]

$$N = \int_\lambda I(\lambda) \bar{y} \mathrm{d}\lambda. \tag{13.19}$$

Finally, $(X, Y.Z)$ can be converted to Lab with

$$L = 116 f_y - 16, \tag{13.20a}$$
$$a = 500(f_x - f_y), \tag{13.20b}$$
$$b = 200(f_y - f_z). \tag{13.20c}$$

The functions $f_x$, $f_y$ and $f_z$ are explained, e.g., in http://www.brucelindbloom.com. I think the spectral distribution can be measured by the ColorMunki Photo. But such undertaking is probably a touch to much for the time being.

## 13.5. Matte paper with toner ink

Printing on matte paper with PK and MK inks and with a toner ink three kinds of pigments need to be taken care of. The respective pigment coverages (probabilities) as function of the actual ink amount printed are[8]

$$A_{\mathrm{PK}}(K) = \frac{R_{\mathrm{PK}}(K)}{L_p - L_{LK}^\infty}, \tag{13.21a}$$
$$A_{\mathrm{MK}}(K) = \frac{L_p - L_K[I_K(K)]}{L_p - L_K^\infty} = 1 - \exp\left\{-s_K [I_K(K)]^{n_K}\right\} \tag{13.21b}$$
$$A_{\mathrm{toner}}(K) = \frac{L_p - L_{LLK}[I_{LLK}(K)]}{L_p - L_{LLK}^\infty} = 1 - \exp\left\{-s_{LLK} [I_{LLK}(K)]^{n_{LLK}}\right\}. \tag{13.21c}$$

[7] The $\bar{y}(\lambda)$ color matching function is exactly equal to the photopic luminous efficiency function $V(\lambda)$ for the CIE standard photopic observer. I think this is the reason why it enters in the normalizing factor $N$.

[8] If $LK$ is the only the glossy ink ($LM$, $LC$, etc. are not printed) one could also use

$$A_{\mathrm{PK}} = \frac{L_p - L_{LK}[I_{LK}(K)]}{L_p - L_{LK}^\infty}$$

instead of (13.21a). But in general several glossy inks are employed when using the GCVT ink set. In that case the $LK$ ink would not be used for the lightest tones which would result in a (wrong) zero pigment coverage. Therefore, in general (13.21a) must be used.

In (13.21a) $I_{LLK}(K)$ must be understood as the actual toner ink amount used.

From the probabilities in (13.21) to find the respective type of pigment within a pixel we obtain the probabilities when all three types of pigments are combined. The probability (coverage) of finding a point at which all three pigments stacked ($A_3$), a point at which two pigments are stacked ($A'_{2a}, A'_{2b}, A'_{2c}$) and a point at which one finds only a single type of pigment ($A'_{1a}, A'_{1b}, A'_{1c}$) are then given by

$$A_3 = A_{\mathrm{MK}} A_{\mathrm{PK}} A_{\mathrm{toner}}, \tag{13.22a}$$
$$A'_{2a} = A_{\mathrm{MK}} A_{\mathrm{PK}} - A_3, \tag{13.22b}$$
$$A'_{2b} = A_{\mathrm{PK}} A_{\mathrm{toner}} - A_3, \tag{13.22c}$$
$$A'_{2c} = A_{\mathrm{MK}} A_{\mathrm{toner}} - A_3, \tag{13.22d}$$
$$A'_{1a} = A_{\mathrm{MK}} - A'_{2a} - A'_{2c} - A_3, \tag{13.22e}$$
$$A'_{1b} = A_{\mathrm{PK}} - A'_{2a} - A'_{2b} - A_3, \tag{13.22f}$$
$$A'_{1c} = A_{\mathrm{toner}} - A'_{2b} - A'_{2c} - A_3. \tag{13.22g}$$

The luminance reductions, considering independent ink/pigment placing, are then given by

$$R_3 = A_3 \left[ L_p - \frac{L_K^\infty}{3} - \frac{L_{LK}^\infty}{3} - \frac{L_{LLK}^\infty}{3} \right], \tag{13.23a}$$
$$R'_{2a} = A'_{2a} \left[ L_p - \frac{L_K^\infty}{2} - \frac{L_{LK}^\infty}{2} \right], \tag{13.23b}$$
$$R'_{2b} = A'_{2b} \left[ L_p - \frac{L_{LK}^\infty}{2} - \frac{L_{LLK}^\infty}{2} \right], \tag{13.23c}$$
$$R'_{2c} = A'_{2c} \left[ L_p - \frac{L_K^\infty}{2} - \frac{L_{LLK}^\infty}{2} \right], \tag{13.23d}$$
$$R'_{1a} = A'_{1a} \left[ L_p - L_K^\infty \right], \tag{13.23e}$$
$$R'_{1b} = A'_{1b} \left[ L_p - L_{LK}^\infty \right], \tag{13.23f}$$
$$R'_{1c} = A'_{1c} \left[ L_p - L_{LLK}^\infty \right]. \tag{13.23g}$$

This yields the luminance prediction for a toned print on matte paper

$$L_{\mathrm{pred}}^{\mathrm{matte,toner}}(K) = L_p - R'_{1a} - R'_{1b} - R'_{1c} - R'_{2a} - R'_{2b} - R'_{2c} - R_3. \tag{13.24}$$

If the ink overlap parameter $\Delta K_o$ is increased very much such that all inks print over a very wide range of $K$, the theoretically predicted luminance of a nominally linear ink distribution (all channels linearized) can be larger than the linear target for PR308. For instance, an overlap parameter of $\Delta K_o = 50$ may yield $\Delta L \approx 1$ above the linear target at $K \approx 40$. This is caused by the $LK$ channel being used at medium to light gray tones. The reason is the linearization of the ink channels is based on the fit of the real luminance data from the calibration print, whereas the luminance prediction is based on the pigment coverage in which the stacking

effect within a single ink droplet of $LK$ is not taken into account.[9] In deriving the luminance prediction only the stacking of different types of pigment is considered, not the stacking within an individual ink droplet. The slight overprediction of the brightness on matte paper for large overlap parameters can be neglected for moderate overlap parameters $\Delta K_o \lesssim 30$. For glossy paper for which the $LK$ ink serves as the PK black at the dark end of the blackness scale the overprediction effect does not seem to play a role.

## 13.6. Superposition of an arbitrary number of inks

[10]To arrive at a prediction of the luminance of an arbitrary number $N$ of inks $i \in [1, N]$ combined and printed in different amounts, one has to make some model assumptions. Here we assume that all pigments are completely opaque and have luminances $L_i^\infty$ depending on the paper. Furthermore, it is assumed that the ink droplets are placed randomly in time and space. If $N$ inks are printed with ink amounts $K_i^{\text{ink}}(K)$ then any point of the reference area may be covered by no pigment, one sort of pigment, or a superposition (stacking) of any number of pigments. In my model, the luminance is determined by the uppermost (top) pigment. A partial overlap of pigments may not have to be considered, if a sufficiently large number of pigments is printed (which seems to be the case).

The model is based on the linear interpolation of the eye (13.6). From this and the ink parameters the ink/pigment coverage (13.7) of the unit reference area is deduced and it is interpreted as a probability of finding the respective pigment within the reference area. Owing to the multiple inks being printed all possible combinations of inks must be considered and the probability for each case to occur must be calculated. In the previous section for $N = 3$ we have seen from (13.22) that 7 different ink combinations (cases) arise. If the number $N$ of inks increases, the possible ink combinations rises very quickly.

Let $n$ be the number of inks which are printed on the unit reference area. Then the number $M_n$ of possible combinations of $n$ inks out of a total of $N$ inks is given by the binomial coefficients

$$M_n = \frac{N!}{(N-n)!n!}. \tag{13.25}$$

Table 13.2 gives an example for $N = 8$. The total number of cases to be considered for $N = 8$ thus amounts to $M_{\text{all}} = \sum_n M_n = 255$. Following (13.21) and according to (13.7) the probability of finding a point covered with the pigment of ink $i$

[9]See fig. 6.1 for the brighter appearance (due to pigment stacking) of the $LK$ ink on the matte paper PR308 as compared to the other diluted ink channels.

[10]This section might be difficult to understand, because considering the luminance prediction for a combination of many inks is a little complicated.

**Table 13.2.:** Number $M_n$ of possible combinations of $n$ inks out of a total on $N = 8$ inks.

| $n$ | 1 | 2 | 3 | 4 | 5 | 6 | 7 | 8 |
|---|---|---|---|---|---|---|---|---|
| $M_n$ | 8 | 28 | 56 | 70 | 56 | 28 | 8 | 1 |

(regardless of the other inks) is obtained from the ink amount $I_i(K)$[11]

$$P_{[i]}(K) = 1 - \exp\{-s_i[I_i(K)]^{n_i}\}, \quad i \in [1, ..., N]. \tag{13.26}$$

The probability of finding a point with a combination of two inks $i$ and $j$ is then

$$P^{(2)}_{[ij]} = P_{[i]}P_{[j]}, \quad i \neq j, \quad i, j \in [1, ..., N], \tag{13.27}$$

where the superscript indicates the number of participating inks and the dependence on the blackness $K$ is suppressed. Then the probability of finding a combination of 3 inks $[i, j, k]$ is the product of the respective individual ink probabilities

$$P^{(3)}_{[ijk]} = P_{[i]}P_{[j]}P_{[k]} = \prod_{t=i,j,k} P_{[t]}, , \quad i, j, k \in [1, ..., N], \tag{13.28}$$

where $i, j, k$ are mutually different. In general, the probability of finding any combination of $n$ inks is

$$P^{(n)}_{[...]} = P_{[i]}P_{[j]}... = \prod_{t} P_{[t]}, \tag{13.29}$$

where the index $t$ runs over the $n$ mutually different participating inks, here symbolized as [...].

In order to obtain the probability of finding a single type of pigment of ink $i$ only (and not a pigment of any other ink), the order-1 probability (13.26) must be reduced by all the probabilities of finding the pigment of another or of several other inks in combination with the pigment of ink $i$. Similarly, to get the probability of finding the pigments of three specific inks only, the probability $P^{(3)}_{[ijk]}$ must be reduced by the probability of finding pigments of 1 or more inks in addition to the three inks $i, j, k$, and so on.

This reduction of the above basic probabilities $P$ is necessary, because the luminance depends on the specific combination of pigments being found in one point.[12] As (13.22) has shown, to obtain the reduced probabilities (indicated by a tilde (˜)

[11] At this stage the ink amount is converted into a probability of finding pigment. This probabilistic approach allows to understand and compute (within the present model) the effect on the luminance when many inks are combined. Of course reality will deviate from the model prediction due to effects which are not captured by the present model. Here $I_i(K)$ is the ink amount of ink $i$ printed.

[12] This is certainly true for the PK and MK inks on matte paper, but perhaps not critical here (GCVT ink set) for dilutions of the PK ink which all contain the same pigment.

below) it is useful to proceed from the highest to the lowest order, starting from order $n = 8$ and then work back to the order $n = 1$.

In the order $n = 8$ there is only one case to be considered for finding all $N = 8$ inks. The probability is

$$\tilde{P}^{(8)}_{[ijklmnop]} = P^{(8)}_{[ijklmnop]} = \prod_{t=i,j,k,l,m,n,o,p} P_{[t]}, \tag{13.30}$$

with all inks $i, j, k, l, m, n, o, p$ being mutually different. Now the probability of finding 7 inks where ink $o$ is lacking is given by

$$\tilde{P}^{(7)}_{[ijklmn\ p]} = P^{(7)}_{[ijklmn\ p]} - P^{(8)}_{[ijklmnop]}. \tag{13.31}$$

This applies to all $M_n = 8$ combinations of order $n = 7$, because all inks are participating in $P^{(8)}_{[ijklmnop]}$, thus

$$\tilde{P}^{(7)}_{[*******]} = P^{(7)}_{[*******]} - P^{(8)}_{[ijklmnop]}. \tag{13.32}$$

On the next higher level, the probability of finding only 6 inks is obtained by reducing $P^{(6)}_{[******]}$ by $P^{(8)}_{[ijklmnop]}$ and by those probabilities $\tilde{P}^{(7)}_{[*******]}$ of 7th order for which the 6 inks from the 6th order are contained in the 7 inks of the 7th order. Hence

$$\tilde{P}^{(6)}_{[ijklmn]} = P^{(6)}_{[ijklmn]} - \left( \sum_{\substack{i,j,k,l,m,n \\ \text{participate}}} \tilde{P}^{(7)}_{[*******]} \right) - P^{(8)}_{[ijklmnop]}. \tag{13.33}$$

In the 6th order we have 28 cases (ink combinations) and the sum over the $\tilde{P}^{(7)}_{[*******]}$ has 2 cases each, because out of the 7 inks of $\tilde{P}^{(7)}_{[*******]}$ 6 inks are fixed (determined by the 6th order) and the 7th ink can only be one of the $8 - 6 = 2$ two remaining inks out of the 8.

This procedure has to be continued up to the eight terms of order 1

$$\tilde{P}^{(1)}_{[i]} = P^{(1)}_{[i]} - \Big(\text{2nd-, 3rd-, 4th-, 5th-, 6th-, 7th-order } \tilde{P} \text{ terms}\Big) - P^{(8)}_{[ijklmnop]}. \tag{13.34}$$

In total one has to compute 255 $\tilde{P}$ terms from the different orders. To obtain these terms, say for a particular order, one has to find those higher order contributions which contain the same inks and subtract the higher-order probabilities from the probability of the term considered at the current oder.

Once the true probabilities $\tilde{P}$, i.e. the probabilities for finding a particular combination of inks exclusively, one can obtain the luminance reduction due to the specific combination of inks. The luminance reduction then is the product of the probability $\tilde{P}$ and the luminance reduction $L_p - L_j^\infty$ from paper white to the luminance of the pigment. Here the luminance reduction is the mean value of the

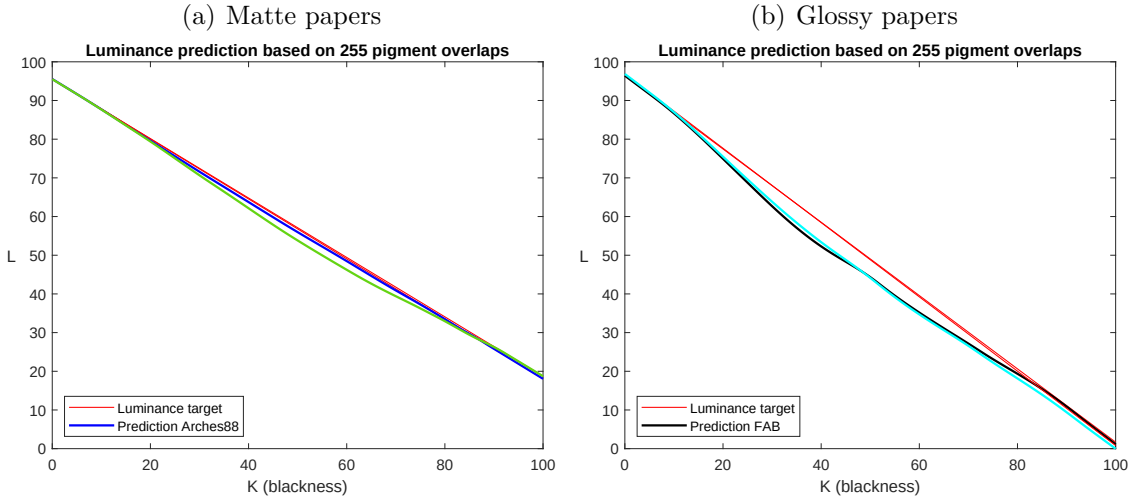


**Figure 13.8.:** Luminance prediction according to (13.36) for nominally linearly printing GCVT ink distributions for matte papers (a) and for glossy papers (b). The red lines represent the linear targets. The colors indicate the paper: Arches 88 (blue), PR308 (green), FAB (black), PRP (cyan).

luminance reductions of all participating pigments, because in this consideration all pigments are equally probable (see the geometrical interpretation in fig. 13.2 at lower order). Thus one obtains the luminance reduction at order $n$ for a particular ink combination

$$\tilde{R}^{(n)}_{[*]}(K) = \tilde{P}^{(n)}_{[*]}(K) \left[ L_p - \frac{\sum_j^{N_j} L_j^{\infty}}{N_j} \right], \tag{13.35}$$

where the subscript $[*]$ denotes the particular ink combination, the index $j$ runs over all inks contributing to $\tilde{P}^{(n)}_{[*]}$ and $N_j$ is the number of these contributing inks.

From the luminance reductions of all the 255 ink combinations one obtains the luminance prediction as

$$L^{\text{pred}}(K) = L_p - \sum_{n,[*]} \tilde{R}^{(n)}_{[*]}(K), \tag{13.36}$$

where the sum runs over the total of 255 cases which we have obtained at orders $n$ and with all possible ink combinations $[*]$.

The prediction according to (13.35) is shown in fig. 13.8 for different papers in combination with the GCVT ink set. In all cases the luminance is predicted for a standard ink distribution for which each channel has been mapped to print linearly as described in section 5.4. Therefore, it is expected that the luminance prediction reproduces the linear behavior (red lines). The present method (13.36) which is based on the consideration of all 255 different ink combinations possible[13] is only

[13] Not all these combinations must arise. For my present standard ink functions typically only three inks overlap. This is also true for the ink distributions on which fig. 13.8 is based.

(a) Ink distribution by QTR (b) Luminance by (13.36)

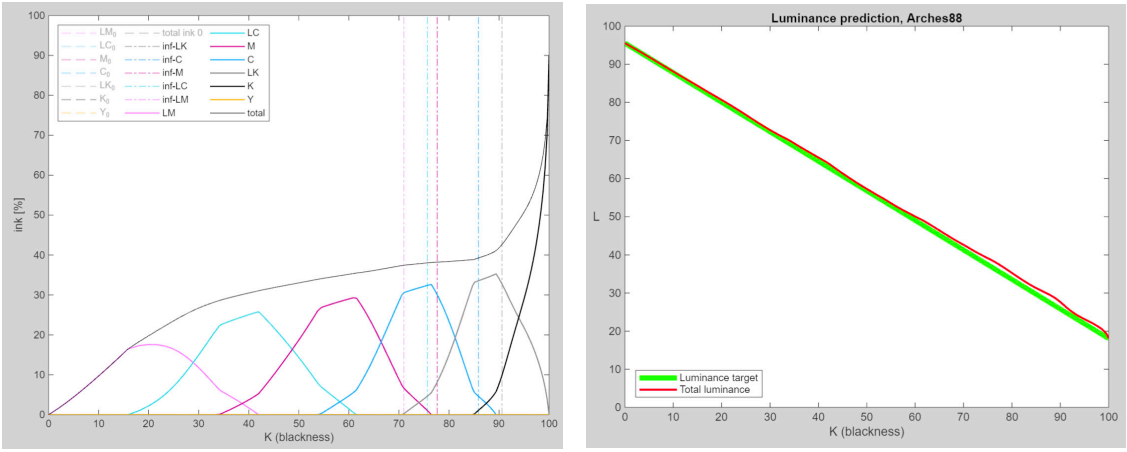


**Figure 13.9.:** (a) GCVT ink distribution by QTR which prints linearly on Arches 88. The vertical dash-dotted lines have no meaning here. (b) Luminance prediction (red) using (13.36) based on data from the quad file.

reliable for Arches 88 (blue line in (a)) and fair for PR308 (green line in (a)). For the glossy papers FAB (black line in (b) and PRP (cyan line in (b)) the prediction is too dark in the midtones. In contrast to this poor prediction, the prediction based on the pigment mapping described in section 13.5 does an excellent job for all these four cases (not shown). From these experiments it is concluded that the luminance prediction based on (13.36) works best on smooth matte papers. The more structure the surface of the paper has, in particular in case of natural glossy papers (FAB,PRP), the more the luminance of the midtones is underpredicted.

All tests and the good luminance prediction for Arches 88 which involves all inks except for the toner ($LLK$) and the $Y$ channel (second MK) suggests that the implementation is correct. Since the luminance produced by quad files created by other applications, e.g. by QTR, cannot be predicted by (13.24) (the ink ansatz functions are not known), one must resort to the method (13.36). Figure 13.9(a) shows an example for an ink distribution from a quad file created with QTR which is expected to print linearly. The luminance prediction by (13.36) is shown in fig. 13.9(b). It yields an almost satisfactory result. Unfortunately, (13.36) underpredicts the luminance for glossy papers.

To better pinpoint the problem, I created nominally linearly printing ink distributions where the inks overlap is very narrow with overlap parameter $\Delta K_o = -5$. From fig. 13.10 for PRP the $K$ ranges in which only a single ink is printing lie on the linear target curve. This is not surprising, because the fit parameters of the calibration plot are obtained for the individual inks printing. But in the narrow ranges where two inks are combined, the luminance is too low. Hence, it is the combination of inks which is not correctly predicted. Since the prediction for the smooth matte Arches88, it is likely that combined inks print too dark due to effects related to the paper surface (structure, reflectivity) and the ink amount. Also the

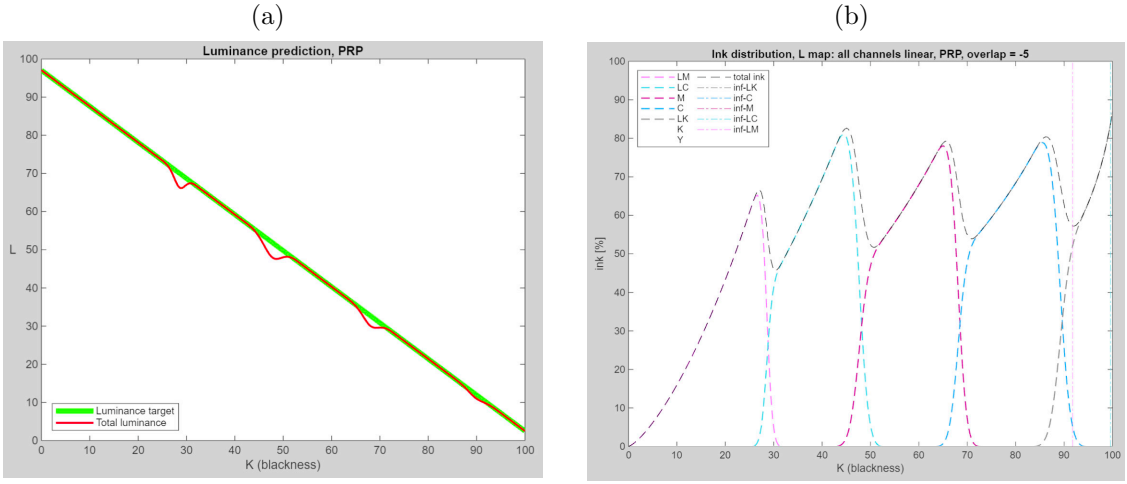


**Figure 13.10.:** (a) Luminance prediction acording to (13.36) and (b) corresponding nominally linearly printing ink distribution with narrow overlap $\Delta K_o = -5$ for the glossy paper HFA PRP.

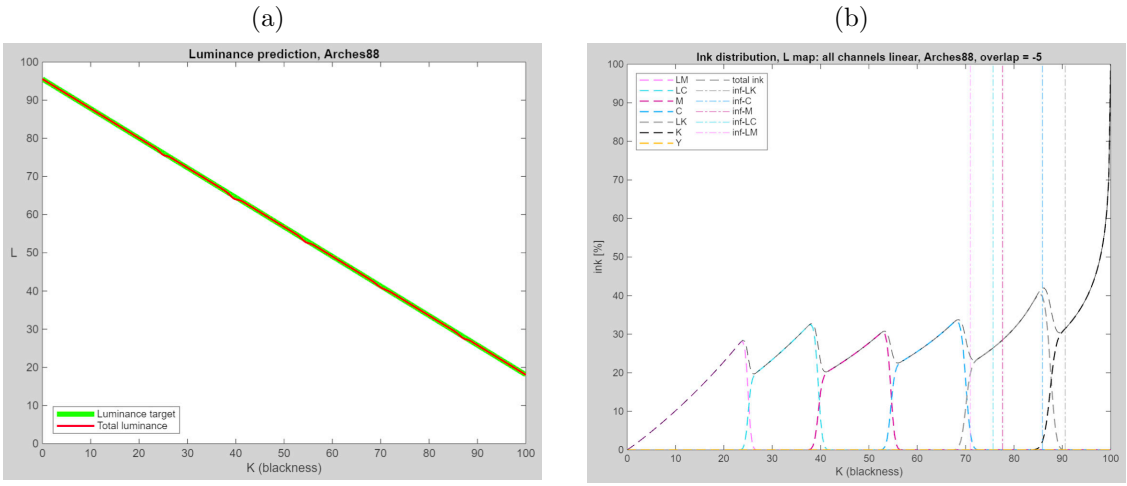


**Figure 13.11.:** (a) Luminance prediction acording to (13.36) and (b) corresponding nominally linearly printing ink distribution with narrow overlap $\Delta K_o = -5$ for the matte paper Arches 88.

assumption that the ink droplets are placed randomly in time is not correct. But the effect of the this violated assumption does not seem to be crucial in view of the good result for Arches 88.

A possible explanation is as follows. It is well known that the luminance of a printed structured surface is reduced from that of a perfectly smooth surface. Since the light of the measurement device has an angle of incidence of 45° with respect to the surface (or the normal), parts of the structured surface may be in the shadow leading to a kind of micro shadowing. Furthermore, the light scattered from a

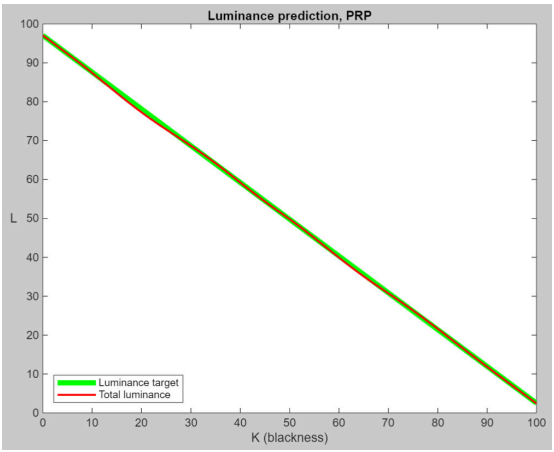


**Figure 13.12.:** Luminance prediction for PRP (linear target) according to (13.36) after replacing $P^{(2)}_{[ij]}$ by $a_{[ij]}P^{(2)}_{[ij]}$ with some phenomenological factors $a_{[ij]}$. This result must be compared with the cyan curve in fig. 13.8(b).

pigment particle sitting in a valley of a structure may be scattered multiple times and may thus reduce the light being detected by the measurement device at an angle of 90° with respect to the surface. These effects are already included in the measured luminance of the single inks from the calibration plot. But if these effects are present, the pigment coverage/probability (13.26) deduced from the luminance by (13.6) and (13.7) is estimated too low for structured surfaces. As a result, the probability $P_{[ij]}$ in (13.27) for two pigments to overlap (and higher orders as well) is also predicted too small. When the luminance is then reconstructed from the probabilities using (13.36), first order terms $P_{[i]}$ are treated correctly, because they represent contributions from only one ink, and these contributions rely on the measured luminances. But in regions where two (ore more) inks are combined the second- and higher-order terms are subtracted from the first-order ones to obtain the luminance in the overlap region of inks. Since the subtracted terms from higher orders are too small and the pigment luminance is essentially the same for all (glossy) inks, the effective pigment covered region is predicted too large. As a result of this error in the higher-order terms, the predicted luminance is too small (see e.g. figs. 13.10(a)).

To phenomenologically compensate this error the luminance prediction can be improved by introducing empirical factors by which the overlap areas/probabilities $P_{[ij]}$ are increased (reducing the total pigment coverage in the ink overlap regions). For instance, introducing correction factors $a_{[ij]} = 2.2$, 1.44, 1.13 and 1.02 for the ink overlap regions from bright to dark and replacing $P_{[ij]} \to a_{[ij]}P_{[ij]}$ one can achieve the luminance prediction shown in fig. 13.12 for PRP. This method seems to be relatively robust with respect to variations of the ink overlap parameters or, more generally, to the ink distribution functions. However, the set of factors $a_{[ij]}$ has to be determined empirically for each paper–ink combination and they may also depend on the blackness $K$ where the overlap arises.

# 14. Hahnemühle Fine Art Baryta (FAB)

In the following some further experimental results with Hahnemühle's Fine Art Baryta (FAB) are described. As mentioned above, the general parameters for FAB are $L_p = 96.41$, $L_m = 2.5$, $\alpha = 80\%$. The linear curve

$$L_{\text{tar}}(K) = L_p - (L_p - L_m)\frac{K}{100} \tag{14.1}$$

is targeted. For this glossy paper only the PK subset of the GCVT ink set are used.

## 14.1. Linearization

Based on the linearization of all ink channels, fig. 14.1 shows the initial distribution of the amount of pigment (full lines), the necessary targeted pigment (from the LK channel) (black line), and the actual ink amounts (dashed lines). The ink limit is 80%.

Figure 14.2 shows the necessary shift to make the raw luminance curve linear. I also used a new smoothed shift curve, which was obtained by first linearly interpolation the 21 shifts (based on measuring the step wedge) to the 256 grid points. These data were then smoothed by moving averages using a span of 20. The resulting curve, shown in blue, represents the original data better than the 6th-order polynomial fit (red dashes), while being much smoother. It seems that the smoothing adds to the well behavior of the final curve. I also found a remark about smoothing in the documentation of Richard Boutwell's software.[1] Obviously the 6th-order polynomial fit is very smooth, but cannot sufficiently capture the character of the necessary shift.

Luminance curves are shown in fig. 14.3. The initial curve (black circles) shown qualitatively the same very small deviations from the linear target curve as PR308 (compare with fig. 13.6) and Arches88 (cf. fig. 7.2), i.e., slightly to dark in the mid tones and highlights and slightly to bright in the shadows. The shifted, i.e. linearized, ink distribution is shown by orange dots. The linearization has been accomplished satisfactorily.

[1] https://www.bwmastery.com/.

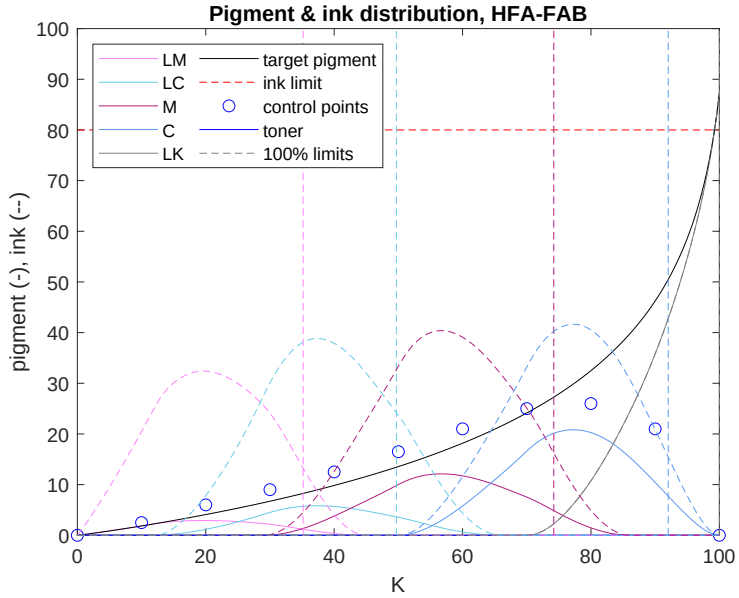


**Figure 14.1.:** A possible ink distribution for GCVT on FAB. Shown are the targeted pigment amount for a linear response (black line), the pigment amounts of the inks (full lines) and the corresponding ink amounts (dashed lines). The vertical dashed lines indicate the $K$ value at which the repective ink would reach $K_i^{\text{ink}} = 100\%$ if it would be printed along a linear output curve. The blue circles are posssible control points in case of neutralization.

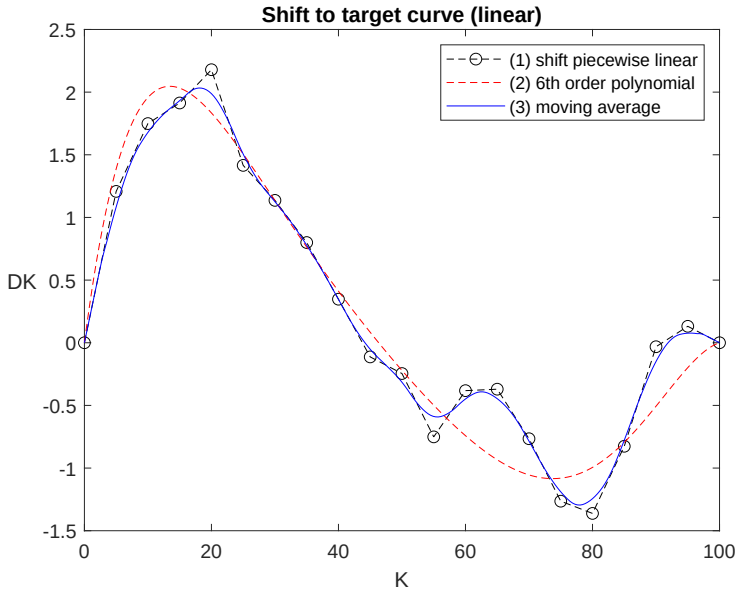


**Figure 14.2.:** Necessary shifts for linearization determined by measuring the 21 step wedge. Shown are the linear interpolation of the measurement points (circles, black dashed line), the smoothed curve by running averages (full blue line) and the 6th order polynomial fit (red dashed line). GCVT on FAB.

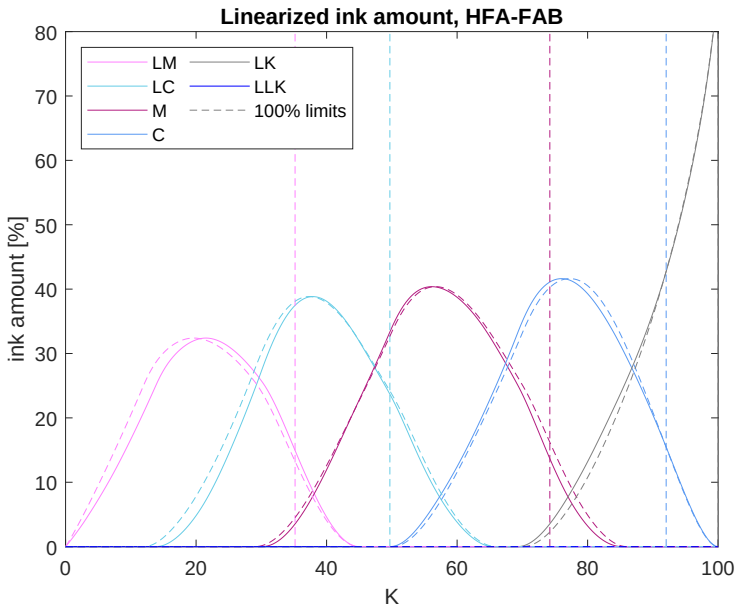


**Figure 14.3.:** Shifted ink distribution after linearization (full lines) in comparison with the non-linearized ink distribution (dashed lines) for GCVT on FAB.

## 14.2. Neutral version

I needed two iterations to arrive the current neutral version of the quad. During the process I had to increase the amount of blue ink repeatedly. From fig. 14.4 it is seen that the quad still prints sightly too warm for $K = 90$ and 95. The luminance of the neutralized version (open black triangles) deviates from the linear curves. The linearization (green triangles) still prints slightly to light for $K \lesssim 40$. I have no explanation for this. Most likely, the small residual deviations from the linear target are due to the uncertainty of the printer output and the ColorMunki measurements.

The print out of a bull's eye is shown in fig. 14.5. While the carbon version appears to be smooth enough, the neutral version has a tendency towards banding. Presumably, the overlap parameter[2] of $\delta = 0.08\%$ (corresponding to $\Delta K = 8$) still seems too small.[3] This demonstrates again how important a smooth transition and overlap between the inks is.

Finally, fig. 14.6 shows the shift $\Delta K$ necessary to shift the neutralized luminance curve to the linear curve. As a result of the shift, the ink curves are moved in $K$ as shown in fig. 14.7.

[2]The overlap parameter $\delta$ is the fraction (of 100) by which the ink of one channel reaches (is non-zero) beyond the maximum points of the neighboring channels; see e.g. fig. 14.3 for $\delta = 0.08$.
[3]For PR308 (carbon) I had to use $\delta = 0.12$.

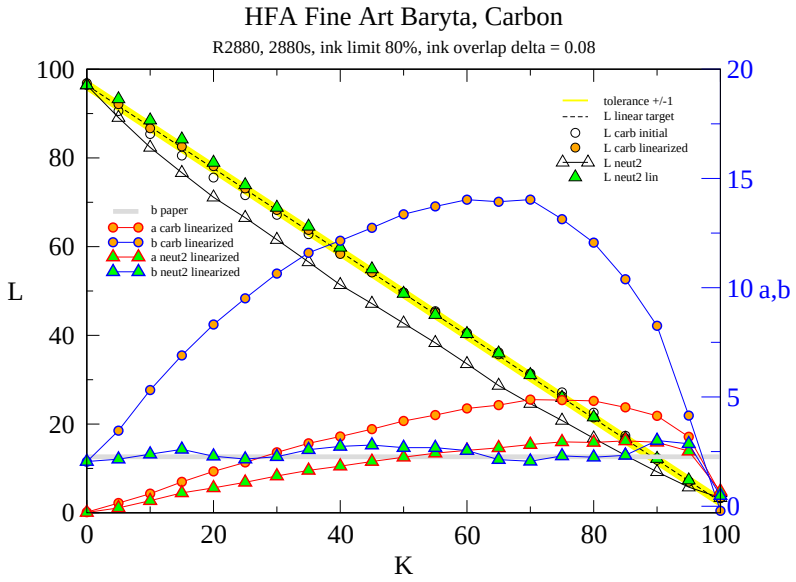


**Figure 14.4.:** ColorMunki measurements of the luminance of the 21 step wedge for GCVT on FAB. Shown are the original luminance curves (from linearizing all ink channels) in comparison with the linearized luminance (by $K$ shift) for both the carbon and the neutral version (see legend). The linear target curve is dashed, surrounded with a yellow tolerance level of $\Delta L = \pm 1$. Also shown are the Lab-$b$ and Lab-$a$ curves for both cases. The Lab-$b$ of the paper is indicated by the thick gray line.

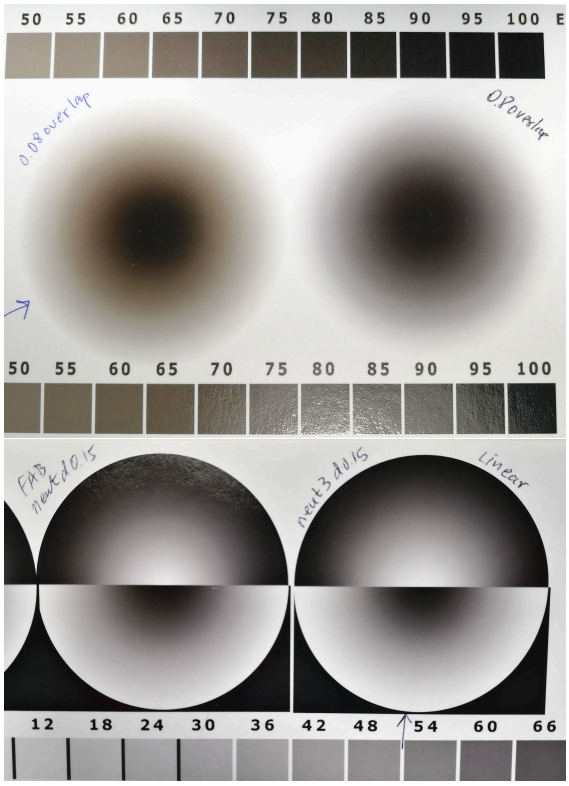


**Figure 14.5.:** Bull's eyes on FAB for overlap parameter $\delta = 0.08$ ($\Delta K = 8$, top row) and $\delta = 0.15$ ($\Delta K = 15$, bottom row). Top left: Carbon version, top right: neutralized version, bottom left: neutral version before linearization, bottom right: neutral version after linearization.

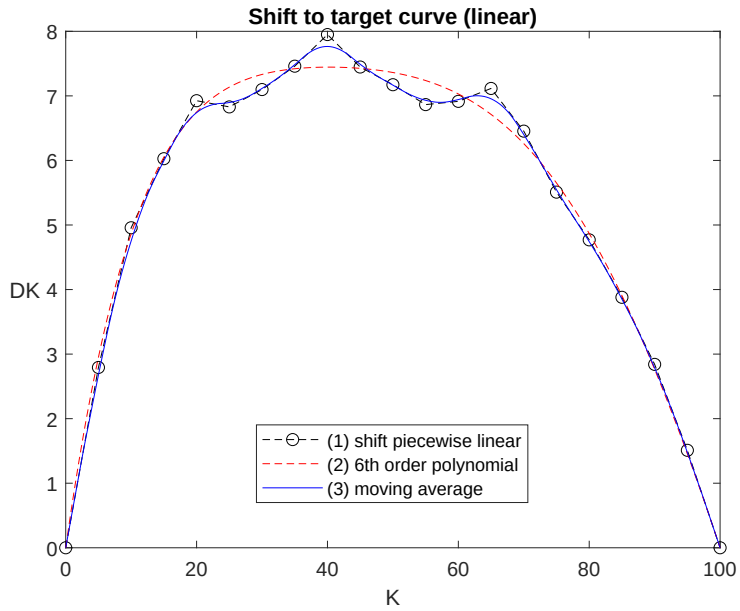


**Figure 14.6.:** Shift $\Delta K$ necessary to linearize the neutral luminance curve (open black triangles in fig. 14.4).

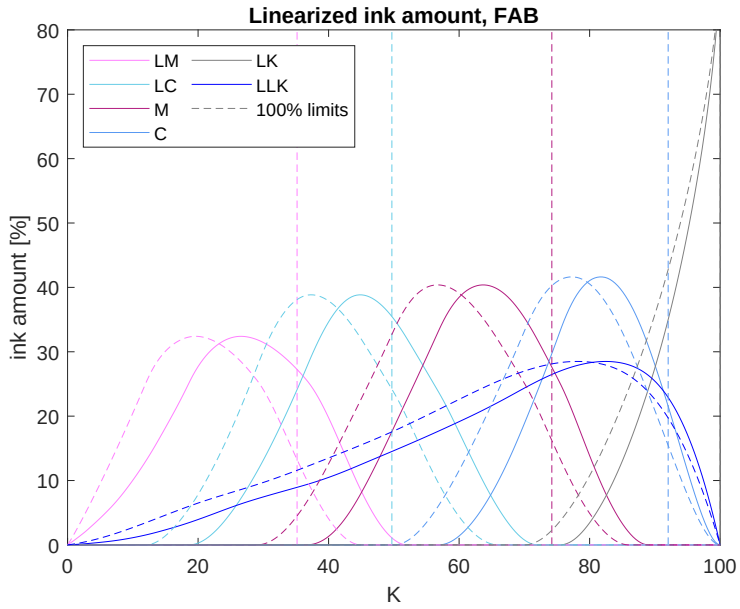


**Figure 14.7.:** Luminance curves for the neutralized ink distribtion before (dashed lines and open black triangles in fig. 14.4) and after linearization (full lines and green triangles in fig. 14.4).

# 15. Hahnemühle Photo Rag Pearl (PRP)

## 15.1. Calibration

Figure 15.1 shows the calibration plot on the full scale with ink limit $\alpha = 100$. The curves show the well known behavior. The data almost collapse to a single curve when plotted on the pigment scale $c_i K_{\text{ink}}$ (fig. 15.2). An exception is the $LLK$ toner curve, which is not considered. As we have seen previously, the luminance of the $LK$ channel is larger than the luminance of the diluted inks in the lower third of the pigment scale when the same amount of pigment is printed. This effect is (as mentioned before) hypothesized to be due to a pigment stacking effect of the pigments within a single droplet of ink. The stacking is caused by the high concentration of pigment in the $LK$ ink. Therefore, the stacked pigment particles cannot contribute to a reduction of the luminosity of the paper. But this does not play a major role when using a linearization of all ink channels independently and the $LK$ ink is printed in the dark regions only. Finally, fig. 15.3 shows the global modified exponential fit (red curve) for which all luminance data values have been multiplied by the weight factor $c_i$ (pigment concentration weight). The modified exponential fit parameters are given in table 15.1.

The asymptotic values $L_i^\infty$ which fit the ink characteristics of $LM$ and $LLK$ are unrealistic. The reasons seem to be as follows. (a) for $LM$ the luminance range over which a fit is possible is relatively narrow which results in a large uncertainty about $L_{LM}^\infty$. But this is not a big problem as long as the ink is used in the range for which data are available. (b) The luminance of the toner ink has been acceptably fitted by a modified exponential. The true dependence is, however, more complicated, because the toner ink is composed of a mixture of two different pigments (Roark, 2023) which will have different decay rates with $K_{\text{ink}}$ and different asymptotic luminances. Therefore, the value for $L_{LLK}^\infty < 0$ serves the fit in the accessible luminance range, but is not a meaningful asymptotic limit.

## 15.2. Carbon version

Luminance curves for PRP are shown in fig. 15.4. All data gave been created with my code `MakeQuad`. Based on the fit, a value $L_m = L_{LK}(K = 100) = 0.81$ might be expected. This value is automatically suggested by `MakeQuad`. But linearizing with respect to $L_m = 0.81$ shows that the ink–paper combination is not really

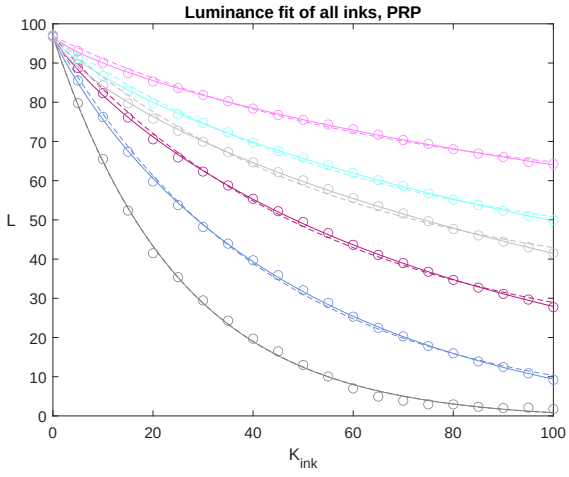


**Figure 15.1.:** Fit of the calibration print for PRP. Shown are the measured data (circles), the exponential fit (dashed lines) and the modified exponential fit (full lines) on the ink-amount scale $K_{\text{ink}}$.

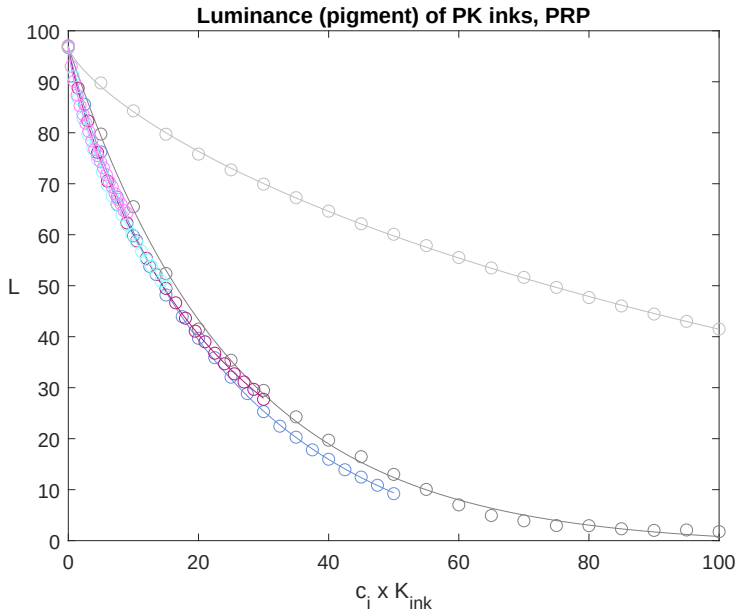


**Figure 15.2.:** Fit of the calibration print for PRP on the pigment scale. The toner curve ($LLK$) has not been scaled, because it a PK pigment concentration does not make sense for this ink.

able to produce such a deep black (red crosses in fig. 15.4). Linearization (red squares) does not change the result very much, because the result obtained within the straight approach (linearizing all ink channels) is already almost linear, except for the deepest blacks. Therefore, the $K$ shift during the linearization is very small.

In another attempt, the target $L_m = 2.5$ has been selected, corresponding to the luminance values achieved for $K = 100$. Surprisingly, the measured luminance data are almost indistinguishable from those for $L_m = 0.81$. I have checked that the quad files are indeed different. For example, at $K \approx 60$ at which the $M$ channel peaks, the maximum ink values in the quad files are 32532 ($L_m = 0.81$) and 31448 ($L_m = 2.5$). This is 3.3% less ink in case of $L_m = 2.5$, but the difference

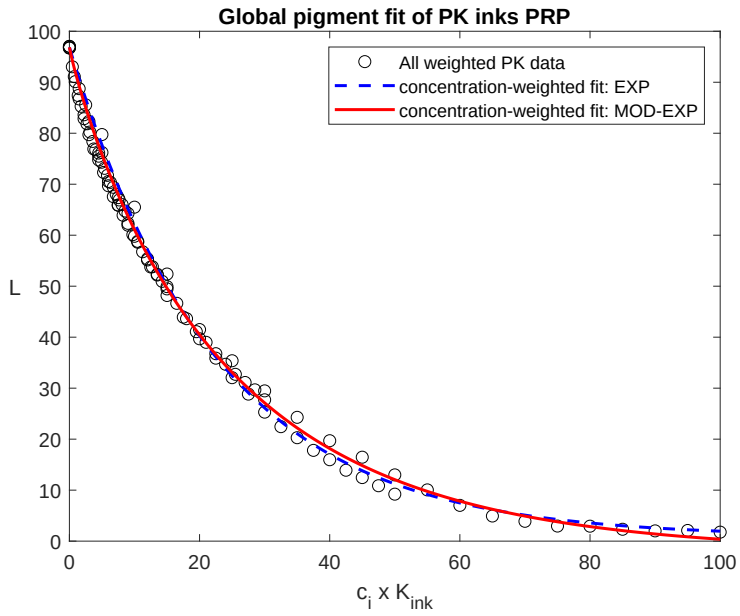


**Figure 15.3.:** Fit of the calibration data for PRP in which all data points have been weighted by the concentration $c_i$ shown on the pigment scale. The toner ink is not shown.

**Table 15.1.:** Fit parameters for the GCVT ink on Hahnemühle Photo Rag Pearl (PRP) obtained by least-squares curve fitting for $\alpha = 100\%$. The white point is at $L_p = 96.9$. The channel $G$ indicates the pigment fit of the concentration weighted data (red curve in fig. 15.3).

| Channel | $L_i^\infty$ | $s_i$ | $n_i$ |
|---|---|---|---|
| $LM$ | 17.929 | 0.0153 | 0.773 |
| $LC$ | −1.372 | 0.0186 | 0.773 |
| $M$ | −0.918 | 0.0230 | 0.862 |
| $C$ | −6.637 | 0.0284 | 0.909 |
| $LK$ | −0.997 | 0.0391 | 1.004 |
| $LLK$ | −24.942 | 0.0201 | 0.740 |
| $G$ | −2.235 | 0.0552 | 0.909 |

is not visible in the luminance plot. Therefore, one may tend to conclude that the deviation of the measurement (green circles) from the green target line is due to a lack of reliability of the printer. In fact, the luminance of the linearization yields the opposite deviation: the luminance of the linearized data (open and full green diamonds) is somewhat to high. As similar effect has been observed before for Arches88 (fig. 7.2). Perhaps one cannot do better with the current equipment.

Ink distribution curves are shown for PRP in fig. 15.5 for a linear luminance target curve with $L_m = 2.5$. During the linearization the curves are shifted to the right. Therefore the luminance is increased (compare green circles and green

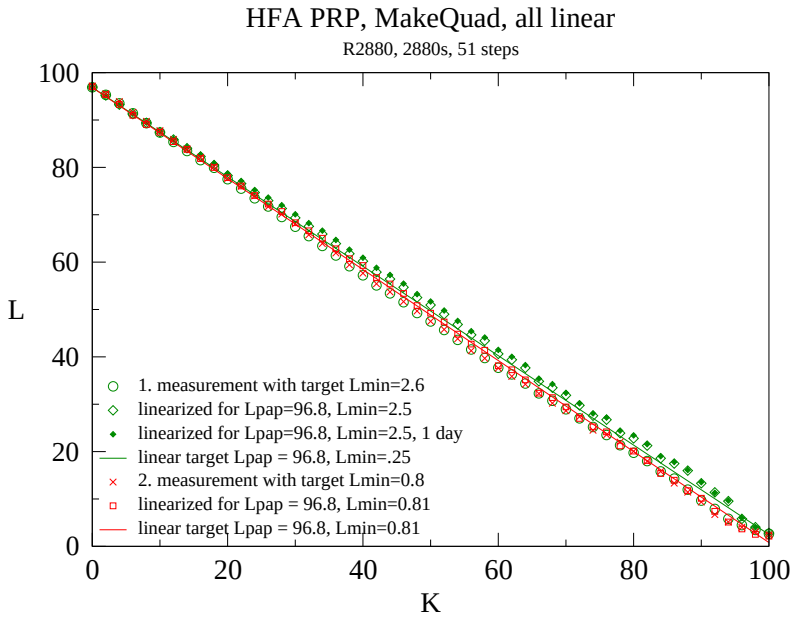


**Figure 15.4.:** Luminance curves for Photo Rag Pearl (PRP). Non-linearized and linearized data are shown for two black point targets: $L_m = 0.81$ (red) and $L_m = 2.5$ (green). The symbols are explained in the legend.

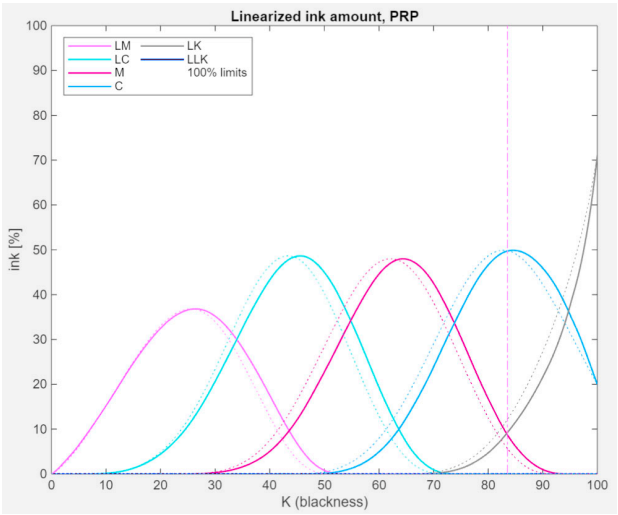


**Figure 15.5.:** Ink amounts on Photo Rag Pearl (PRP) for a linear target with $L_m = 2.5$. Curves are shown before (dotted) and after (full) linearization. Pure carbon – no toner applied.

diamonds in fig. 15.4). The linearization was based on running averages over 25 data points out of the 256 values for $K$ to which the 51 measured data points (green circles in fig. 15.4) were linearly interpolated. All data and graphs in this section were obtained using the code `MakeQuad`.

**Table 15.2.:** Toner amount $K^{\text{ink}}_{LLK}(K)$ required for neutrality of the ink on HFA Fine Art Baryta (FAB) and Photo Rag Pearl (PRP), before linearization. For PRP the value Lab-$b = 1.88$ was targeted.

| $K$ | 0 | 10 | 20 | 30 | 40 | 50 | 60 | 70 | 80 | 90 | 100 |
|---|---|---|---|---|---|---|---|---|---|---|---|
| FAB | 0 | 3 | 6.5 | 9.7 | 14 | 18 | 23 | 27 | 28.5 | 25 | 0 |
| PRP | 0 | 2.7 | 6.1 | 10.0 | 14.6 | 19.5 | 24.6 | 28.7 | 30.6 | 26.2 | 0 |

## 15.3. Neutralization

For the neutralization I targeted $L_m = 2.5$ and added to the pure carbon ink distribution (printing according to green circles in fig. 15.4) toner ink according to the toner ink curve previously obtained for FAB. When the toner is adapted such as to match as good as possible the Lab-$b$ value of the paper white (Lab-$b = 1.88$) the toner curve needed only a slight modification. Table 15.2 shows the different values on the grid of control points (see section 8).

## 15.4. Linearization

Figure 15.6 shows the Lab values before and after linearization. Lab-$b$ of the carbon version (cyan dashed) is pretty large with a maximum of 14.0 at $K = 60$. The neutralized version before linearization is shown as full lines in brown, magenta and cyan. The toner darkens the output (brown line). In a first print of the 21 step wedge using the linearized quad with QTR yields the black curve for luminance and the blue curve (with circles) for the Lab-b values.The Lab-$b$ is well controlled near Lab-$b = 1.88$ (black dotted line).[1] The Lab-$a$ still remains with a maximum of Lab-$a \approx 3$ near $K = 80$. But the toner has also reduced the Lab-$a$ by a factor of two.

The shift $\Delta K$ with values up to $\Delta K \approx 10$ required for linearization of the neutral version is shown in fig. 15.7. The shifted ink curves are shown in fig. 15.8.

The luminance curve (black) in fig. 15.6 is close to the theoretical linear line (green), but deviations exist. The maximum deviations are about $\Delta L \approx +2.0$. I am not fully satisfied with this result. Therefore, I made a second measurement of the printed step wedge on the other day. The result is indicated by the orange circles. This luminance (orange circles) agrees very closely with the first measurement (black lines), thus showing the same deviation. This confirms that the reproducibility of the ColorMunki is pretty good. Therefore, it might not be the main culprit for the deviations from the ideal linear luminance curve. On the same day, I printed the 21 step wedge again and measured it with the ColorMunki immediately. The ColorMunki did not need a re-calibration. It was thus in the same calibration state as for the orange circles. The measurement of the second print

[1] The toner amount resulted from the fourth iteration step, because I first targeted Lab-$b = 0.5$. Then I noticed that this resulted in cooler tones than the paper white.

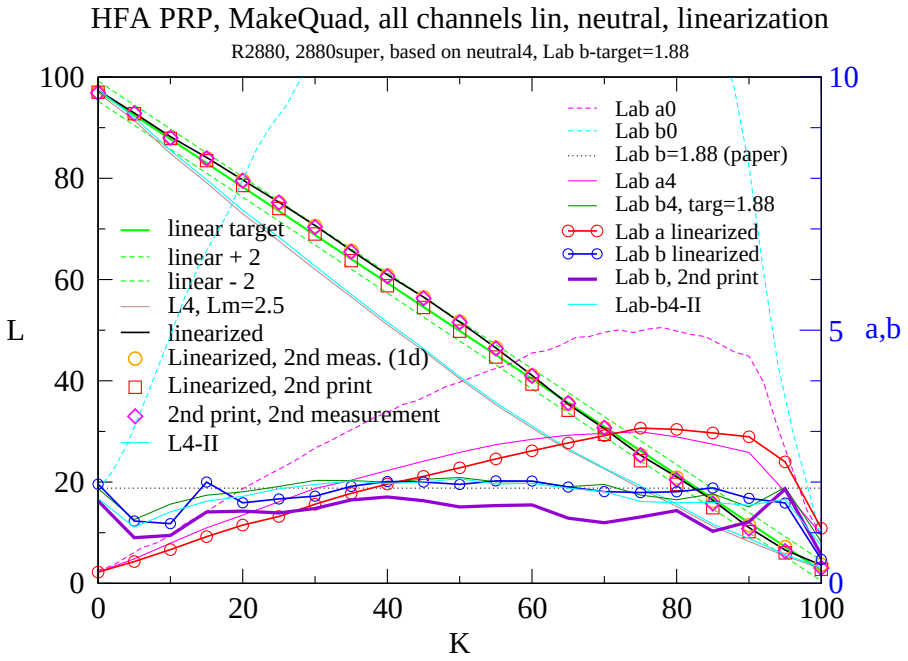


**Figure 15.6.:** Linearization of the neutralized version of the quad for HFA PRP. The final luminance curves is indicated by red squares and the final Lab- curve is the thick violet line. For an explanation, see the text. The green dashed lines mark ±2-deviations from the linear target curve (green). $L_m = 2.5$.

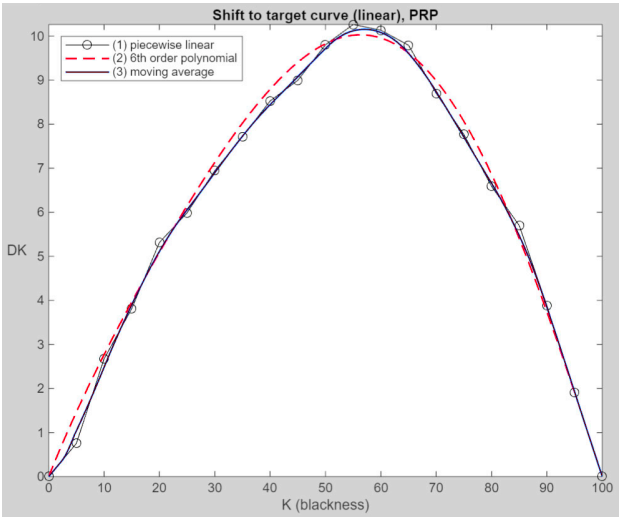


**Figure 15.7.:** Shift function $\Delta K(K)$ required to linearize the neutral version of the curves for PRP. Smoothing span for the moving averages is 25 data points.

yielded the red squares. This time the luminance (red squares) reproduce the ideal linear curve very well. For larger $K$ the luminance is slightly too low, though. But this deviation seems well acceptable.[2] This seems to suggest that the main factor of uncertainty is the present R2880 printer. The resulting Lab-$b$ for the second print

[2] In fact, for the second print $L_m = 2.76$ (close to the target $L_m = 2.5$), while the first print had $L_m = 3.68$, almost $\Delta L = 1$.

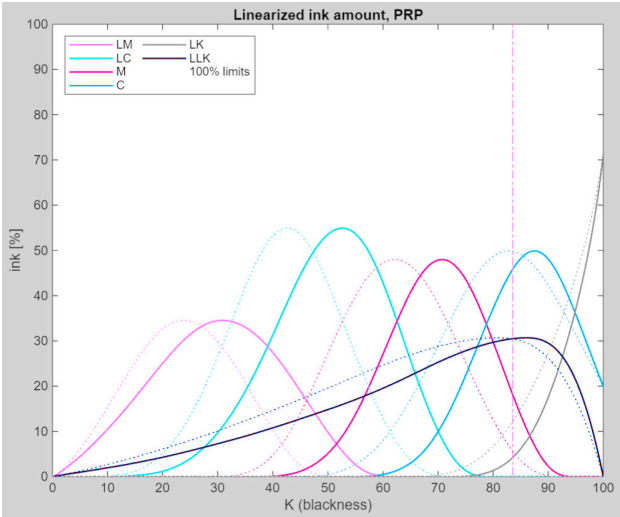


**Figure 15.8.:** Shifted ink curves (full lines) which linearize the original toned (neutral) curves(dotted lines).

is the thick violet line in fig. 15.6.

## 15.5. Effect of the drying time on luminance

But wait. On the next day I made a second measurement of the second print. As a result the luminance curve returned very close to the one of the ones of the first print (black line, orange circles). It now seems as if there is a drift of the luminance of the printed patches while drying. It is commonly accepted that such drift occurs. But I may not have paid enough attention to it (my bad), because I deemed it to have a very small effect. But here we are considering small deviations and this drying time may become important. From the measurements, I must conclude that the drift (if existent) mainly leads to a brightening of the print. This brightening should then be of the order of magnitude of the deviation of the black line from the linear curve. If the drift exists, I must have measured the luminance data of the linearized output (red squares) too early after the printing (I don't remember it, but I certainly did not wait for an hour). To preclude that also the neutral but non-linearized curve (brown line) was measured too early, I measured the step wedge once again. The luminance result is shown as a cyan line L4-II in fig. 15.6. The deviation from the original luminance curve L4 (brown line) is very small.

To better assess the effect of the drying time after printing before the step wedge is measured I made measurements with different time delays. This is illustrated in fig. 15.9 which shows the deviation of the measured luminance from the target luminance (here linear with $L_m = 2.5$). One can see that $L - L_{\text{tar}}$ is negative. This means the print is too dark in the mid tones. As time proceeds the print brightens in the mid tones. All measurements (up to 3h) were made with the same calibration state of the ColorMunki. The brightening effect may well be up to 2 units of Lab-$L$. In the present case there remains a small negative deviation from the target of the order of $\Delta L = 1$. For the measurement after 1d the ColorMunki

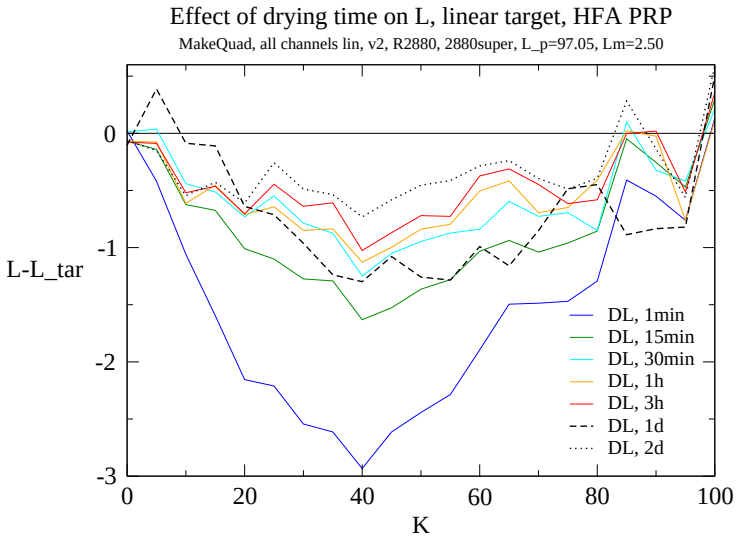


**Figure 15.9.:** Deviation of the luminance from the target luminance $L - L_{\text{tar}}$ (here $L_{\text{tar}}$ is linear) as a function of the drying time (see legend) of the printed 21 step wedge. The data were measured after linearization based on a well-dried step wedge and should, therefore, theoretically be zero.

had to be re-calibrated. The resulting measurement (black dashed line) does not continue the trend of brightening. The black dotted line is achieved after 2 days and re-calibration. Since the print is expected not to change any more after 1d, the deviation between the dashed (1d) and dottel (2d) line can be considered a measure for the reproducibility of the ColorMunki measurements. The associated error appears to be of the order of 0.5 Lab units in the mean.

If the step wedge printed with a quad that would perfectly fit the target is measured too early, then the measurement may fake the print being too dark. The following linearization based on the this print would then tend to make the linearized quad print lighter. If a print using this linearized quad is then measured after a sufficiently long drying time, it would appear too bright. Perhaps this is what had happened with the data in fig. 7.2.

I made also further prints and measurement, but I was not able to ultimately pinpoint or eliminate all uncertainties. From my experiments so far, I conclude

1. The drying time has an effect. Probably, a drying time of 1h is enough for the luminance of the print to stabilize. A drying time of one day is certainly safe.

2. The ColorMunki has a good reproducibility but it may, at times, also add to the uncertainty.

3. There exists uncertainties due to the fit functions from the measured data in the calibration print not exactly reproducing the measured luminance data (which also have an error). Perhaps a spline interpolation would be better.

But then the calculation of the ink amounts necessary for linearization would have to be made purely numerically on the $2^8$ grid. This is possible and would provide a way to evaluate the error propagation from the modified exponential fit to the computed luminance of the linearized ink distribution functions.

4. My impression is the output of the printer also has some variation. This was already seen in fig. 4.1 where the luminance functions $L(K_{\text{ink}})$ for the $K$ and $Y$ channels deviate from each other (may have to do with the cartridges and the priming). But also in fig. 15.1 one can notice an non-monotonous slope of the luminance of the $K$ channel in the region from $K_{\text{ink}} = 40$ and $K_{\text{ink}} = 60$ (almost a little jump from 55 to 60).

The two last aspects are probably the most important factors for deviations from the theoretical result. However, the linearization process does not depend on errors made by the fitting, because during the linearization a given combination of inks with fixed amounts is just printed at a blackness which differs by the shift $\Delta K$. And the errors made in computing $\Delta K$ (fig. 15.7) are much smaller than the deviation seen in fig. 15.6. Given the good reproducibility of the ColorMunki, the main culprit is probably the printer itself.

I was trying to use the fine art papers sparingly. Therefore, I made rather slender step wedges of which 14 fit on an A4 sheet such that about 1" at the leading and the trailing edge are not printed. Nevertheless, if a glossy paper is printed on ten or more times, the increasing number of slightly offset pizza wheel tracks the R2880 leaves on the paper (due its transportation mechanism) may slightly brighten the darkest black if their effect accumulates. I could see these traces only under a loupe.

# 16. Conclusions

The method presented allows to create a quad file for use in QTR which prints with carbon inks along a predefined target luminance curve $L_{\text{target}}(K)$, including a linear curve and a gamma corrected curve. The quad file is created in one go without the need to iterate. Iteration is required, however, when an additional toner ink is used.

The method requires a good fit of the characteristic ink curves $L(K_{\text{ink}})$ on which the mapping to the target curve relies. The method has been demonstrated for the GCVT ink set of Paul Roark for matte and for glossy paper. When using the method for matte paper care must be taken not to use light inks for very dark tones at high blackness $K$. The reason is the PK inks of this ink set cannot produce the darkest tones on matte paper if they are printed alone. Expressed mathematically, the linearization transformation becomes singular at the infinity limits of the respective inks.

To remedy this deficit, the individual linearization of all ink channels can be given up. In that case a luminance prediction for an arbitrary combination of inks would be very useful. Therefore, a luminance prediction method has been presented which can accurately predict the luminance of a combination of PK inks, MK inks and toner ink on matte and glossy paper. This allows to freely design the ink distributions, while still arriving at a very good approximation of the target luminance curve in one go. Yet, for matte paper the use of PK inks of the GCVT ink set at and beyond $K = 100$ is not recommended, because the PK inks would necessarily increase the black point $L_m$ which could be achieved with MK ink only. Such limitation does not apply to glossy paper.

An important factor to avoid banding is a smooth transition between inks with a sufficient overlap in $K$ of the ink curves. If the overlap is insufficient deviations from the perfect reproduction of the target luminance curve may arise. These deviations may not show up in the 21 step wedge. But printing a bull's eye is a critical test to unravel any banding phenomenon which (among other reasons) may be amplified by errors made by the printer (R2880) and the measurement device (ColorMunki Photo).

It is hoped that the methods presented will also prove useful for creating negatives for various alternative printing processes which often require particular density distributions as functions of $K$. In fact, any bijective density curve can be targeted. The adaptation to transmissive media seems to be straightforward.

# Bibliography

Arney, J. S. and Yamaguchi, S. (1999), The physics behind the Yule–Nielsen equation, *in* 'Proceedings of the Conference on Image Processing, Image Quality and Image Capture Systems (PICS-99)', pp. 381–385.

Beer, A. (1852), 'Bestimmung der Absorption des rothen Lichts in farbigen Flüssigkeiten', *Ann. Phys. Chem.* **162**, 78–88.

Lambert, J. H. (1760), *Photometria sive de mensura et gradibus luminis, colorum et umbrae (in Latin)*, Eberhardt Klett, Augsburg (Germany).

Moore, T. (2005), *Quad Tone Rip – User Guide.*
**URL:** *http://www.quadtonerip.com/User Guide.pdf*

Roark, P. (2023), *Universal – Glossy or Matte – Carbon Variable-Tone (Originally written 2016) Black and White Inkset Epson 7800, 9800 and other Epson printers.*
**URL:** *http://www.paulroark.com/BW-Info/7800-9800-Glossy-Carbon-Variable-Tone.pdf*

Vermont PhotoInkjet (2014), *The New Piezography Users Manual.*

# A. Remarks on fine tuning by changing the amount of ink

In section 7 we have accomplished the fine tuning or the linearization by $K$-shifting the ink distribution curves. This requires several interpolations as described. It seems the linearization in QTR is also based on $K$-shifting the ink functions.

Alternatively, one could think of changing the luminance by adapting the ink amount at the given equidistant $K$ values. The problem is that the ink amount required for a correction of the luminance depends on the inks. Therefore, for each ink a dedicated ink-amount correction is required as a function of $K$. Although this is doable, it seems too much effort in comparison to shifting the ink distribution functions described in chapter 7. On the other hand, for pure carbon printing (no toner) the corrections of the ink amount are expected to be very small such that a linearization of the ink curves $L_i(K_{\text{ink}})$ should be admissible to compute the ink amount correction (for fixed blackness $K$).

# B. Further calibration and linearization results

## B.1. HFA Photo Rag 308 (PR308)

The mapping used for PR308 with ink limit $\alpha = 60\%$ is shown in fig. B.1. The fit of the ink characteristics was made over the full range up to 100% ink. The ink ansatz functions (Gauß) for PR308 differ only in the data for $LC$ and $M$ from those used for Arches 88. The parameters are given in table B.1. Combining the ansatz functions and the ink mapping yields the final ink distribution for pure carbon printing shown in fig. B.2. It should be noted that the 100%-limits (vertical dashed lines) only apply to the non-linearized ink amount curves. Since the linearization by shifting the ink amount curves is made for constant luminance, the shift does not mean that the luminance is being changed by changing the ink amount. Table B.2 provides the numerical data which accomplish the linearization from the colored lines to the dashed lines in fig. B.2 (see also fig. 9.3).

Finally, fig. B.3 shows the luminance (black line) and Lab-$b$ (blue line) which

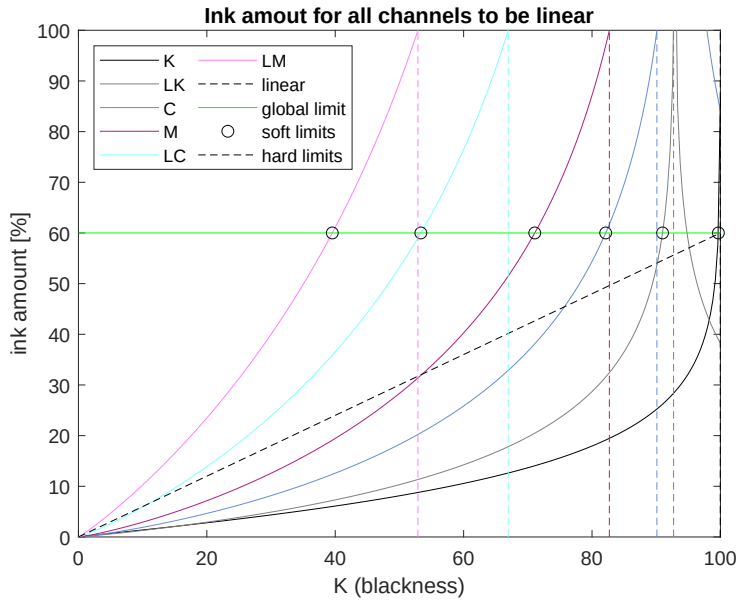


**Figure B.1.:** Mapping of the ink curves for HFA PR308 using $\alpha = 60\%$ and $L_m = 18.7$. The fit of the ink characteristics was carried out over the full range of ink delivery $[0, 100]\%$.

**Table B.1.:** Parameters for the Gauß ink ansatz functions used. The Gauss functions are centered at $\hat{K}_i$ and the full width at half maximum is $d_i$. $\alpha = 60\%$. The fit is made over $K_{\text{ink}} \in [0, \alpha]$ (Arches 88) and $K_{\text{ink}} \in [0, 100\%]$ (PR308).

| | HFA PR 308 | | Arches 88 | |
|---|---|---|---|---|
| channel | $\hat{K}_i$ | $d_i$ | $\hat{K}_i$ | $d_i$ |
| $K$ | 1.00 | 0.20 | 1.00 | 0.20 |
| $LK$ | 0.68 | 0.14 | 0.68 | 0.14 |
| $C$ | 0.55 | 0.16 | 0.55 | 0.16 |
| $M$ | 0.37 | 0.20 | 0.35 | 0.20 |
| $LC$ | 0.24 | 0.18 | 0.26 | 0.18 |
| $LM$ | 0.05 | 0.22 | 0.05 | 0.22 |

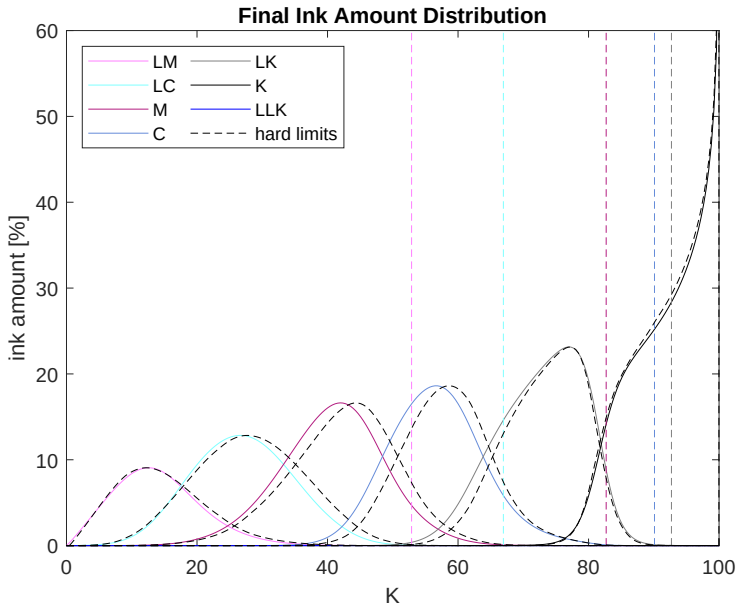


**Figure B.2.:** Final linearized distribution of the ink amount (dashed) for pure carbon printing on HFA PR 308 with $\alpha = 60\%$, $L_m = 18.7$, ink functions (6.3) with parameters according to table B.1. The fitting of the ink charactersitics was carried out over the full range $[0, 100]\%$.

**Table B.2.:** Numerical data for the linearization of the quad for HFA PR 308 (black curve in fig. 9.3 and fig. B.2). The luminance values at $K$ are shifted to $K_{\text{shifted}} = K + \Delta K$.

| $K$ | $K_{\text{shifted}}$ | $\Delta K$ |
|---|---|---|
| 0 | 0.0000 | 0.0000 |
| 5 | 4.4792 | −0.5208 |
| 10 | 9.7910 | −0.2090 |
| 15 | 15.5063 | 0.5063 |
| 20 | 21.0686 | 1.0686 |
| 25 | 26.0362 | 1.0362 |
| 30 | 31.6112 | 1.6112 |
| 35 | 37.1600 | 2.1600 |
| 40 | 42.4347 | 2.4347 |
| 45 | 47.2383 | 2.2383 |
| 50 | 52.3764 | 2.3764 |
| 55 | 57.0000 | 2.0000 |
| 60 | 61.9472 | 1.9472 |
| 65 | 66.2696 | 1.2696 |
| 70 | 70.5915 | 0.5915 |
| 75 | 75.3039 | 0.3039 |
| 80 | 79.7017 | −0.2983 |
| 85 | 84.7791 | −0.2209 |
| 90 | 89.2309 | −0.7691 |
| 95 | 94.5703 | −0.4297 |
| 100 | 100.0000 | 0.0000 |

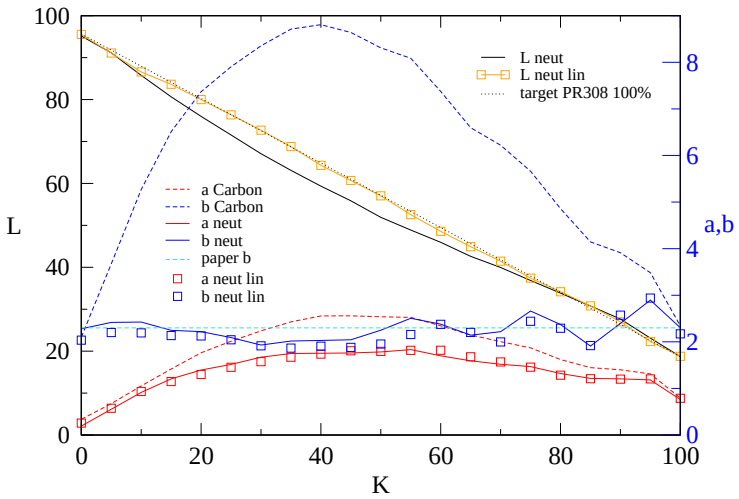


**Figure B.3.:** Neutralization of the GCVT ink on PR308. Shown are the luminance before (black line) and after linearization (organge line and squares). Also shown are the Lab-$b$ values before toning and linearization (blue dashed line), after tioning (full blue line) and after toning and linearization (blue squares).

**Table B.3.:** Amount of blue toner at the control points to make HFA PR 308 appear neutral. The ink limit is $\alpha = 60\%$. The resulting distribution of Lab $b$ is shown in fig. B.3 (full blue line).

| control point $K$ | 0 | 20 | 40 | 60 | 80 | 0 |
|---|---|---|---|---|---|---|
| ink amount [%] | 0 | 3.0 | 5.9 | 7.1 | 6.3 | 0 |

accomplishes neutrality. The toner amout (table B.3) was adjusted such as to move Lab-$b$ of the print to the Lab-$b$ value of the paper (cyan dashed line). The linearized data are indicated by squares. The luminance at $K = 10$ after linearization seems a little bit too low. But I have no plausible explanation for it other than the combined uncertainty of the printer and the measurement of the Lab-$L$ values before and after linearization.

Figure B.4 shows the final ink amount distribution required for a neutral and linear output. Since even more blue ink was used for PR308 as compared to Arches 88, the output is considerable darkened by the toner (fig. B.3). Therefore, a larger shift of the ink distributions was necessary to make the output linear. The numerical data are given in table B.4. In the shifted curves for the $K$ and $LLK$ (toner) channel one can recognize a slight discontinuity of the slope near $K \approx 90$. I trace this back to the relatively strong change of the slope of $\Delta K$ at $K = 90$ (fig. B.5). The 21 shifted $K$ values $K_{\text{shifted}}$ were linearly interpolated to the $2^8$ grid necessary for the quad. Spline interpolation of $K_{\text{shifted}}$ made the curves visually smoother near $K \approx 90$, but introduced artifacts near $K = 0$. Therefore, $K_{\text{shifted}}$ was interpolated linearly.

One might think of representing the $K$-shift $\Delta K$ by a low-order Fourier representation yielding a smooth continuous function $\Delta K(K)$. This is shown in fig. B.5. But the gain in making the ink curves in fig. B.4 even smoother than they are already, would be counteracted by the insufficient representation of extreme shifts $\Delta K$. I conclude again, the deviations from the linear response (even after linearization) in fig. B.3 is due to the printer/cartridges variability and the uncertainty of the Lab-$L$ measurements. But the reproducibility of the ColorMunki data is quite good.

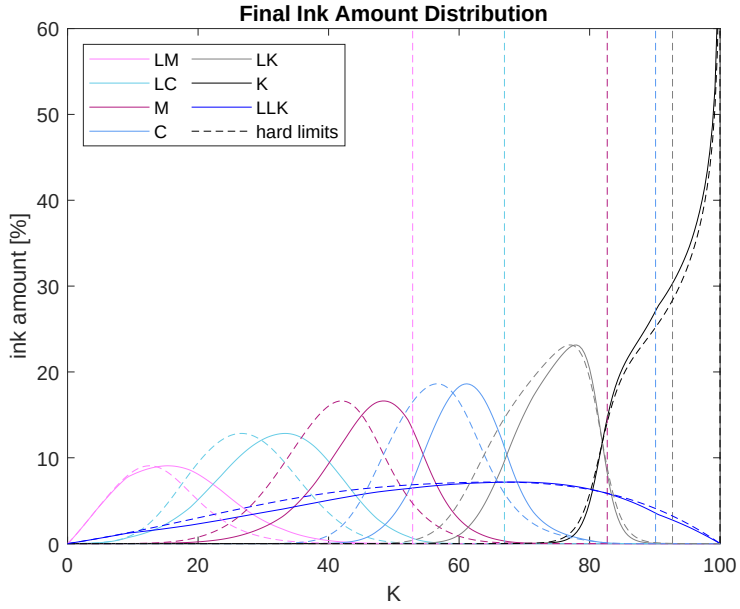


**Figure B.4.:** Final ink amount distribution for a neutral and linear output of GCVT ink on HFA PR 308. Shown are the ink distributions before (dashed lines) and after linearization (full lines). $L_p = 95.65$, $L_m = 18.7$. 100%-limits only apply to the ink curves before linearization (dashed).

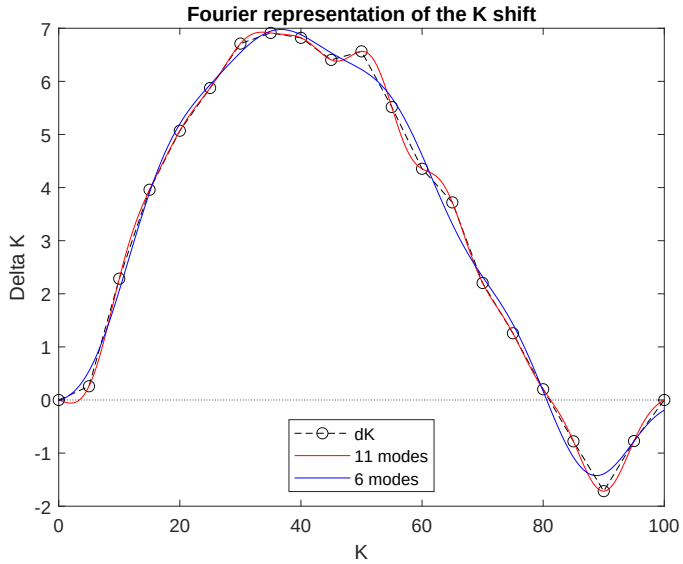


**Figure B.5.:** Required $K$-shift $\Delta K$ (circles and dashed line, table B.4) based on ColorMunki measurements and Fourier representations with different trucation order $N$. For 21 data points the maximum truncation order is $N = 11$ (red line).

**Table B.4.:** Numerical data for the linearization of the quad for HFA PR 308 after toning for neutrality. The luminance values at $K$ are shifted to $K_{\text{shifted}}$ by the amount $\Delta K$.

| $K$ | $K_{\text{shifted}}$ | $\Delta K$ |
|---|---|---|
| 0 | 0.0000 | 0.0000 |
| 5 | 5.2585 | 0.2585 |
| 10 | 12.2850 | 2.2850 |
| 15 | 18.9594 | 3.9594 |
| 20 | 25.0706 | 5.0706 |
| 25 | 30.8760 | 5.8760 |
| 30 | 36.7112 | 6.7112 |
| 35 | 41.9126 | 6.9126 |
| 40 | 46.8199 | 6.8199 |
| 45 | 51.4042 | 6.4042 |
| 50 | 56.5652 | 6.5652 |
| 55 | 60.5174 | 5.5174 |
| 60 | 64.3543 | 4.3543 |
| 65 | 68.7213 | 3.7213 |
| 70 | 72.2036 | 2.2036 |
| 75 | 76.2565 | 1.2565 |
| 80 | 80.2020 | 0.2020 |
| 85 | 84.2220 | −0.7780 |
| 90 | 88.2833 | −1.7167 |
| 95 | 94.2271 | −0.7729 |
| 100 | 100.0000 | 0.0000 |

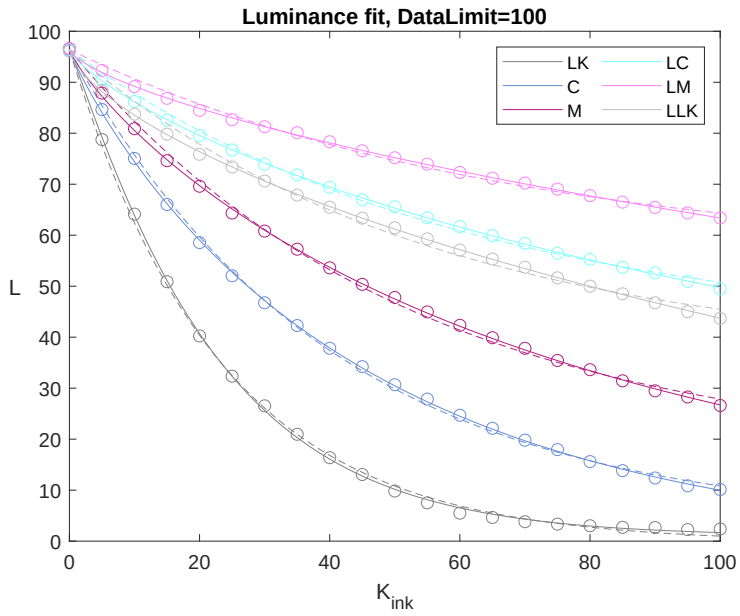


**Figure B.6.:** Luminance of the different glossy inks on Hahnemühle FineArt Baryta as function of the ink amount $K_{\text{ink}}$ on the full scale.

## B.2. HFA Fine Art Baryta (FAB)

The fit of the ink characteristics, i.e. the luminance as functions of the ink amount, when printing on Hahnemühle Fine Art Baryta (FAB) using the glossy part of the GCVT ink set is shown in fig. B.6 (full lines). One can notice certain deviations for the pure exponential decay (dashed) of the luminance. In particular, the luminance of the lightest ink ($LM$) has an almost linear dependence on $K_{\text{ink}}$, except for $K_{\text{ink}} \lesssim 20$, where there is a relatively rapid decay of $L$. I speculate this is due to the gloss effect the PK ink brings along with it. The pigment coverage is always glossier than the paper base. Thus if there would be no pigment in the ink, more light would be reflected away from the paper surface and the paper surface would indeed appear darker than without the GLOP cover.[1] This effect seems to be the reason for the relatively strong reduction of the luminance for $K_{\text{ink}} \lesssim 10$.

Figure B.7 shows the data and the fitting of the luminance as function of the amount of pigment $c_i K_{\text{ink}}$. Once again a good correlation is found. It is somewhat surprising that the collapsed curves are quite good resembled by the pure exponential fit according to (3.4) with

$$L = L^{\infty} + (L_p - L^{\infty}) \exp(-0.048 \times c_i K_{\text{ink}}),$$

with the paper white $L_p = 96.41$ and the *deepest black* of $L^{\infty} = 0.9$. This fit is

[1] The standard conditions for luminance measurements (also realized in the ColorMunki Photo) is an illumination of the surface under an angle of incidence of 45° with a measurement of $L$ perpendicular to the surface.

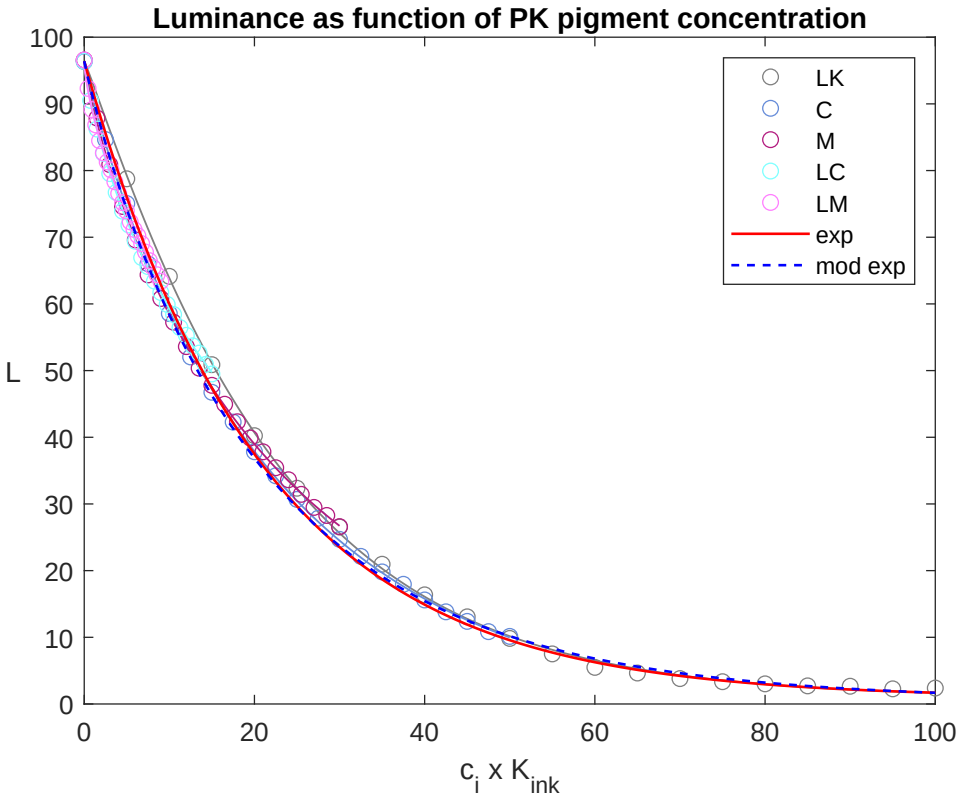


**Figure B.7.:** Luminance of all glossy inks on Hahnemühle FineArt Baryta as function of the pigment amount $c_i K_{\text{ink}}$. The data are very well fitted by the pure exponential decay according to (3.4) (red line). The modified exponential law (9.1) (blue dahes) provides little improvement, if any.

shown as the red line. Little is to be gained by the modified exponential fit

$$L = L^{\infty} + (L_p - L^{\infty}) \exp[-0.058 \times (c_i K_{\text{ink}})^{0.94}],$$

with $L_p = 96.41$ and the *deepest black* of $L^{\infty} = 0.5$ (blue dashed line). Both fits were made by the eye, because a standard curve fitting gives equal weight to all data points such that, due to the uneven distribution of the points, emphasis would be on the lower values of $K_{\text{ink}}$ and such fit would fail completely for large $K_{\text{ink}}$.[2]

Similar as for the matte paper PR308 (fig. 6.1) the most concentrated ink in the $LK$ channel (PK ink) prints lighter than expected for small $c_i K_{\text{ink}} \lesssim 30$. This is consistent with my hypothesis regarding the stacking of pigment particles. But different from PR308 the fine ordering of the curves is just the other way around (compare with fig. 6.1(b)).

When the luminance of all individual inks is mapped to a linear curve according to (5.2), the required ink amount as a function of the blackness $K$ is shown in fig. B.8. By comparing the curves with those for the matte papers (figs. 5.4 and B.1)

[2]Later, I have introduced an automatic fit using proper weights.

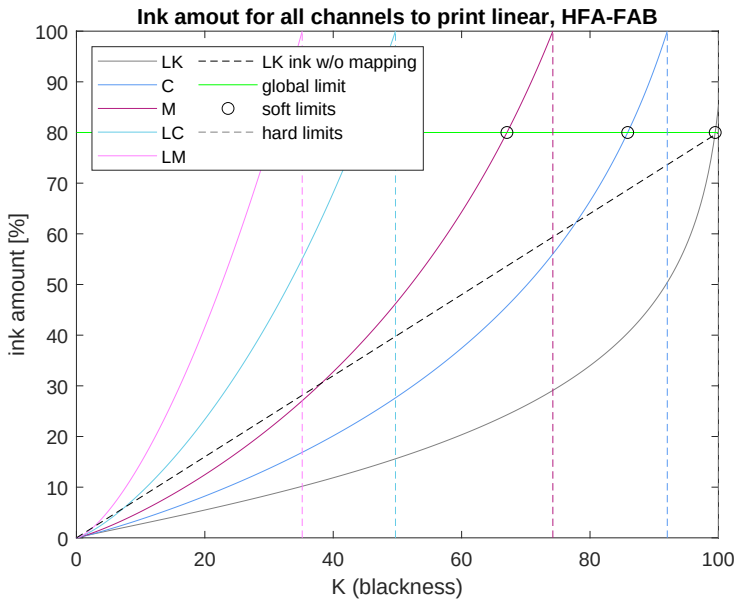


**Figure B.8.:** Ink amount $K_{\text{ink}}$ as function of the blackness $K$ required to print linearly on HFA FAB. The ink limit is $\alpha = 80\%$ and the black point was set to $L_m = 2.5$.

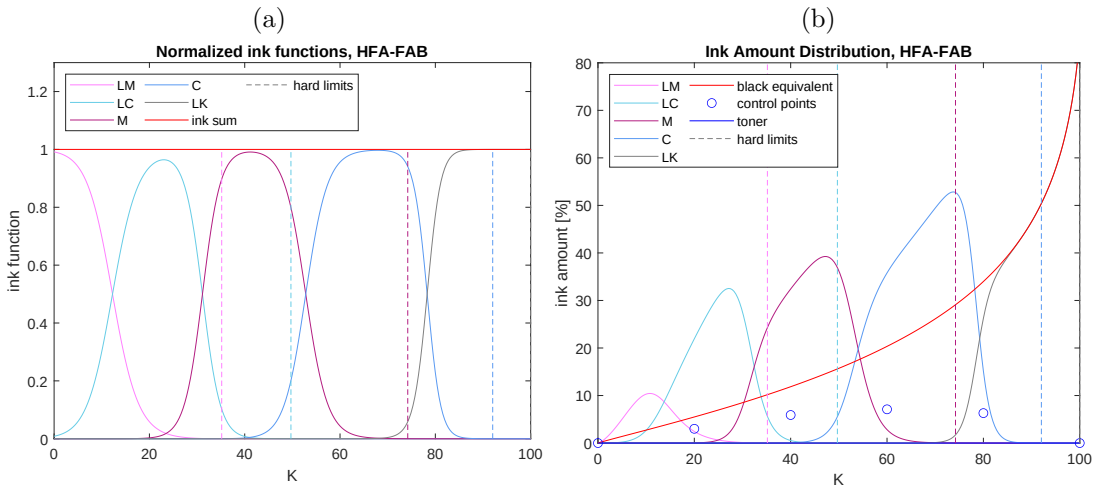


**Figure B.9.:** (a) Normalized ink functions for FAB according to (6.2). (b) Final ink distribution functions according to (6.3), without toner.

one can already notice that more ink is necessary to print linearly on Fine Art Baryta (FAB).

Finally, the normalized Gauß-type ink functions and a possible ink distribution is shown in fig. B.9. The ink distribution parameters are given in table B.5. They have been selected to distribute the inks evenly and to prevent the inks to exceed their ink limit on the blackness $K$ scale.

The linearity of the quad file produced for pure carbon printing is shown in fig. B.10. When comparing the measured data (squares, pluses) to the linear curve

**Table B.5.:** Parameters for the Gauß-type ink functions (6.1) for HFA FAB.

| | $LM$ | $LC$ | $M$ | $C$ | $LC$ |
|---|---|---|---|---|---|
| $\hat{K}_i$ | 0.04 | 0.20 | 0.43 | 0.62 | 1 |
| $d_i$ | 0.16 | 0.15 | 0.16 | 0.15 | 0.20 |

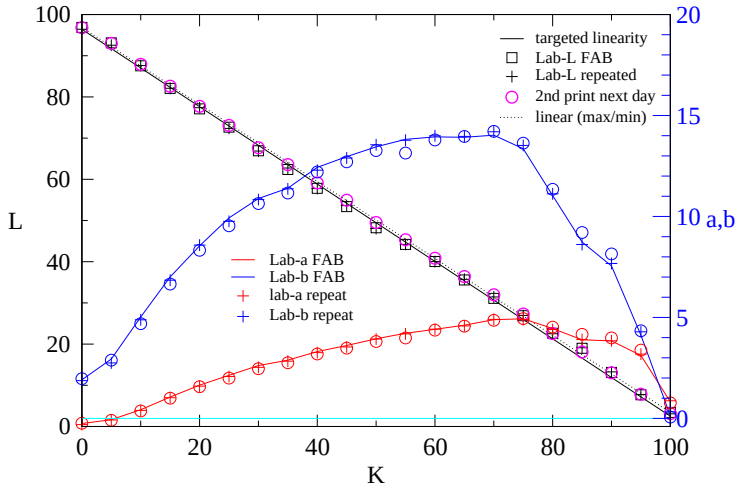


**Figure B.10.:** Linearity of the quad created for FAB with pure carbon inks. The global ink limit is $\alpha = 80\%$. Ink data measured over 100%. The targeted linearity was $L_p = 96.41$ and $L_m = 2.5$.

made by the two extreme values at $K = 0$ and $K = 100$ (dotted line), it seems as if the print is slightly too dark in the middle part. The maximum deviation from the curve connecting the extreme values linearly is about $-4\%$. I have no explanation at the moment. For instance, at $K = 40$ almost all ink is used from the $M$ channel (fig. B.9(b)), and the ink amount printed is about 32% (also fig. B.9(b)). From fig. B.6 the ink delivered by the $M$ channel at $K_{\text{ink}} = 32$ should very accurately be represented by the fit (full line). But if one compares the measured data with the actually targeted curve using the values $L_p = 96.41$ and $L_m = 2.5$, then the data scatter more equally about the target curve. As a test a new step wedge was printed the next day and measured. The data for Lab-$L$ are indicated by pink circles. Now the data in the mid range fit nicely with the target curve, but are slightly too bright at the extreme ends of the $K$ scale. The deviation of the measured data (circles versus squares) indicates the error made by the combination of the printer and the measurement. Probably one cannot do better with the current equipment. So there seems to be no systematic problem with the method. Occasionally, there ares some outliers, as for Lab-$b$ at $K = 55$.

# C. ColorMunki Photo versus ColorChecker24

The following tables provide reference data from https://babelcolor.com/colorchecker.htm for the colors contained in the ColorChecker24 of X-rite. The two sets of reference data do not deviate much from each other and the deviations are typically smaller than those of the measurements. The ColorChecker was stored dry in the dark over several years. The reference data are compared with the measured data from my ColorMunki Photo. Most of the deviations are less than 1 in Lab values. But the largest deviations were found for the white (A4) and strong red (C3). The maximum deviation was for white (A4) in the old reference data set with $\Delta b = 2.7$. The maximum deviation for the newer version of the ColorChecker was smaller with a maximum for strong red (C3) with $\Delta L = -2.0$. Thus the measured red was lighter than the reference. Perhaps red is the most unstable color in the ColorChecker? But usually the blue is fading the fastest, here $\Delta L \approx 1...1.5$.

The deviations for the gray colors were always positive with deviations for the mid grays below $\Delta L < 1$ and the maximum deviations up to $\Delta L \approx 1.4$ for black (all for the newer version of the reference data). The positive deviations indicate that the measured values are slightly darker than the reference values. From the data it is plausible to assume a typical error for the ColorMunki to be less than $\pm 1$ in any of the Lab channels, but sometimes larger deviations may occur up to $O(2)$.

| Before Nov 2014 | | Reference value | | | Measured | | | Difference | | |
|---|---|---|---|---|---|---|---|---|---|---|
| | | L | a | b | L | a | b | $\Delta L$ | $\Delta a$ | $\Delta b$ |
| A1 | Mod. Brown | 37.860 | 13.555 | 14.059 | 38.055 | 13.338 | 13.851 | -0.195 | 0.217 | 0.208 |
| A2 | Str. Orange | 62.661 | 36.067 | 57.096 | 63.092 | 35.828 | 57.544 | -0.431 | 0.239 | -0.448 |
| A3 | Str. Purplish Blue | 28.778 | 14.179 | -50.297 | 28.570 | 14.490 | -48.917 | 0.208 | -0.311 | -1.380 |
| A4 | White | 96.539 | -0.425 | 1.186 | 94.605 | -0.409 | 3.865 | 1.934 | -0.016 | -2.679 |
| B1 | Dark Yell-Pink | 65.711 | 18.13 | 17.81 | 64.666 | 19.244 | 18.067 | 1.045 | -1.114 | -0.257 |
| B2 | Str. Purp-Blue | 40.020 | 10.41 | -45.964 | 41.026 | 10.484 | -44.295 | -1.006 | -0.074 | -1.669 |
| B3 | Str. Yell-Green | 55.261 | -38.342 | 31.37 | 55.206 | -39.573 | 32.052 | 0.055 | 1.231 | -0.682 |
| B4 | Light Bl-Gray | 81.257 | -0.638 | -0.335 | 80.589 | -0.566 | 0.037 | 0.668 | -0.072 | -0.372 |
| C1 | Mod. Blue | 49.927 | -4.88 | -21.905 | 48.628 | -4.381 | -22.234 | 1.299 | -0.499 | 0.329 |
| C2 | Str. Red | 51.124 | 48.239 | 16.248 | 51.019 | 49.005 | 17.701 | 0.105 | -0.766 | -1.453 |
| C3 | Strong Red | 42.101 | 53.378 | 28.19 | 44.477 | 52.464 | 29.217 | -2.376 | 0.914 | -1.027 |
| C4 | Light Gray | 66.766 | -0.734 | -0.504 | 66.654 | -0.677 | -0.325 | 0.112 | -0.057 | -0.179 |
| D1 | ModÓl-Green | 43.139 | -13.095 | 21.905 | 43.192 | -12.968 | 21.751 | -0.053 | -0.127 | 0.154 |
| D2 | Dark Purple | 30.325 | 22.976 | -21.587 | 30.338 | 23.256 | -21.562 | -0.013 | -0.280 | -0.025 |
| D3 | Viv. Yellow | 81.733 | 4.039 | 79.819 | 82.569 | 2.722 | 81.303 | -0.836 | 1.317 | -1.484 |
| D4 | Medium Gray | 50.867 | -0.153 | -0.27 | 50.451 | -0.540 | 0.149 | 0.416 | 0.387 | -0.419 |
| E1 | Light Violet | 55.112 | 8.844 | -25.399 | 54.598 | 9.571 | -24.878 | 0.514 | -0.727 | -0.521 |
| E2 | Bril. Yel-Green | 72.532 | -23.709 | 57.255 | 73.049 | -25.268 | 57.909 | -0.517 | 1.559 | -0.654 |
| E3 | Deep P-Pink | 51.935 | 49.986 | -14.574 | 51.578 | 50.917 | -14.450 | 0.357 | -0.931 | -0.124 |
| E4 | Dark Gray | 35.656 | -0.421 | -1.231 | 35.187 | -0.509 | -0.644 | 0.469 | 0.088 | -0.587 |
| F1 | Light Bl-Green | 70.719 | -33.397 | -0.199 | 70.692 | -32.526 | 0.749 | 0.027 | -0.871 | -0.948 |
| F2 | Str. Or-Yellow | 71.941 | 19.363 | 67.857 | 72.579 | 19.163 | 68.203 | -0.638 | 0.200 | -0.346 |
| F3 | Viv. Gr-Blue | 51.038 | -28.631 | -28.638 | 50.414 | -27.933 | -28.130 | 0.624 | -0.698 | -0.508 |
| F4 | Black | 20.461 | -0.079 | -0.973 | 19.308 | 0.251 | -0.354 | 1.153 | -0.330 | -0.619 |

| Nov 2014 & newer | | Reference value | | | Measured | | | Difference | | |
|---|---|---|---|---|---|---|---|---|---|---|
| | | L | a | b | L | a | b | $\Delta L$ | $\Delta a$ | $\Delta b$ |
| A1 | Moderate Brown | 37.540 | 14.37 | 14.92 | 38.055 | 13.338 | 13.851 | -0.515 | 1.032 | 1.069 |
| A2 | Strong Orange | 62.730 | 35.83 | 56.5 | 63.092 | 35.828 | 57.544 | -0.362 | 0.002 | -1.044 |
| A3 | Strong Purplish Blue | 28.370 | 15.42 | -49.8 | 28.570 | 14.490 | -48.917 | -0.200 | 0.930 | -0.883 |
| A4 | White | 95.190 | -1.03 | 2.93 | 94.605 | -0.409 | 3.865 | 0.585 | -0.621 | -0.935 |
| B1 | Dark Yellowish Pink | 64.660 | 19.27 | 17.5 | 64.666 | 19.244 | 18.067 | -0.006 | 0.026 | -0.567 |
| B2 | Strong Purplish Blue | 39.430 | 10.75 | -45.17 | 41.026 | 10.484 | -44.295 | -1.596 | 0.266 | -0.875 |
| B3 | Strong Yellowish Green | 54.380 | -39.72 | 32.27 | 55.206 | -39.573 | 32.052 | -0.826 | -0.147 | 0.218 |
| B4 | Light Bluish Gray | 81.290 | -0.57 | 0.44 | 80.589 | -0.566 | 0.037 | 0.701 | -0.004 | 0.403 |
| C1 | Moderate Blue | 49.320 | -3.82 | -22.54 | 48.628 | -4.381 | -22.234 | 0.692 | 0.561 | -0.306 |
| C2 | Strong Red | 50.570 | 48.64 | 16.67 | 51.019 | 49.005 | 17.701 | -0.449 | -0.365 | -1.031 |
| C3 | Strong Red | 42.430 | 51.05 | 28.62 | 44.477 | 52.464 | 29.217 | -2.047 | -1.414 | -0.597 |
| C4 | Light Gray | 66.890 | -0.75 | -0.06 | 66.654 | -0.677 | -0.325 | 0.236 | -0.073 | 0.265 |
| D1 | Moderate Olive Green | 43.460 | -12.74 | 22.72 | 43.192 | -12.968 | 21.751 | 0.268 | 0.228 | 0.969 |
| D2 | Dark Purple | 30.100 | 22.54 | -20.87 | 30.338 | 23.256 | -21.562 | -0.238 | -0.716 | 0.692 |
| D3 | Vivid Yellow | 81.800 | 2.67 | 80.41 | 82.569 | 2.722 | 81.303 | -0.769 | -0.052 | -0.893 |
| D4 | Medium Gray | 50.760 | -0.13 | 0.14 | 50.451 | -0.540 | 0.149 | 0.309 | 0.410 | -0.009 |
| E1 | Light Violet | 54.940 | 9.61 | -24.79 | 54.598 | 9.571 | -24.878 | 0.342 | 0.039 | 0.088 |
| E2 | Brilliant Yellow Green | 71.770 | -24.13 | 58.19 | 73.049 | -25.268 | 57.909 | -1.279 | 1.138 | 0.281 |
| E3 | Deep Purplish Pink | 50.630 | 51.28 | -14.12 | 51.578 | 50.917 | -14.450 | -0.948 | 0.363 | 0.330 |
| E4 | Dark Gray | 35.630 | -0.46 | -0.48 | 35.187 | -0.509 | -0.644 | 0.443 | 0.049 | 0.164 |
| F1 | Light Bluish Green | 70.480 | -32.26 | -0.37 | 70.692 | -32.526 | 0.749 | -0.212 | 0.266 | -1.119 |
| F2 | Strong Orange Yellow | 71.510 | 18.24 | 67.37 | 72.579 | 19.163 | 68.203 | -1.069 | -0.923 | -0.833 |
| F3 | Vivid Greenish Blue | 49.570 | -29.71 | -28.32 | 50.414 | -27.933 | -28.130 | -0.844 | -1.777 | -0.190 |
| F4 | Black | 20.640 | | -0.46 | 19.308 | 0.251 | -0.354 | 1.332 | -0.251 | -0.106 |